Virginia Commonwealth University
VCU Scholars Compass

Theses and Dissertations | Graduate School

2013

# INTRA-MITOCHONDRIAL INJURY DURING ISCHEMIA-REPERFUSION

Hema Aluri
*Virginia Commonwealth University*

Follow this and additional works at: https://scholarscompass.vcu.edu/etd

 Part of the Physiology Commons

© The Author

Downloaded from
https://scholarscompass.vcu.edu/etd/474

This Dissertation is brought to you for free and open access by the Graduate School at VCU Scholars Compass. It has been accepted for inclusion in Theses and Dissertations by an authorized administrator of VCU Scholars Compass. For more information, please contact libcompass@vcu.edu.

**© Hema S. Aluri 2013**

**All Rights Reserved**

# INTRA-MITOCHONDRIAL INJURY DURING ISCHEMIA-REPERFUSION

A dissertation submitted in partial fulfillment of the requirements for the degree of Doctor of Philosophy at Virginia Commonwealth University School of Medicine
by

**Hema S. Aluri**

MS, Chemistry, Virginia Commonwealth University, 2009

**Director: EDWARD LESNEFSKY, Jr. M.D.**
Professor of Internal Medicine (Cardiology),
Physiology and Biophysics
Biochemistry and Molecular Biology

Virginia Commonwealth University
Richmond, Virginia
May 18, 2013

**Acknowledgement**

This dissertation would not have been possible without the guidance and the support of several individuals who in one way or another contributed and extended their valuable assistance in the preparation and completion of this study.

I would like to express the deepest appreciation to Dr. Edward Lesnefsky who has the attitude and the substance of a genius. He continually and convincingly conveyed a spirit of adventure in regard to research. Without his guidance and persistent help this dissertation would not have been possible. It's because of Dr. Edward Lesnefsky, I truly considered myself as one of those rare graduate students who enjoy graduate school wholeheartedly accompanied with a rich learning experience.

I would like to thank my committee members, Professors: Roland Pittman, Clive M. Baumgarten, Srinivasa Karnam, Jessica K. Bell, Fadi N. Salloum, for their constant support and insightful suggestion to strengthen my research project and honed up my overall analytical aptitude.

My sincere gratitude to Dr. Diomedes E. Logothetis as it was under his tenure as a departmental chair, I got admittance to Medical Campus of Virginia (MCV). My heartiest regards to Dr. Louis J. De Felice, the former program director for his inevitable support and contribution to help me succeed in my graduate life. I also extend my unparalleled respect to Department of Physiology and Biophysics. I feel such fortunate to work in this department. I have learned a great deal of science and professionalism by pursuing Ph.D. in this department.

Apart from the efforts of me, the success of any project depends largely on the encouragement and guidelines of colleagues. I take this opportunity to express my gratitude to Dr. Qun Chen, Ms. Ying Hu, Dr. Karol Szczepanek and Dr. Aijun Xu who have been instrumental in the successful completion. The guidance and support received from all the members who contributed and who are contributing to this dissertation, was vital for the success of the dissertation. I am grateful for their constant support and help. Very special thanks to Dr. Karol Szczepanek for being such a good friend and tremendously helpful teacher who assisted me in learning new techniques during the entire period of my doctoral program.

Also, I thank all of my dearest and wonderful friends: Suresh Narayanasamy, Balamurali Kannan, Daniel Amalanayagame Gerard, Gunjan Saxena, Ketan Vidwans, Deboleena Mitra, Devnath Vasudevan, Spandana Kankanala, Pooja Desai and Krasnodara Cameron for their unconditional support during all times. Last but of course not least, this work would not have been achieved without the support and encouragement from my family.

Finally, I am dedicating this thesis to my mom Naga Durga Aluri and my husband, Kalyan Valluripalli. They were always there cheering me and also stood by me through the good and bad times to make me happy and successful in my life. Without both of them this wouldn't have been possible.

## Table of contents

## LIST OF TABLES

## LIST OF FIGURES

## ABBREVIATIONS

A.A - Antimycin A

ADP - Adenosine diphosphate

AMBRA1 - Activating molecule in BECLIN1-regulated autophagy

ANOVA - Analysis of variance

ANT - Adenine-nucleotide translocator

ARF - Animal Research Facility

ASK1 - Apoptosis signaling kinase 1

ASK1-i - Apoptosis signaling kinase 1-inhibitor

ATP - Adenosine triphosphate

Ag - Antigen

Asn - Asparagine

BAK - BCL2-antagonistic/killer

BAX - BCL2-associated X protein

BCL-2 - B-cell lymphoma 2

BCL-XL - B-cell lymphoma-extra large

BID - BH3 interacting domain death agonist

BNIP3 - BCL2/adenovirus E1B 19-kDa protein-interacting protein 3

BNIP3L - BCL2/adenovirus E1B 19-kDa protein-interacting protein 3-like

BSA - Bovine serum albumin

C18:2 - Linoleic acid

CCC - C-terminal coiled-coil

CL - cardiolipin

$CN^-$ - cyanide anions

CO - carbon monoxide

COX - Cytochrome c oxidase

CP1 - Chappell-Perry 1

CRC - Calcium retention capacity

CaMKII - Calcium/calmodulin-dependent protein kinase type II

CoQ - Coenzyme Q

CyP-D - Cyclophilin-D

DCPIP - Dichlorophenolindophenol

DIABLO - Direct IAP-binding protein with low pI

DMSO - Dimethyl sulfoxide

DNP - Dinitrophenol

DTNB - 5,5'-dithiobis-(2-nitrobenzoic acid)

DTT - Dithiotreitol

Drp 1 - Dynamin-related protein 1

EDTA - Ethylenediaminetetraacetic acid

EGTA - Ethylene glycol-bis(2- aminoethylether)-N,N,N′,N′-tetraacetic acid

EPR - Electron paramagnetic resonance

EQ - Equilibration

ER - Endoplasmic reticulum

ESR - Electron spin resonance

ETC - Electron transport chain

ETF - Electron transfer flavoprotein

FAD - Flavin adenine dinucleotide

$FADH_2$ - Flavin adenine dinucleotide

FMN - Flavin mononucleotide

FRET - Förster resonance energy transfer

Fe-Met - Iron-methionine

Fis1 - Mitochondrial fission 1 protein

$GP_x$ - Glutathione peroxidase

GSH - Glutathione

GSSG/GSH - Glutathione disulfide/Reduced glutathione couple

GTP - Guanosine triphosphate

$H_2O_2$ - Hydrogen peroxide

$H_2S$ - Hydrogen sulfide

HOCl - Hypochlorous acid

HRP - Horse Radish Peroxidase

IMM - Inner mitochondrial membrane

IMS - Intermembrane space

IP - Immunoprecipitation

ISC - Ischemia

ISC-REP - Ischemia-Reperfusion

JNK - c-Jun NH(2)-terminal kinase

LDH - Lactate dehydrogenase

LPS - Lipopolysaccharide

LTQ XL - Linear trap Quadrupole

LVDP - Left ventricular developed pressure

Lys - Lysine

MAM - Mitochondria-associated ER-membrane

MAPK - Mitogen-activated protein kinase

MDM2 - Mouse double minute 2

MEFS - Mouse embryonic fibroblasts

MKK - Mitogen-activated protein kinase kinase

MOMP - Mitochondrial outer membrane permeabilization

MPTP - Mitochondrial permeability transition pore

MSRB - Methionine sulfoxide reductase B

Met - Methionine

Met(O) - Methionine sulfoxide

Mfn - Mitofusin

MnSOD or SOD2 - superoxide dismutase

$N_3^-$ - Azide anion

NADH - Nicotinamide adenine dinucleotide

NADPH - Nicotinamide adenine dinucleotide phosphate

NCC - N-terminal coiled-coil

NFR - NADH ferricyanide oxidoreductase

NIX - Nip3-like protein X

NO - Nitric oxide

$O_2^{\bullet -}$ - Superoxide

OAA - Oxaloacetic acid

OMM - Outer mitochondrial membrane

Opa1 - Optic atrophy protein 1

PGC-1α - Peroxisome proliferator-activated receptor-γ coactivator 1α

PINK1 - Putative kinase 1

PKC - Protein kinase C

PLS-3 - Phospholipid scramblase-3

PMF - Proton motive force

PP2Cε - Serine/threonine protein phosphatase

PUMA - p53 upregulated modulator of apoptosis

PVDF - Polyvinyldifluoridine

$P_i$ - Phosphate

QTrap - Quadrupole/linear ion trap

RCR - Respiratory control ratios

REP - Reperfusion

RET - Reverse electron transfer

ROS - Reactive Oxygen Species

Rot - Rotenone

SDS-PAGE - Sodium dodecyl sulfate-Polyacrylamide gel electrophoresis

SEM - standard error of the mean

SMAC - second mitochondria-derived activator caspase

STEMI - ST segment elevation myocardial infarction

Ser - Serine

Succ - Succinate

TC - Time control

TCA - Tricarboxylic acid cycle

TCEP - Tris(2-carboxyethyl)phosphine

TIM - Translocase of inner membrane

TMPD - N,N,N′,N′-tetramethyl-*p*-phenylenediamine

TMRM – Tetramethyl rhodamine methyl ester

TMT - Tandem mass tag

TNF-α - Tumor necrosis factor-α

TOM - Translocase of the outer membrane

TRAIL - TNF-related apoptosis-inducing ligand

TTFA - Thenoyltrifluoroacetone

TXNIP - Thioredoxin-interacting protein

Thr - Threonine

Trx - Thioredoxin

VDAC - Voltage-dependent anion channel

VDUP1 - VitaminD3 upregulated protein-1

PARIS - Parkin-interacting substrate

mtDNA - Mitochondrial DNA

rRNAs - Special mitochondrial ribosomes

tRNAs - Transfer RNAs

ΔpH - Proton gradient

$\Delta\Psi_m$ - Mitochondrial membrane potential

αGPDH - α-Glycerophosphate dehydrogenase

αKGDH - α-Ketoglutarate dehydrogenase

$^{\bullet}OH^{-}$ - Hydroxyl radical

## ABSTRACT


**INTRA-MITOCHONDRIAL INJURY DURING ISCHEMIA-REPERFUSION**

By Hema Santhi Aluri

A thesis submitted in partial fulfillment of the requirements for the degree of Doctor of Philosophy at Virginia Commonwealth University.

Virginia Commonwealth University, 2013

Director: **EDWARD LESNEFSKY, Jr. M.D.**
Professor of Internal Medicine (Cardiology), Physiology and Biophysics, Biochemistry and Molecular Biology

Cardiac injury is increased following ischemia-reperfusion. Mitochondria are the “effector organelles” that are damaged during ischemia (ISC) when there is no blood flow. Resumption of metabolism by damaged mitochondria during reperfusion (REP) results in increased cell injury. Current therapeutic interventions to pre-condition and post-condition the heart during ISC are ineffective during certain conditions like aging and diabetes due to defects in the signaling cascades. In contrast, mitochondrial-based strategies are effective in protecting the heart during ISC-REP. Hence direct therapeutic targeting of dysfunctional mitochondria will provide the potential to bypass the upstream signaling defects and intervene directly upon the effector organelle.

Novel mitochondrial-targeted therapy relies on understanding the sites in the electron transport chain (ETC) that are damaged by ISC and produce cell-injury during REP. This project identifies a novel pathological role of cytochrome c in depleting cardiolipin during ischemia after which the mitochondria are in a defective condition that leads to additional cell death during reperfusion. During ischemia oxidants from complex III oxidize cytochrome c*,* forming a peroxidase, which causes oxidative damage and depletion of cardiolipin. Depletion of cardiolipin disrupts normal physiology and augments cell death. Identification of the innovative pathobiology during ISC-REP recognizes a novel therapeutic target, cytochrome c peroxidase, which can be a focal point for new therapeutic interventions to decrease cardiac injury.

In order to maintain homeostatis, living organisms have the methionine sulfoxide reductase system, which reduce both free and protein bound Met(O) back to methionine (Met) in the presence of thioredoxin. Oxidized Trx is inactive and unable to bind to ASK1 thereby activating ASK1 and causing cell death via p38/JNK pathways thereby

contributing to the pathogenesis of myocardial ISC-REP injury. In this study we have shown that inhibition of ASK1 protects the heart during REP via the modulation of mitochondria that sustained damage during ISC. The mitochondrial-based mechanism of cardioprotection with ASK1 inhibition enhanced the functional integrity of the inner mitochondrial membrane retaining cytochrome c thereby decreasing cell death. This therapeutic intervention is a key step to achieve the ultimate goal to improve clinical outcomes in patients that suffer an acute myocardial infarction.

# CHAPTER I: INTRODUCTION

## I. 1. Mitochondria biology and structure

Mitochondria are distinct, membrane-bound organelles found in most eukaryotic cells. The size of these organelles range from 0.5 to 1.0 μm in diameter and their number in a cell varies in each organism and tissue type from one to over a thousand. Since mitochondria generate most of the cell's adenosine triphosphate (ATP), they are often termed "powerhouse of the cell". In addition to generating energy, mitochondria are involved in other cellular processes such as calcium homeostasis, ammonia detoxification (urea cycle), fatty acid oxidation, certain heme synthesis reactions, steroid synthesis, cell signaling, cellular differentiation and cell death [1, 2]. Mitochondria are implicated in diseased conditions including cardiac dysfunction, neurodegeneration and congenital metabolic disorders, as well as, aging [3-5]. The mitochondrion has its own independent genome that is replicated and transcribed entirely in this organelle similar to bacterial genome, presumably due to the bacterial origin of mitochondria [6-8]. As

shown in **Figure 1.1**, the organelle is composed of compartments that include the outer membrane, the intermembrane space, the inner membrane, the cristae and the matrix, each responsible for specialized functions. Both the outer and inner membranes are made of phospholipid bilayers and have different properties [6-8].

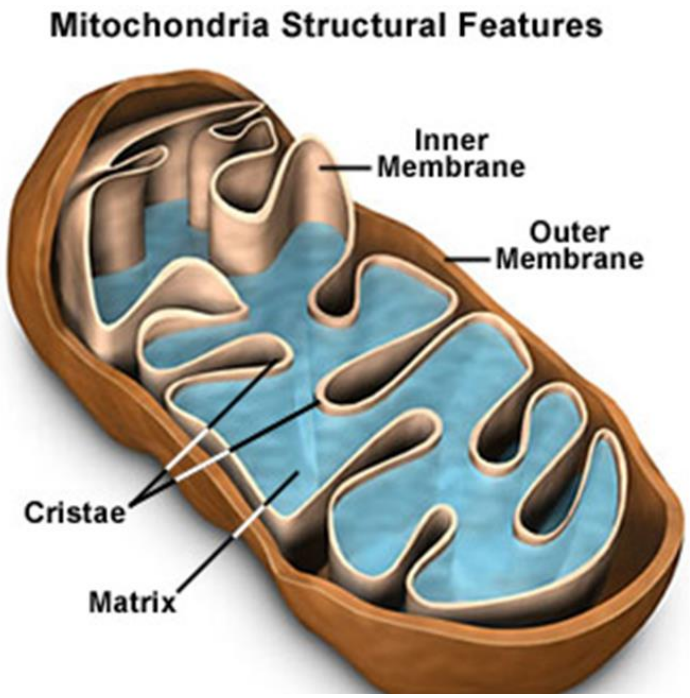


**Figure 1.1. Schematic depiction of a mitochondrion.** The organelle is composed of compartments that include the outer membrane, the intermembrane space, the inner membrane, the cristae and the matrix [8].

The outer mitochondrial membrane (OMM) encloses the entire organelle and has a 1:1 weight ratio of protein: phospholipid which is similar to that of the plasma membrane [6, 8]. The membrane allows passage of molecules 5000 Daltons or less through channels which are formed by a large variety of integral proteins called porins. Larger proteins are transported across the outer membrane by binding to the multisubunit protein complex called translocase of the outer membrane (TOM) [9]. Studies have been reported that the outer membrane associates with the endoplasmic reticulum (ER) forming a structure called MAM (mitochondria-associated ER-membrane) which is involved in lipid transfer between ER and mitochondria and also in calcium signaling [10-12].

The space between the outer membrane and the inner membrane is termed the mitochondrial intermembrane space (IMS). IMS contains small molecules including ions, carbohydrates and sugars that are permeable to the outer membrane resulting in a similar concentration as the cytosol. However, large proteins like cytochrome c are transported across the outer membrane via the TOM complex [6, 13-15].

The inner mitochondrial membrane (IMM) has numerous invaginations called cristae which increase the surface area of the inner membrane. Proteins are embedded in the inner membrane that perform important functions including oxidative phosphorylation, specific transport of proteins that regulate metabolite passage, protein import and mitochondrial fusion. The IMM is enriched with phospholipids, particularly cardiolipin, which makes the membrane impermeable to molecules [6, 16]. Proteins are transported across the inner membrane using translocase of inner membrane (TIM) and metabolite transporters comprising malate-aspartate shuttle system and glycerol-3-phosphate

shuttle that allow tightly controlled exchange of metabolites and protein import across the IMM [9].

The space enclosed by the inner membrane is called the matrix. It contains proteins, enzymes, special mitochondrial ribosomes (rRNAs), transfer RNAs (tRNAs), and circular forms of mitochondrial DNA (mtDNA) present in two to ten copies per mitochondrion [17]. Some key functions of matrix localized enzymes include oxidation of pyruvate and fatty acids, the citric acid cycle and the urea cycle (in liver and kidney mitochondria) [6].

Mitochondria have their own genetic material and fully functional machinery to synthesize their own RNAs and proteins. Mitochondrial DNA is a double-stranded circular sequence which consists of 16,569 base pairs that encodes a total of 37 genes: 22 tRNA, 2 rRNA, and 13 polypeptides. The thirteen polypeptides encode for the subunits of electron transport chain complexes I, III, IV, and ATP synthase **(Table 1.1)**. The rest of the mitochondrial proteins are encoded by nuclear DNA which are subsequently translocated and integrated into the mitochondria using TOM/TIM system [17, 18].

Significant oxidative stress generates reactive oxygen species (ROS) from the electron transport chain (ETC) which result in spontaneous and relatively frequent mutations in mtDNA due to close proximity of mtDNA to the electron transport chain (ETC) and due to the lack of the efficient defense mechanisms [19, 20]. Mitochondrial DNA mutations trigger a vicious cycle that lead to enzymatic abnormalities and further oxidative stress. Such mutations are inherited (only maternal mtDNA is passed to the offspring) and lead

to diseases that include Kearns-Sayre syndrome, MELAS syndrome and Leber's hereditary optic neuropathy [21]. However, mutations in nuclear genes lead to mitochondrial abnormalities such as coenzyme Q10 deficiency, Barth syndrome and a wide variety of clinical disease phenotypes, including certain mitochondrial myopathies [22, 23].

**Table 1.1. The mtDNA encodes proteins of the electron transport chain complexes**

| Complex | Number of subunits | Subunits encoded by mtDNA |
|---|---|---|
| Complex I | 46 | ND1, ND2, ND3, ND4, ND4L, ND5, ND6 |
| Complex III | 11 | CytB |
| Complex IV | 13 | COX1, COX2, COX3 |
| Complex V | 8 | Atp6, Atp8 |

**COX- Cyclooxygenase; ND- NADH dehydrogenase; Cyt- Cytochrome; ATP- adenosine triphosphate.**

## I. 2. Cellular respiration and oxidative phosphorylation

The most important role of mitochondria is to generate energy for cellular respiration in the form of ATP by phosphorylation of ADP. The key pathways localized to the inner membrane and matrix include the tricarboxylic acid cycle, fatty acid β-oxidation and pyruvate dehydrogenase which lead to oxidation of amino acids, fatty acids and pyruvate [6]. The initial steps involve conversion of pyruvate (by pyruvate dehydrogenase) or fatty acids (in β-oxidation pathway) to acetyl CoA. The acetyl-CoA is oxidized to $CO_2$ by the citric acid cycle also known as the tricarboxylic acid cycle (TCA)/Krebs cycle. Oxidation of one pyruvate molecule generates three molecules of nicotinamide adenine dinucleotide (NADH), one flavin adenine dinucleotide ($FADH_2$) and one guanosine triphosphate (GTP) molecule [24, 25]. NADH and $FADH_2$ are cofactors that transfer electrons into the respiratory chain to drive ATP synthesis. The respiratory chain is localized in cristae of the IMM. NADH is diffusible but impermeable to inner membrane whereas $FADH_2$ (from TCA cycle) is covalently bound to the succinate dehydrogenase which is the only enzyme of TCA cycle located in the inner membrane. GTP is readily converted into ATP. NADH and $FADH_2$ generated by the TCA cycle transfer electrons to $O_2$ through four multimeric respiratory complexes (I-IV) resulting in an electrochemical gradient across the membrane which in turn is used by by the $F_0F_1$ complex (ATP synthase) to generate ATP. The coupled processes of the electron transport chain-dependent NADH and $FADH_2$ oxidation and the phosphorylation of ADP to ATP driven by electron transport chain (ETC) dependent proton motive force (PMF) are termed oxidative phosphorylation [26-28].

Oxidative phosphorylation is a highly sophisticated system evolutionarily developed to increase recovery of energy contained in glucose molecules [29]. Oxidation of glucose through glycolysis, citric acid cycle and oxidative phosphorylation theoretically generates a maximum of 38 ATP molecules (3 ATP per NADH and 2 ATP per $FADH_2$). However, this number is not reached in reality due to the losses in energy, such as the cost of moving two equivalents of NADH (generated in glycolysis) from cytoplasm to matrix, translocation of Pi and ADP into the mitochondria, and ATP out of the mitochondria. Furthermore, inefficiencies in oxidative phosphorylation due to leakage of protons across of the mitochondrial membrane and slippage of the ATP synthase/proton pump reduce the ATP yield. Therefore, the theoretical efficiency of oxidative phosphorylation is not reached and the observed yield is closer to 30 ATP molecules per one molecule of glucose (2.5 ATP per NADH and 1.5 ATP per $FADH_2$) [30].

### I. 3. Mitochondrial Electron Transport Chain

The electron transport chain (ETC) is comprised of multi-subunit enzyme complexes and additional mobile electron carriers, ubiquinone (coenzyme $Q_{10}$) in the inner membrane and cytochrome c located in the intermembrane space [26, 28]. These complexes diffuse in the inner mitochondrial membrane individually or are organized into larger supercomplexes called respirasomes [31].

Electrons are transferred from complex I (NADH: ubiquinone oxidoreductase; EC 1.6.5.3) and II (succinate: ubiquinone oxidoreductase, EC 1.3.5.1) to ubiquinone, which carries them to complex III (ubiquinol: cytochrome c oxidoreductase, EC 1.10.2.2). From complex III, the mobile cytochrome c carries the electrons to complex IV (cytochrome c oxygenase, EC 1.9.3.1) where molecular oxygen is reduced to water. However, other

enzymes comprising the electron-transferring flavoprotein (ETF): ubiquinone oxidoreductase; s, n-glycerophosphate dehydrogenase; dihydroorotate dehydrogenase provide electrons to the ETC at the ubiquinone and the reactions occur usually at a very low rate. Additionally in the liver, electrons generated during oxidation of sulfur-containing amino acids by sulfite oxidase can be fed into the ETC at cytochrome c [29].

Electrons are transferred via productive collisions from high redox potential molecules such as NADH, $FADH_2$ with ETC complexes. The energy lost as a result of the transfer of electrons is utilized by complexes I, III and IV to pump protons from the mitochondrial matrix into the IMS **(Figure 1.2)**. The released energy generates a potential difference ($\Delta\Psi_m$) and proton gradient (ΔpH) across the membrane. This electrochemical proton gradient is used by the ATP synthase which allows the flow of $H^+$ through the enzyme back into the matrix to generate ATP from adenosine diphosphate (ADP) and inorganic phosphate. Apart from the ATP synthesis, proton motive force is used for chemical, osmotic and mechanical work such as mitochondrial $Ca^{2+}$ uptake, ATP/ADP exchange by the adenine-nucleotide translocator (ANT), import of nDNA-encoded preproteins, functioning of mitochondrial antiporters (aspartate/glutamate, $H^+/K^+$, $H^+/Na^+$, $2H^+/Ca^{2+}$) and symporters ($H^+$/pyruvate and $P_i$/ADP) [29, 32-34]. The proton motive force is dominated by $\Delta\Psi_m$ and the ΔpH component contributes approximately 15% to its total. Therefore, $\Delta\Psi_m$ can be considered as a crucial indicator of mitochondrial function and metabolic activity [29, 35, 36].

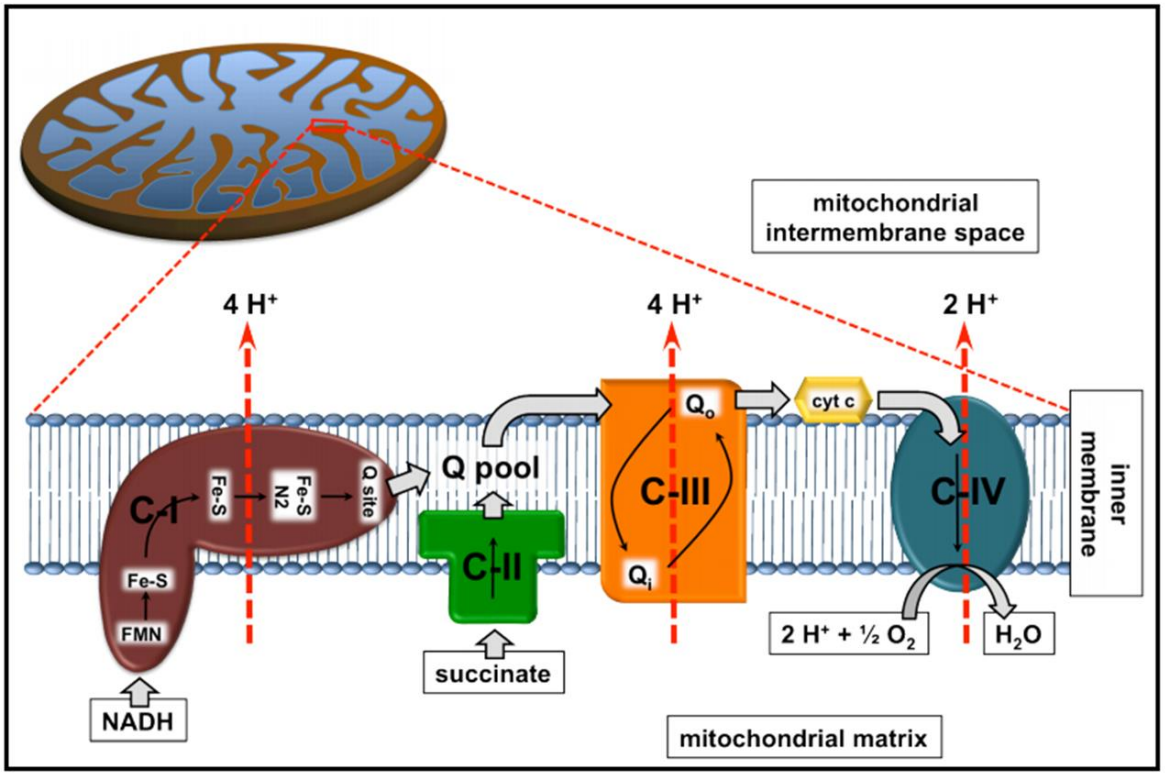


**Figure 1.2. Schematic representation of mitochondrial electron transport chain.** The sites of proton pumping (red arrows) are located in complex I, III and IV. From each NADH two electrons are passed into molecular oxygen ($O_2$) resulting in translocation of ten protons ($H^+$). Six protons are pumped into IMS when succinate/$FADH_2$ is used as an electron donor. NADH, nicotinamide adenine dinucleotide; FMN, flavin mononucleotide; Fe-S, iron-sulfur cluster; Q, ubiquinone; cyt c, cytochrome c; C, complex. Adapted from [37].

### I. 3. 1. NADH: ubiquinone oxidoreductase

During oxidative phosphorylation complex I transfers two electrons from NADH to ubiquinone with pumping of four protons from the matrix to the intermembrane space [6]. Complex I is comprised of forty six unique protein subunits with an approximate total size of 980 kDa. Despite such complexity, only fourteen subunits are essential for its catalytic function: seven highly hydrophobic mtDNA-encoded subunits (ND1, ND2, ND3, ND4, ND4L, ND5, ND6) and seven hydrophilic nuclear-encoded subunits (NDUFV1, NDUFV2, NDUFS1, NDUFS2, NDUFS3, NDUFS7, NDUFS8). The function of the remaining 31 additional proteins is largely unknown. Electron microscopy analysis reveals that complex I assumes an L-shaped conformation and consists of a peripheral, matrix-protruding arm and an inner membrane-embedded arm. The matrix protruding arm contains NADH dehydrogenase activity with flavin mononucleotide (FMN) and an inner membrane-immersed arm consisting of all mtDNA-encoded subunits with ubiquinone-and rotenone-binding site [38, 39].

Fully assembled mammalian complex I accepts electrons from NADH into FMN cofactor located in the NDUFV1 subunit. Then electrons are transported through the protein by eight iron-sulfur clusters: N3 (NDUFV1), N1b (NDUFS1), N4 (NDUFS1), N5 (NDUFS1), N6a (NDUFS8), N6b (NDUFS8) and N2 (NDUFS7). In six of the FeS clusters (N2, N3, N4, N5, N6a, and N6b) iron atoms are coordinated to four sulfur atoms ([4Fe-4S]) and the other two (N1a, N1b) display a [2Fe-2S] configuration. After reaching FeS N2 cluster, electrons are transferred to the coenzyme Q or ubiquinone-binding site [38, 40]. The *Thermus thermophiles* crystal structure studies predict that coenzyme Q binding is located at subunits NDUFS2 and NDUFS7. Another study using site-directed

mutagenesis of NDUFS2 and NDUFS7 subunits confirm this observation [41]. Complex I inhibitors act at the terminal electron donating step by inhibition of ubiquinone reduction. One of them is the naturally found plant alkaloid rotenone, commonly used to study complex I dependent effects in the mitochondria. Photoaffinity labeling techniques and mutagenesis studies from *Y. lipolytica, R. capsulatus* reveal that NDUFS2, NDUFS7, ND1 and ND5 subunits contribute to the rotenone inhibition site within complex I [42]. The net reaction of complex I activity is summarized below:

$$NADH + Q + 5H^{+}_{matrix} \longrightarrow NAD^{+} + QH_2 + 4H^{+}_{IMS}$$

Altered complex I activity during pathologic conditions is often observed in a variety of diseases resulting from mutations in mtDNA that leads to decreased integrated respiration [21, 43, 44]. Mutations in the subunits of complex I have been associated with neurological and neuromuscular diseases, including Leigh syndrome [45-47], Leber's hereditary optic neuropathy [48, 49] and even with etiology of Parkinson's disease [50, 51]. Moreover, enzymatic activity may be regulated by specific post-translational modifications of particular subunits which include phosphorylation [52], glutathionylation [53-55], acetylation/deacetylation [56] and even S-nitrosylation [57, 58].

### I. 3. 2. Succinate: ubiquinone oxidoreductase

Complex II is the only enzyme that participates both in TCA cycle and ETC by catalyzing the oxidation of TCA intermediate succinate to fumarate with the electron transfer directly to the quinone pool. Complex II consists of four protein subunits and a bound flavin adenine dinucleotide (FAD) cofactor, iron-sulfur clusters, and a heme group [6]. The protein subunits are encoded by nuclear-DNA that include two

hydrophilic subunits, SDHa and SDHb which protrude into matrix and two hydrophobic subunits SDHc and SDHd embedded in inner membrane. The heme group does not participate in electron transfer to coenzyme Q, but is important in decreasing production of reactive oxygen species. The electrons from succinate are accepted at FAD cofactor located in SDHa. Next, the electrons are transferred through three iron-sulfur clusters, ([2Fe-2S], [4Fe-4S] and [3Fe-4S]), within SDHb into membrane-anchored subunits that contain the quinone-binding site [6, 59]. However, transfer of electrons through complex II does not transport protons across the membrane as summarized in equation below:

$$FADH_2 + Q \longrightarrow FAD + QH_2$$

Molecules such as TTFA (thenoyltrifluoroacetone) bind to the ubiquinone pocket and are speculated to play a protective role in blocking the unfavorable reverse electron flow from complex II into I, which can result in superoxide generation by complex I [29, 60]. The activity of succinate:ubiquinone oxidoreductase is tightly regulated despite its simple structure. However, post-translational modifications such as acetylation/deacetylation [61], glutathionylation [62] and phosphorylation [63] in the flavoprotein part of the complex (SDHa) result in altered enzymatic activity. On the other hand, mutations in SDHa subunit have been reported to cause a classical mitochondrial neurogenerative disease, encephalomyopathy in childhood while the mutations found in the genes of the other three subunits have been associated with sporadic paragangliomas and/or pheochromocytomas and the inherited autosomal cancer-susceptibility syndromes [64]. Also, mev-1 mutation in C. elegans gene encoding the homolog of SDHc subunit results in premature aging and hypersensitivity to oxidative stress [65].

### I. 3. 3. Ubiquinone: cytochrome c oxidoreductase

Complex III or mitochondrial bc1 complex is a multi-subunit enzyme encoded by both the mtDNA (cytochrome b) and the nuclear genome (remaining ten peptides). Structural studies have shown that the functional complex III is present as a dimer wherein each monomer contains three protein subunits with redox prosthetic groups: cytochrome b (two b-type hemes, $b_L$and $b_H$); cytochrome c1 (c-type heme, $c_1$); and the Rieske iron-sulfur protein harbors a [2Fe-2S] cluster [66].

Complex III has two reaction centers for ubiquinol, $Q_o$ and $Q_i$. $Q_o$ is located on the outer face of the inner membrane while $Q_i$ is localized facing the mitochondrial matrix [67]. Electron transport through bc1 complex, termed Q cycle, involves a concerted oxidation of $QH_2$ coupled with proton pumping across the membrane. Initially, $QH_2$ is oxidized at the $Q_o$ site resulting in bifurcation of the electron transfer. One electron is given to the [2Fe-2S] cluster within Rieske subunit, which is then oxidized by cytochrome c1. Further, cytochrome c1 is oxidized by cytochrome c resulting in transfer of a single electron and translocation of two protons into the IMS. The second electron bifurcated at the $Q_o$ site, as a result of oxidation of $QH_2$ results in formation of a semiquinone which subsequently is oxidized by donating the electron to the chain of hemes $b_L$ and $b_H$. Reduced heme $b_H$ gives one electron to $Q_i$ site resulting in the formation of semiquinone. The second half of the cycle is initiated again by a second round of $QH_2$ oxidation at $Q_o$ resulting in another molecule of reduced cytochrome c, another two protons translocation into the intermembrane space. The successive reduction of hemes $b_L$ and $b_H$ causes the complete reduction of semiquinone at $Q_i$ to ubiquinone. The quinone reduction at $Q_i$ involves an uptake of two protons from matrix. Therefore,

as a result of the Q cycle, for every pair of electrons taken from $QH_2$ to two molecules of cytochrome c, four protons are translocated to the intermembrane space and two protons are removed from the mitochondrial matrix [68]. The overall reaction is summarized below:

$$QH_2 + 2\text{cyt-c}\ (Fe^{3+}_{ox}) + 2H^+_{matrix} \longrightarrow Q + 2\text{cyt-c}\ (Fe^{2+}_{red}) + 4H^+_{IMS}$$

Two types of complex III-specific inhibitors have been reported based on their targets. Myxothiazol and stigmatellin bind to the distinct pockets within the $Q_o$ site and block the transfer of electrons into complex III from reduced $QH_2$. Antimycin A (second class inhibitor) blocks the electron transfer from $b_H$ heme to oxidized $Q_i$ site by binding to the ubiquinone [69].

Complex III gene mutations cause exercise intolerance and cardiomyopathy [19]. Additionally, mutations in mtDNA-encoded cytochrome b have been reported to cause septo-optic dysplasia [70] and multisystem disorders like deafness, mental retardation, retinitis pigmentosa, cataract, growth retardation and epilepsy [71]. Furthermore, Bjornstad syndrome (deafness, hair abnormalities) [72] and the Finnish lethal GRACILE syndrome (growth retardation, amino aciduria, iron overload, lactic acidosis and cholestasis) [73] are due to mutations in BCs1L assembly protein which assists in the maturation of the Rieske protein.

### I. 3. 4. Cytochrome c oxidase

Complex IV (cytochrome c oxidase) belongs to the heme-copper oxygen reductase superfamily which catalyzes the complete reduction of dioxygen to water and

translocates protons to the intermembrane space [8]. Complex IV can exist as a monomer, which is sufficient for electron transfer and oxygen reduction but for proton translocation across the inner membrane the cytochrome c oxidase must be present as a dimer. Each monomer is composed of several metal prosthetic groups (two hemes and two copper centers) and thirteen proteins. Among the thirteen proteins, three of them are encoded by mtDNA (COX1, COX2, and COX3) and the other ten by nuclear DNA. COX1 contains twelve transmembrane α helices that are organized in three groups of four helices with a central pore. The first group contains heme *a*, the second contains a heme $a_3$-copper CuB center, and the third group is empty. Subunit COX2 contains a binuclear copper center CuA. The nuclear encoded subunits (COX4 -COX8) are considered to contribute to the stability, assembly and regulation of the oxygenase. However, their exact functions are only partially understood [6, 25, 74].

Electrons from reduced cytochrome c are transferred to the binuclear CuA center in COX2 and then to heme *a*. Finally electrons are transferred to heme $a_3$-CuB center from heme *a* resulting in conversion of ½ $O_2$ to $H_2O$ at the heme $a_3$-CuB center which involves a rapid four electron reduction along with immediate oxygen-oxygen bond cleavage to avoid superoxide formation. Electron transfer through complex IV is coupled with the translocation of four protons from the matrix to the intermembrane space [25, 29]. The net reaction is summarized below:

$$\mathbf{4cyt\text{-}c\ (Fe^{2+}_{red}) + 8H^{+}_{matrix} + O_2 \longrightarrow 4cyt\text{-}c\ (Fe^{3+}_{ox}) + 4H^{+}_{IMS} + 2H_2O}$$

The oxygen binding site of complex IV also binds ligands such as carbon monoxide (CO), nitric oxide (NO), cyanide anions ($CN^-$), azide anions ($N_3^-$), and hydrogen sulfide

($H_2S$), resulting in competitive inhibition of the oxidase activity, which in turn leads to chemical asphyxiation [29].

Genetic mutations altering complex IV functionality and/or structure usually result in very severe and often fatal metabolic dysfunctions. The majority of cytochrome c oxidase disorders are caused by mutations in nuclear-encoded assembly proteins such as SURF1, SCO1, SCO2, COX10 and COX15 [75] that result in oxidase deficiency with variety of clinical phenotypes including Leigh syndrome, fatal infantile hypertophic cardiomyopathy and other neuropathies [76, 77].

### I. 4. Mitochondria as generators of reactive oxygen species

In most mammalian cells, mitochondria are important generators of Reactive Oxygen Species (ROS) [78-80]. Small amounts of ROS can function as “signaling ROS” that trigger ischemic preconditioning by activating protein kinases such as protein kinase C (PKC) or p38 MAP kinase leading to the subsequent translocation of transcription factor NF-κB to the nucleus where it regulates gene expression [81, 82]. However, excessive generation of ROS act as “cytotoxic ROS” that damage cardiomyocytes ultimately permeabilizing the mitochondrial membrane. Increased ROS from mitochondria contribute to the pathological redox signaling, releasing $H_2O_2$ from the organelle to the rest of the cell resulting in oxidative damage of target proteins which alters activity of enzymes, kinases, phosphatases and transcription factors [79, 83].

In mitochondria, superoxide ($O_2^{\bullet -}$) is produced by one-electron reduction of dioxygen ($O_2$). Theoretically, several electron donors and redox couples in the mitochondria can thermodynamically favor the formation of $O_2^{\bullet -}$. However, small-molecule electron

carriers like NADH, NADPH, $CoQH_2$ and glutathione (GSH) do not react with $O_2$ to generate $O_2^{\bullet-}$. Instead, mitochondria produce $O_2^{\bullet-}$ mainly at active sites of redox prosthetic groups within proteins or when reduced electron carriers such as $CoQH_2$ are bound to proteins. Alterations in protein due to mutation, post-translational modification or conformational changes enable $O_2$ to interact more rapidly with the electron carrier which increases dramatically the production of $O_2^{\bullet-}$ [84]. This makes the electron transport chain a perfect candidate for ROS production. Indeed, it is now very well documented that complex I and III are the main sites of superoxide generation during pathologic conditions [85].

Better understanding of mitochondrial ROS production will lead to the rational design of therapies to minimize oxidative damage by $O_2^{\bullet-}$. However, direct measurement of $O_2^{\bullet-}$ within mitochondria is a challenge because MnSOD rapidly dismutates it to form $H_2O_2$. The difficulties in assessing mitochondria-generated superoxide can be overcome by the measurement of $H_2O_2$ release from the mitochondria that has already exceeded the threshold of ROS scavenging systems capacity [86-88].

### I. 4. 1. Complex I-mediated ROS production

As mentioned earlier, Complex I comprises forty six polypeptides which includes FMN, FeS clusters and likely two semiquinones. Oxygen mostly likely has access to electron carriers mainly at FMN, CoQ sites and terminal FeS centers which can possibly donate an electron reducing $O_2$ to $O_2^{\bullet-}$ [89, 90]. Isolated complex I increases $O_2^{\bullet-}$ production in the presence of NADH and inhibitor rotenone. Rotenone binds to the CoQ-binding site of complex I and enhances $O_2^{\bullet-}$ generation I which suggests that the N2 Fe-S or the

tightly bound quinones are the loci for $O_2^{\bullet-}$ release [91, 92]. It is now well understood that complex I produces $O_2^{\bullet-}$ when $O_2$ reacts with fully reduced FMN which in turn is dependent on the NADH/$NAD^+$ ratio. Excess NADH leads to the fully reduced state of FMN, which favors the reduction of $O_2$ at the flavin cofactor [93-95]. Hence inhibition of the electron transport chain by chemicals, damage, mutation, ischemia, loss of cytochrome c or decrease in ATP demand affects respiration thereby increasing NADH/$NAD^+$ ratio ultimately causing excessive ROS generation [84, 93, 96]. In contrast, physiological respiring mitochondria on NADH-linked substrates produce less $O_2^{\bullet-}$ from complex I because the NADH/$NAD^+$ ratio is very low [97].

Reverse electron transfer (RET) is another mechanism by which complex I produces large amounts of superoxide [84, 89, 97]. RET occurs when electrons from succinate, α-glycerophosphate or fatty acid oxidation reduce the CoQ pool which along with significant proton motive pushes electrons back from $CoQH_2$ into complex I ultimately to the FMN site resulting in reduction of $NAD^+$ to NADH [98]. Under above mentioned conditions complex I produces extensive amounts of superoxide, especially in brain, heart, muscle and liver mitochondria [84, 89, 97]. Moreover, this generation of ROS is abolished in the presence of rotenone, which confirms that electrons enter complex I through the Q-binding site during RET [99]. However, the site in complex I of the RET-linked superoxide generation is unclear [100]. One possibility is that RET results in higher generation of $O_2^{\bullet-}$ from reduced FMN by forcing electrons back from complex I to FMN [84]. Additional RET-related $O_2^{\bullet-}$ production occurs at semiquinones formed in the Q-binding site of complex I during proton pumping [94, 99]. However, other reports provide evidence that the one-electron donor to oxygen in complex I is located prior to

the Q-binding site [101]. Their results also suggest that the superoxide generation site can be the iron-sulfur cluster N2, based on its physico-chemical properties and ability to interact with endogenous ubiquinone. Notably, the ROS production from complex I is considered to be directed into the matrix of the mitochondria [102].

### I. 4. 2. Complex III-mediated ROS production

Complex III for a long time has been considered the dominant source of superoxide production. Inhibition of the $Q_i$ center by antimycin A, results in large amounts of $O_2^{\bullet-}$ release due to the reaction of $O_2$ with ubisemiquinone bound to the $Q_o$ site. However, the $Q_i$ center can also be a site of $O_2^{\bullet-}$ production especially when electron flow into $Q_o$ is limited [91, 103]. Complex III exists as dimer which allows adequate residual electron flow into the the complex. As a result, electrons tunnel between the *b* hemes located at the $Q_i$ centers of each monomer [104] which increases ROS generation from the $Q_i$ center [105, 106]. On the other hand, an altered Fe-S center [107] will inactivate the $Q_o$ center which along with loss of cytochrome c, limits electron flow to $Q_o$ center which further augments ROS release from complex III [94, 104]. Superoxide generated at the $Q_o$ site in complex III is released into the intermembrane space but $O_2^{\bullet-}$ from $Q_i$ is targeted to the matrix [108, 109]. Interestingly, under conditions of a high proton motive force, as a result of reduced Q pool (from succinate), the main site of $O_2^{\bullet-}$ generation remains at the complex I through RET mechanism [84].

### I. 4. 3. Other sites of ROS production in the mitochondria

Other sites in the mitochondria located outside the ETC contribute to $O_2^{\bullet-}$ production. However, it is unclear whether they generate quantitatively significant amounts of mitochondrial ROS when compared to the ETC generated ROS [110].

Studies on the lower organisms or from the *in-vitro* isolated mammalian complex II have reported that the catalytic activity of electron transport chain complex II can contribute to $O_2^{\bullet-}$ generation in the mitochondria. Two regions of this enzyme that are suspected for ROS production are: the FAD cofactor which is modulated by $FADH^{\bullet}$ semiquinone and the Q-binding site [111-113]. However, the main source of complex II-driven superoxide generation in intact mitochondria is based on the RET into the complex I, which results in $O_2^{\bullet-}$ release from the sites within complex I. In addition, the damaged or mutated complex II increases $O_2^{\bullet-}$ production by itself [84, 114, 115].

Enzymes containing flavin prosthetic groups in their redox active center are suspected to generate $O_2^{\bullet-}$. These enzymes function mainly by donating electrons into NADH or ubiquinol. However, under conditions of high proton motive force, ubiquinol remains highly reduced, which leads to a blockade of the electron transfer to NADH and in turn to ubiquinol generating $O_2^{\bullet-}$. For example, the α-ketoglutarate dehydrogenase (αKGDH) contains a flavin center which produces ROS when its electron acceptor $NAD^+$ is limiting [116]. Furthermore, enzymes transferring electrons to the ubiquinol pool, such as succinate dehydrogenase and electron transfer flavoprotein (ETF), increase superoxide generation by the RET mechanism by donating electrons to CoQ [86]. Additionally, ETF: CoQ reductase may produce ROS by itself directed to the intermembrane space [109].

Another Q-linked enzyme located on the outer surface of the inner membrane is α-glycerophosphate dehydrogenase (αGPDH) which donates electrons from α-glycerophosphate to ubiquinol. This leads to increased ROS production, mainly by RET, although some is released from the enzyme itself. However, the physiological relevance of αGPDH contribution to $O_2^{\bullet-}$ generation is unclear due to a very low expression of this enzyme in most of mammalian tissues, though it may be important in the brain [116, 117].

In addition, many other mitochondrial enzymes which are not connected to NADH or CoQ can be induced to produce $O_2^{\bullet-}$ or $H_2O_2$. For example, adrenodoxin reductase/adrenodoxin/ cytochrome $P_{450}$ produces ROS in the mitochondrial matrix by receiving electrons from the NADPH pool [118]. Another one which has recently been reported is the mitochondrial intermembrane space protein, $p66^{shc}$, which uses electron transferred from reduced cytochrome c to generate peroxide that in turn appears to activate the apoptotic program [119]. Last but not least, monoamine oxidase is a flavoenzyme (containing FAD) located within the outer mitochondrial membrane, facing the intermembrane space. In mitochondria, monoamine oxidase catalyzes oxidative deamination of monomaines resulting in formation of aldehydes, ammonia and $H_2O_2$ [120]. However, their contribution to the overall production of ROS by mitochondria is still unclear [110].

### I. 4. 4. Mitochondrial ROS scavenging system

Mitochondrial ROS is measured using $O_2^{\bullet-}$-sensitive dyes such as hydroethidine and MitoSOX$^{TM}$ [121-123], spin trapping [88], by measuring the reaction of $O_2^{\bullet-}$ with

compounds to form chemiluminescent products [124, 125] and also by measuring the inactivation rate of aconitase [126]. However, the assessment of $O_2^{\bullet-}$ generation in mitochondria is extremely difficult due to its extremely short half-life and also due to the rapid dismutation into hydrogen peroxide ($H_2O_2$) which further diffuses out from the mitochondria. $H_2O_2$ which diffuses out is typically measured by oxidation reaction of $H_2O_2$ with non-fluorescent dye (eg. Amplex Red) and a peroxidase (Horse Radish Peroxidase) to form a fluorescent product [86, 127, 128].

The process of dismutation of $O_2^{\bullet-}$ to $H_2O_2$ occurs either spontaneously or is catalyzed by mitochondrial antioxidant systems that are capable of neutralizing excess ROS [79]. Tetrameric mitochondrial manganese superoxide dismutase (MnSOD or SOD2) located in the matrix catalyzes the production of $H_2O_2$ from $O_2^{\bullet-}$ as shown in the following reaction [129]:

$$\mathbf{O_2^{\bullet-} + O_2^{\bullet-} + 2H^+ \xrightarrow{MnSOD} H_2O_2 + O_2}$$

Due to a high intra-mitochondrial concentration (3-10 µM) and reaction rate ($k = 2.3 \times 10^9$ $M^{-1}s^{-1}$) of MnSOD, the steady-state superoxide content in matrix of normally respiring mitochondria is very low [130]. However, in the presence of redox-active transition metals like copper and iron, $H_2O_2$ can form very active and damaging hydroxyl radicals ($^{\bullet}OH$). $^{\bullet}OH$ radicals are highly unstable and reactive for which no scavenging enzyme system exists [131]. These forms of ROS may cause direct damage to membrane lipids, proteins and mitochondrial DNA [132, 133]. Therefore, mitochondrial matrix contains a special system of peroxidases that remove $H_2O_2$ before it can react with active forms of metals. These include peroxiredoxins, glutathione peroxidases and trace amounts of

catalase [134, 135]. The glutathione peroxidase (GPx) reaction is coupled to the glutathione disulfide-reduced glutathione couple (GSSG/GSH) and the rate of $H_2O_2$ removal depends on GSH concentration [136, 137].

$$H_2O_2 + 2\,GSH \xrightarrow{GPx} 2H_2O + GSSG$$

The above mentioned highly efficient antioxidant systems in the mitochondria neutralize ROS under normal conditions. Probably this is why the normal respiring mitochondria generate low levels of $H_2O_2$. However, damaged mitochondria during stress produce high levels of ROS that exceed the capacity of the antioxidant system and can result in cell death [87].

### I. 5. Mitochondria regulate apoptosis and mitophagy

During stress, damage to mitochondria concomitantly activate both mitophagy and mitochondrial apoptosis/permeabilization. The final outcome depends on the balance between these pathways. Exposure to modest stress activates mitophagy wherein damaged mitochondria are sequestered by autophagosomes and degraded before apoptosis or necrosis can be triggered. However, during severe stress conditions apoptosis is the major pathway to minimize tissue damage upon cell death [138].

#### I. 5. 1. Intrinsic apoptotic signalling

Apoptosis is programmed cell death. It results in chromatin condensation, DNA fragmentation, cell shrinkage, and plasma membrane blebbing with release of apoptotic bodies, which are phagocytized by other cells in the organism [139]. There are two principal apoptotic pathways: the extrinsic or the death receptor-mediated pathway, and

the intrinsic or the mitochondrial-mediated pathway. The extrinsic pathway is triggered by tumor necrosis factor-α (TNF-α), TRAIL (TNF-related apoptosis-inducing ligand) and Fas receptors which activate downstream caspase 8 and caspase 10 [140, 141]. The intrinsic pathway involves mitochondria to intensify or augment the pathway by responding to stress signals including loss of growth factors, hypoxia, oxidative stress, and DNA damage [142].

Apoptosis by mitochondria is highly regulated by the BCL-2 family of proteins. Antiapoptotic members of the family BCL-2 and BCL-XL promote survival. The pro-apoptotic BCL-2 family proteins are BH3-only proteins, which include BH3 interacting domain death agonist (BID), BCL2/adenovirus E1B 19-kDa protein-interacting protein 3 (BNIP3), Nip3-like protein X (NIX), BCL2/adenovirus E1B 19-kDa protein-interacting protein 3-like (BNIP3L), p53 upregulated modulator of apoptosis (PUMA), and the effector proteins the BCL2-associated X protein (BAX) and BCL2-antagonistic/killer (BAK). The majority of the pro-apoptotic proteins are cytosolic, with the exception of Bak, which is localized at the OMM [143]. The cytosolic BH3-only proteins neutralize the antiapoptotic BCL-2 proteins thereby causing cell death by activating BAX and BAK [144, 145]. Additonally, following apoptotic stimuli, Bid is cleaved by death receptor-dependent caspase-8, after which it translocates to the mitochondria and interacts directly with BAX and BAK to induce their activation. Upon activation, BAK and BAX undergo conformational changes forming homo-oligomers in the OMM. Homo-oligomerization of BAK and BAX, form pores in the OMM causing mitochondrial outer membrane permeabiliation (MOMP) [146]. Permeabilization of the outer membrane results in the release of pro-apoptotic proteins from the IMS such as cytochrome c,

second mitochondria-derived activator caspase (SMAC)/direct IAP-binding protein with low pI (DIABLO), HtrA2/Omi, apoptosis-inducing factor, and endo-nuclease G into the cytosol, which activates apoptosis [138, 147, 148]. In the cytosol, cytochrome c binds to dATP, Apaf-1 and the initiator caspase 9 which forms an apoptosome activitaing caspase 9 which in turn activates caspase-3, the ‘executioner’ of the apoptotic pathway [149]. Smac/DIABLO and HtrA2/Omi promote caspase activation by neutralizing IAPs (inhibitor of apoptosis proteins) in the cytosol [150, 151], whereas EndoG and AIF initiate a caspase-independent pathway by translocation to the nucleus where they trigger DNA fragmentation and chromatin condensation [152, 153].

In parallel, there exists a crosstalk between BCL-2 proteins and mitochondrial permeability transition pore (MPTP). Opening of MPTP in the inner mitochondrial membrane activates the intrinsic pathway leading to cell death [154]. Reports in the literature suggest that MPTP contains a voltage-dependent anion channel (VDAC, porin) in the OMM, the adenine nucleotide translocase (ANT) in the IMM and cyclophilin-D in the matrix, although the exact structure of MPTP is still unknown [155]. Opening of the MPTP causes rapid influx of solutes and water into the mitochondrial matrix. This collapses the proton gradient thereby disrupting ATP synthesis. MPTP opening induces mitochondrial swelling and cell death through apoptosis or necrosis and has been implicated in ischemia-reperfusion injury, cardiomyopathies, and congestive heart failure [147, 156, 157]. It has been reported that BCL-XL can bind directly to the components of MPTP controlling the pore opening and closing whereas BCL-2 increases the calcium threshold which makes the mitochondria more resistant to

MPTP. Also, BAX promotes MPTP opening through a mechanism which is different from MOMP [158-160].

Apoptosis is an energy-dependent process, thus the presence of ATP is necessary to execute the apoptotic program. Therefore, substantial ATP depletion limits caspase activation and leads to necrosis. Necrosis is characterized by cell swelling, plasma membrane disruption releasing cytosolic components which trigger an inflammatory response [142]. During severe oxidative stress, apoptosis progresses to necrosis as a result of ATP loss which inhibits energy-dependent processes (e.g. functioning of ion pumps) resulting in swelling and rupturing of the cell membrane [161]. Rupture of the plasma membrane can be facilitated by proteolytic degradation of crucial cytoskeletal and membrane proteins, such as calpain-mediated cleavage of ankyrin and fodrin, anchor proteins for $Na^+/K^+$-ATPase [162].

### I. 5. 2. Mitochondria and mitophagy

BCL-2 and BCL-XL regulate autophagy via their interaction with activating molecule in BECLIN1-regulated autophagy (AMBRA1) that activates the BECLIN1-VPS34-VPS15 complex which induces autophagy. Upon induction of autophagy, BCL-2 releases BECLIN1 and AMBRA1. However, it is still unclear what triggers the dissociation of AMBRA1 from BCL-2 [163-166]. Similarly, BNIP3, a pro-apoptotic BH3-only protein is a potent inducer of mitophagy [167]. Another protein which regulates both apoptosis and autophagy is the p53 tumor suppressor protein. Under physiological conditions, the E3 ubiquitin ligase mouse double minute 2 (MDM2) degrades p53 maintaining low levels. In response to oxidative stress, p53 escapes degradation by an unknown mechanism

and its levels increase in the cell. P53 causes cell death by regulating gene expression and by direct action on the mitochondria. In the nucleus, p53 activates expression of autophagic genes like AMP-activated protein kinase, tuberous sclerosis protein 2, and sestrin1/2 [168, 169] along with proapoptotic genes which include Bax [170], Bak [170, 171], Noxa [172], and Puma [173]. It also represses the transcription of antiapoptotic BCL-2, BCL-XL, and MCL-1 [171, 174, 175]. In parallel, p53 translocates to mitochondria where it inhibits BCL-2/BCL-XL and activates BAX and BAK causing MOMP [176-178].

The phosphatase and tensin homolog induced putative kinase 1 (PINK1)/Parkin pathway is another important regulator of mitophagy. In normal healthy mitochondria with an intact membrane, serine/threonine kinase PINK1 is rapidly imported and cleaved by mitochondrial proteases. Upon collapse of the $\Delta\psi_m$, the import and degradation of PINK1 are blocked, and PINK1 accumulates on the outer mitochondrial membrane which signals the cytosolic E3 ubiquitin ligase Parkin [179, 180]. Parkin rapidly translocates to mitochondria where it ubiquitinates mitochondrial proteins like VDAC1, MIRO, mitofusin-1 and mitofusin-2. Ubiquinated proteins signal induction of mitophagy [181-183]. However, the exact mechanism on how accumulation of PINK1 on the OMM activates and recruits Parkin is still unclear [138]. Alternatively, mitochondria can also be cleared via an ubiquitin-independent pathway which involves direct binding of ATG8 family proteins to autophagy receptors on the mitochondria [184, 185].

### I. 5. 3. Interplay between Mitophagy, Mitochondrial Biogenesis and Mitochondrial dynamics

In response to mitophagy, cells compensate energy production without affecting contractility using their reserve pool of mitochondria. However, excessive mitophagy results in depletion of the bioenergetic reserve leading to cell death. Under such conditions, the cell replaces the mitochondria cleared by mitophagy through a tightly coupled process called mitochondrial biogenesis. The transcriptional coactivator peroxisome proliferator-activated receptor-γ coactivator 1α (PGC-1α) is a key regulator of mitochondrial biogenesis [186]. PGC-1α is induced at birth wherein there is a striking increase in mitochondrial biogenesis [186, 187]. In addition, Parkin has been shown to be a central regulator of both mitophagy and mitochondrial biogenesis. Recently, PARIS (ZNF746), a Parkin substrate is shown to repress the expression of PGC-1α by binding to insulin response sequences in the PGC-1α promoter. Activation of Parkin during mitophagy promotes degradation of PARIS and subsequent activation of PGC-1α transcription [188].

Mitochondria are highly dynamic organelles capable of changing both size and shape. The main regulators of this process are the fission and fusion proteins [138]. Fission produces mitochondria that are fragmented and discontinuous whereas fusion produces elongated, tubular, interconnected mitochondrial network [189, 190]. Dysfunction or loss of fusion proteins is lethal as it causes the total loss of mtDNA from the cells. In mammals, the fusion proteins are the dynamin-related GTPases mitofusins (Mfn) and optic atrophy protein 1 (Opa1). Mfn exists in two isoforms, Mfn1 and Mfn2, both localized in the outer mitochondrial membrane (OMM) which interact with their

homologous proteins in the adjacent mitochondria causing OMM fusion. Opa 1 is located in the inner mitochondrial membrane (IMM) and plays a role in IMM fusion and cristae remodeling [190]. On the other hand, mitochondrial fission 1 protein (Fis1) and dynamin-related protein 1 (Drp 1) participate in fission. While Fis1 is transmembrane protein which binds to the OMM, Drp1 is located in the cytosol and translocates to mitochondria and interacts with Fis 1 in the event of mitochondrial fission [189]. The loss of fusion responses predisposes toward cell death and following fission, the mitochondrial fragments are selectively degraded through lysosomal machinery. A fine balance exists between mitophagy and biogenesis that is responsible for mitochondrial quality control [191-193]. However, the mechanisms through which mitochondrial dynamics trigger cell death are not fully understood.

### I. 6. Mitochondria and ischemia-reperfusion injury

Heart attack/ myocardial ischemia is a major cause of morbidity and mortality worldwide. Myocardial ischemia exists when there is an inadequate supply of oxygen and nutrients to the myocardium as a result of blockade of blood flow through coronary arteries. The depletion of oxygen and metabolic substrates decreases the energy available to cardiomyocytes and leads to cardiac injury (infarction) [5]. The extent of the injury is determined by various factors including the duration of ischemia and the severity of ischemia (zero-flow versus low-blood flow). Reperfusion following ischemia to restore cardiac tissue survival also increases cardiac injury over and above that sustained during ischemia and independently contributes to myocardial cell death. This phenomenon is called reperfusion injury [78, 149, 194-197]. However, the cardiac response to ischemia-reperfusion insult can be manipulated to decrease the severity of

tissue injury which has motivated intense studies on the mechanisms of cardioprotection.

### 1. 6. 1. Mitochondrial damage during ischemia

Mitochondria are the cellular powerhouses that generate ATP for cell survival. But during cardiac ischemia, they are both sources and targets of cellular damage. Ischemia disrupts the ETC in mitochondria which leads to a decrease in respiration rate and an increase in production of reactive oxygen species (ROS). Global ischemia in animal models decreases the activity of complex I, complex III, cytochrome c content and respiration through complex IV [5, 198]. Studies in different animal models have shown that the consequences of ischemic damage depend on the duration of ischemia. Brief periods of ischemia for 15 min did not damage the ETC; cardiac contractile function is recovered with no myocyte cell death. This phenomenon is called “stunning” wherein the myocardium is not contracting properly and is viable. The stunned myocardium eventually will recover function if blood flow is restored [199, 200]. Ischemia for shorter time periods (15-20 min) decreases complex I activity [201, 202] while prolonged ischemia (30-45 min) results in damage distal to complex I. Longer periods of iscchemia decreases activity of complex III, leads to loss of cardiolipin and cytochrome c content, and impaired complex IV respiration rate [102, 203, 204].

Ischemia decreases complex I activity due to increased ROS generation as a result of electron leakage from the complex [102, 201, 205-207]. Additionally, complex I undergo ischemia-mediated post-translational modifications including phosphorylation [208] and S-nitrosylation [57] (as discussed earlier in section I.3). However, there are conflicting

reports regarding the ischemia-induced damage to NADH ferricyanide oxidoreductase (NADH dehydrogenase, NFR) which is the proximal component of complex I. While some reports have shown that the decreased NFR activity appears likely due to the loss of the flavin mononucleotide (FMN) component [206, 207], other studies have pointed out that the increased ROS production by complex I due to ischemia without apparent decrease in NFR activity indicates a site of damage distal to NADH dehydrogenase part of complex I [102, 209]. During ischemia, complex I is considered to be both the target and a source of damage. Rotenone treatment immediately before ischemia decreased damage to the distal parts of the ETC [210] by preserving complex IV respiration, cardiolipin and cytochrome c content [210]. Consistent with the retention of cytochrome c, proximal blockade of ETC during ischemia preserved the integrity of inner and outer mitochondrial membrane [209]. In addition, complex I blockade with rotenone before ischemia decreased ROS production and mitochondrial $Ca^{2+}$ loading [85, 211, 212]. Therefore, it has been suggested that the proximal electron transport chain mediates the damage to its distal part during the progression of ischemia [210].

Several studies have shown that myocardial ischemia does not damage complex II [5]. However, studies showed that in vivo regional or global ischemia/reperfusion resulted in loss of protective glutathionylation of key sulfhydryl groups in the complex II which results in decreased complex II enzyme activity [62]. Recent work by Quinlan et al. demonstrated that complex II is an important contributor to physiological and pathological ROS production [213]. This work suggests that the flavoprotein subunit of complex II generates ROS in both the forward reaction with electrons supplied by succinate, and the reverse reaction with electrons supplied from the reduced ubiquinone

pool when complex III is inhibited [213]. Thus, complex II can also be a potential source of damage during ischemia or early reperfusion due to distal blocks in the ETC.

Ischemia decreases complex III activity as a result of the functional inactivation of iron-sulfur [2Fe-2S] protein subunit. Ischemic damage did not affect the remaining eleven subunits of the complex. The electron paramagnetic resonance (EPR) signal from [2Fe-2S] cluster decreases after ischemia without loss of the protein, suggesting that it is the disruption of the cluster which decreases the complex activity [214]. Studies with complex III blocker, myxothiazol decreased superoxide generation during simulated ischemia in cardiomyocytes which highlights the role of complex III as a major site of ROS production during ischemia [212]. As discussed in section I.3, the majority of ROS produced in complex III originates from the $Q_o$ center. However, the $Q_i$ center also releases superoxide when electron transfer into $Q_o$ is blocked. ROS generated from complex III causes oxidative modification and depletion of cardiolipin and subsequent release of cytochrome c from the inner membrane. Therefore, apart from complex III damage, progressive loss of cytochrome c during ischemia sets a distal block in the ETC resulting in impairment of $Q_o$ center which in turn increases ROS generation at the $Q_i$ site [104, 105].

During ischemia, the activity of cytochrome c oxidase is decreased by two different mechanisms. First, ischemia leads to posttranslational modifications of complex IV, mainly phosphorylation of COXI, COXIVi1, and COXVb causes functional inactivation of the complex [215]. Second, studies from different animal models (rabbit, rat, canine) suggest that selective depletion of cardiolipin during ischemia affects the cytochrome c oxidase enzyme activity [216-218]. Cardiolipin is a phospholipid enriched in the inner

mitochondrial membrane and is the only phospholipid whose content decreases during ischemia. Decrease in cardiolipin content corresponds to the decrease in intergrated respiration through complex IV [219]. Potential mechanisms of overall cardiolipin loss during ischemia include hydrolysis by phospholipase $A_2$ or oxidative damage [220, 221]. The mechanism of cardiolipin oxidation may result from the formation of cytochrome c-cardiolipin peroxidase, which can occur in pathologic settings, under conditions of oxidative stress (increased $H_2O_2$) [222]. As mentioned earlier, the ROS generated from $Q_i$ center (in complex III) most likely causes cardiolipin modifications [222], although other sites of superoxide generation should not be excluded from the consideration.

Cardiolipin contains linoleic acid (C18:2) acyl groups with two unsaturated cis double bonds. Oxidative damage to cardiolipin during ischemia generates peroxy-groups that are unstable and decompose rapidly leading to direct depletion of cardiolipin from the inner membrane [223]. Alternatively, the peroxy-acyl groups can form complexes with proteins that cause delocalization of cardiolipin from the membrane [221]. Hence, the peroxidation of cardiolipin, if not counteracted by synthesis of new cardiolipin leads to increase in generation of monolysocardiolipin which activates pro-apoptotic factors leading to cell death [224, 225]. However, the remaining cardiolipin in the inner membrane that did not delocalize showed no signs of modification.

Cytochrome c is localized to the the inner membrane via its interactions with cardiolipin [226]. Depletion of cardiolipin results in redistribution of cytochrome c from the inner membrane into the inter-membrane space [227]. In normal conditions the outer membrane is impermeable to cytochrome c, however during ischemia the integrity of the outer membrane lipid bilayer is disrupted [149]. Results from the different

experiments suggest that during ischemia, loss of BCL-2 triggers oligomerization of the pro-apoptotic BAX and BAK in the outer membrane forming pores. This leads to an increase in the permeability of the outer membrane allowing delocalization of cytochrome c from the inter-membrane space into the cytosol following its detachment from cardiolipin (two-step process) [228]. Consequently, cytochrome c and the accompanying pro-apoptotic proteins including SMAC/DIABLO, HtrA2/Omi, apoptosis-inducing factor and endo-nuclease G activate apoptotic pathways leading to cell death [146, 229].

### 1. 6. 2. Mitochondrial damage during reperfusion

The restoration of blood flow to an organ or to tissue is termed reperfusion. The presence of damaged mitochondria following ischemia persist during reperfusion leading to reduced energy production, increased ROS and activation of cell death programs by cytochrome c release [222]. Pathological ETC function as a consequence of ischemic damage is supported by experimental evidence that blockade of complex I with amobarbital or nitric oxide before ischemia followed by reperfusion improved contractile recovery and decreased infarct size following reperfusion [211, 230-232]. Also, the distal blocks in ETC during ischemia due to damage of complex III and loss of cytochrome c result in excessive ROS generation which causes increased cardiac injury during reperfusion. Interestingly, the net release of ROS from ischemic damage can be abolished by proximal blockade of the ETC with rotenone [210].

Amobarbital (Amytal®) is a short-acting barbiturate that reversibly inhibits complex I at the rotenone-binding site [233, 234]. Amobarbital treatment during ischemia protects the

distal electron transport chain by preserving respiration through complex III and complex IV, improving complex I activity along with retention of cytochrome c within mitochondria, all of which are measured following reperfusion [209, 230]. This demonstrates that though rotenone and amobarbital are chemically distinct compounds, inhibiting the rotenone binding site protected mitochondrial ETC from ischemic damage. Moreover, this inhibition of electron transport during ischemia reduced calcium loading during reperfusion. Diminished calcium loading along with lower ROS levels would result in decreased susceptibility to MPTP opening and smaller cardiac infarction [211, 232]. Therefore, the reduction of electron flow through ETC applied before the ischemic insult exhibits cardioprotection following reperfusion. Hence, ischemic damage to the electron transport chain is considered an important link between ischemia and the progression of cardiac injury during reperfusion [222].

There are conflicting reports on the damage caused to mitochondria during reperfusion. Some studies suggest that ischemic damage to complexes I, III and IV further deteriorates oxidative phosphorylation [201] and complex activities [201, 235] during reperfusion, suggesting that additional mitochondrial injury occurs. Also, early in reperfusion, a detectable burst ROS generation is recorded [194, 236-239]. Damage to the ETC during ischemia increases net release of $H_2O_2$ during reperfusion with glutamate as a substrate [102]. With succinate and rotenone the $H_2O_2$ generated following ischemia from complex III is substantially increased [85, 88, 240]. Hence, ischemic damage to the ETC augments oxidative injury during reperfusion, especially at complex I and III wherein there is an increase in ROS generation due to distal blocks in the ETC which could result in additional damage [201, 235]. In addition, post-ischemic

mitochondria generate reactive and damaging hydroxyl radical (•OH) measured by electron spin resonance (ESR) spin-trapping [194, 241].

Prompt reperfusion or reoxygenation rapidly restores the substrates essential for ATP generation, increases the oxygen supply and normalizes the extracellular pH to restore cellular homeostasis. However, abrupt normalization concurrently causes reperfusion injury [242]. Rapid normalization of the extracellular pH creates an extreme $H^+$ gradient across the plasma membrane that triggers $Na^+/H^+$ exchange leading to high $Na^+$ influx which in turn triggers $Na^+/Ca^{+2}$ exchanger in a "reverse mode," resulting in intracellular $Ca^{+2}$ overload [243]. The increase in intracellular $Ca^{+2}$, enhances mitochondrial calcium overload triggering mitochondrial permeability transition (MPTP) that contributes to additional cardiac injury during reperfusion [244, 245]. The MPTP can be blocked by pharmacological inhibitor, cyclosporine A. Opening of the MPTP can lead to cell death through apoptosis (release of cytochrome c) or necrosis (depletion of ATP) [246, 247]. Morphological and biochemical studies suggest that mitochondria are largely intact following ischemia [204, 216]. However, during reperfusion increased calcium availability enhances mitochondrial calcium loading as result of which mitochondria "swell" and cause cell death [244, 248].

In contrast, experimental studies suggest that ischemic damage to the mitochondria persists during reperfusion without apparent evidence of additional substantial damage to the distal ETC caused by reperfusion. The decreased cardiolipin and cytochrome c contents as well as cytochrome c oxidase respiration persist but do not worsen during reperfusion [203, 223]. However, during ischemia, distal blocks formed as a result of loss of cardiolipin and cytochrome c [216], functional inactivation of Fe-S peptide of

complex III [214] result in decreased respiration through complex IV [204] following reperfusion. Apart from this, ischemia increases ROS generation during reperfusion from complex I even in the absence of complex I damage [78, 92, 219]. From these studies it is clear that enhanced mitochondrial damage, increased ROS along with calcium loading predispose MPTP pore opening during early reperfusion which translates the ischemic mitochondrial damage into reperfusion injury [222]. Amobarbital treatment before ischemia along with postconditioning during early reperfusion improved calcium tolerance and inner membrane potential recorded following reperfusion [249]. In another study, postconditioning (brief periods of ischemia) during early minutes of reperfusion, inhibited MPTP opening by reducing oxidative stress at the cellular level without any effect on oxidative phosphorylation or membrane polarization [250]. These results suggest that reperfusion injury can be minimized if the mitochondrial damage during ischemia is prevented.

Current therapeutic interventions to pre-condition, post-condition, or pharmacological treatment to activate signaling pathways of protection in the heart are ineffective during certain conditions including aging and diabetes due to defects in the signaling cascades [251-253]. Hence direct therapeutic targeting of dysfunctional mitochondria will provide the potential to bypass the upstream signaling defects and intervene directly with the effector organelle. Novel mitochondrial-targeted therapy relies on understanding the sites in the ETC that are damaged by ischemia and produce cell-injury during reperfusion. The main objective of the current study is to delineate sites of ETC that are responsible for ischemic damage. This will allow us to identify a key mechanism of

ischemic damage after which the mitochondria are in a “locked in” defective condition and lead to additional cell death during reperfusion.

# CHAPTER II: Electron flow into cytochrome c and reactive oxygen species from the electron transport chain convert cytochrome c to a peroxidase during ischemia-reperfusion

## II. 1. Introduction

Mitochondria are the cellular powerhouses that generate ATP for cell survival. But during a pathological condition like cardiac ischemia, they are both sources and targets of cellular damage [5]. The sequence of events leading to myocardial ischemic damage involves increased generation of reactive oxygen species (ROS) [102], mitochondrial membrane permeabilization [154], depletion of cytochrome c and activation of apoptotic pathways [149]. Blockade of electron transport chain during ischemia decreases myocardial damage. This supports the concept that ETC itself plays a major role in ischemic damage [209].

### II. 1. 1. Localization of the segment of mitochondrial ETC responsible for ischemic damage

Given the importance of ETC as a source of damage during ischemia, blocking it with inhibitors to manipulate electron flow through the respiratory complexes allows one to isolate the segment responsible for ischemic damage [254]. Experiments using *an in-situ* global ischemic model with rotenone, an irreversible inhibitor of complex I, markedly attenuated the ischemic damage to cardiolipin, cytochrome c and respiration through complex IV. This observation provides evidence that proximal blockade of ETC during ischemia protects distal respiration [210]. Similar to rotenone, a chemically distinct compound, amobarbital competes for binding at the “rotenone-site” of complex I [233]. Amobarbital treatment immediately before ischemia decreases the net release of $H_2O_2$ due to the preservation of oxidative phosphorylation and cytochrome c content [230]. Thus, the site within ETC that causes damage is located distal to complex I.

To localize the site of ischemic damage distal to complex I, antimycin A, an irreversible inhibitor, is used to block the electron transport distal to complex III. Antimycin A, inhibits the $Q_i$ center of complex III thereby causing a net increase in ROS production from the semiquinone bound $Q_o$ site [109]. The ROS generated from the $Q_o$ site in complex III is released into the intermembrane space [78, 108]. Antimycin A, given immediately before ischemia, preserves complex IV respiration, cardiolipin and cytochrome c content. This evidence suggests that the site of ETC responsible for ischemic damage is located distal to quinol oxidation site of complex III [255].

Lastly, the contribution of complex IV in mediating ischemic damage was studied. Isolated perfused rabbit hearts which underwent global ischemia for 30 min were used.

Azide was given immediately before ischemia which blocked the ETC at complex IV. Interestingly, treatment with azide did not protect the ischemia-mediated decrease in respiration. Also, a decrease in cytochrome c content was observed similar to that of untreated ischemic hearts [254]. This evidence strongly supports that the segment located between the quinol oxidation site of complex III and complex IV is responsible for the ischemic damage to the ETC [254]. One of the key components of this site is the cytochrome c and cardiolipin complex located between complex III and complex IV which can potentially play an important role in ischemia mediated cardiac injury and is the focus of my research **(Figure 2.1)** [222].

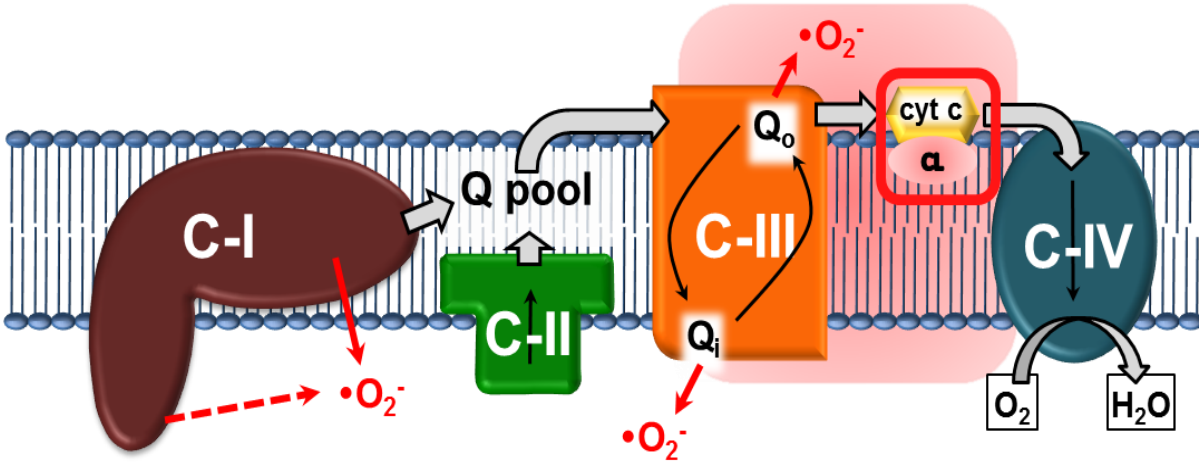


**Figure 2.1. Schematic representation of the mitochondrial electron transport chain localizing the ischemic defect.** The segment located between the quinol oxidation site of complex III and complex IV is responsible for the ischemic damage to the ETC. Key components of this site are the cytochrome c and cardiolipin complex. Q, ubiquinone; cyt c, cytochrome c; CL-cardiolipin. Adapted from [37].

### II. 1. 2. Cytochrome c-cardiolipin interactions

Cytochrome c is a small heme protein that transfers electrons between respiratory complexes III and IV located in the inner membrane of mitochondria. Cytochrome c is a positively charged protein with an iso-electric point of approximately pH 10, with approximately 30% of the protein surface having binding sites for anionic lipids [256-259]. Complex interactions of cardiolipin with cytochrome c are responsible for localizing the later at the inner membrane. Various forces including electrostatic, hydrogen bonding and hydrophobic interactions are responsible for the formation of cytochrome c/cardiolipin complex. Under physiological conditions, electrostatic forces existing between negatively charged phosphate groups of the cardiolipin and positively charged lysine residues of cytochrome c are predominant [259]. Experimental studies have shown that anionic phospholipids have contact sites on cytochrome c at residues $Lys_{72}$ and $Lys_{73}$ [256, 257]. Also, studies from interactions of the spin-labeled protein with spin-labeled phospholipids have shown that $Lys_{72}$, $Lys_{86}$, and $Lys_{87}$ residues of cytochrome c are involved in cytochrome c-cardiolipin binding [226]. Recent studies have shown that additional electrostatic binding sites on cytochrome c which interact with membrane include $Lys_{22}$, $Lys_{25}$, $His_{26}$, $Lys_{27}$, and $His_{33}$ [258]. Other than electrostatic interactions, hydrogen bonding between protonated acidic phospholipids and $Asn_{52}$ stabilizes the protein binding with lipids [256, 257]. FRET studies depicted that the interactions between cytochrome and lipids are classified into two modes: an electrostatic low-affinity binding to deprotonated cardiolipin molecules and a high-affinity binding to partially protonated cardiolipin stabilized by electrostatic and hydrogen bonding. However, the type of interaction depends on pH, ionic strength, and the mole

fraction of cardiolipin [260]. Another type of interaction in the cytochrome- cardiolipin complex that are a result of nonpolar acyl residues of the lipid molecules and nonpolar regions of cytochrome c (normally buried inside the protein) are the hydrophobic interactions [259, 261, 262]. Thus, a single cardiolipin molecule interacts with cytochrome c by electrostatic interaction of a negatively charged phosphate groups with $Lys_{72}$ as well as hydrophobic interaction by acyl chain insertion either in the channel surrounded by $Asn_{52}$, $Lys_{72}$, and $Lys_{73}$ or between the nonpolar polypeptide strands 67-71 and 82-85 [260, 263]. Experimental evidence from nuclear magnetic resonance studies suggests that the high affinity interactions between cytochrome c and cardiolipin are also a result of partial unfolding and partial insertion of the protein into the membrane [261, 264]. However, to a large extent, the interactions by insertion depend on pH, ionic strength, lipid composition and lipid/protein ratio. Hence, a decrease in cardiolipin content or alterations in the linoleate-fatty acyl chain saturation would diminish the affinity of cytochrome c to cardiolipin [264].

### II. 1. 3. Structural rearrangements and peroxidase activity of cytochrome c

Interactions of cytochrome c with negatively charged lipids in the membrane can disrupt the native structure of cytochrome c resulting in an intermediate conformation, between the native and the fully unfolded state, called a “molten globule” [265-268]. Exceptionally, solubilized cytochrome c is a heme-containing protein that reacts very slowly with $H_2O_2$ (0.2 $M^{-1}s^{-1}$ at pH 7.0) [269] since the heme iron is occupied by ligands in all the six coordination positions [270]. The heme iron in cytochrome c has two axial bonds, one with $His_{18}$ and the other with $Met_{80}$ **(Figure 2.2)**. In normal conditions, it is the $Met_{80}$ bond with heme that blocks the interaction of iron with NO, $O_2$, CO and $H_2O_2$

[271]. However, conditions including pH and temperature affect the heme binding to $Met_{80}$ ligand in cytochrome c. Several *in-vitro* studies that include oxidation by HOCl [272], nitration of $Tyr_{67}$ by $ONOO^-$ [273] or carboxy-methylation of $Met_{80}$ [274] were shown to disrupt the Fe-$Met_{80}$ bond which facilitates the reactivity of iron thereby inducing the peroxidase activity. This change in reactivity of iron is a two-step process initiated with disruption of Fe-S($Met_{80}$) bond further resulting in rearrangements of the protein's tertiary structure [275]. The changes in the heme environment are detected by looking at the CD spectra shifts in the 375-425 nm region (heme moiety), changes in the UV region (250-280 nm) as well as the quenching of the $Trp_{59}$ fluorescence due to the closely located heme group. In addition, the disruption of the Fe-$Met_{80}$ bond can be detected by measuring its characteristic absorbance at 695 nm [264, 271]. In short, structural changes along with loss of axial ligand ($Met_{80}$) alter the redox catalytic reactivity of cytochrome c by enhancing its peroxidase activity in the presence of negatively charged phospholipid membranes [264, 271].

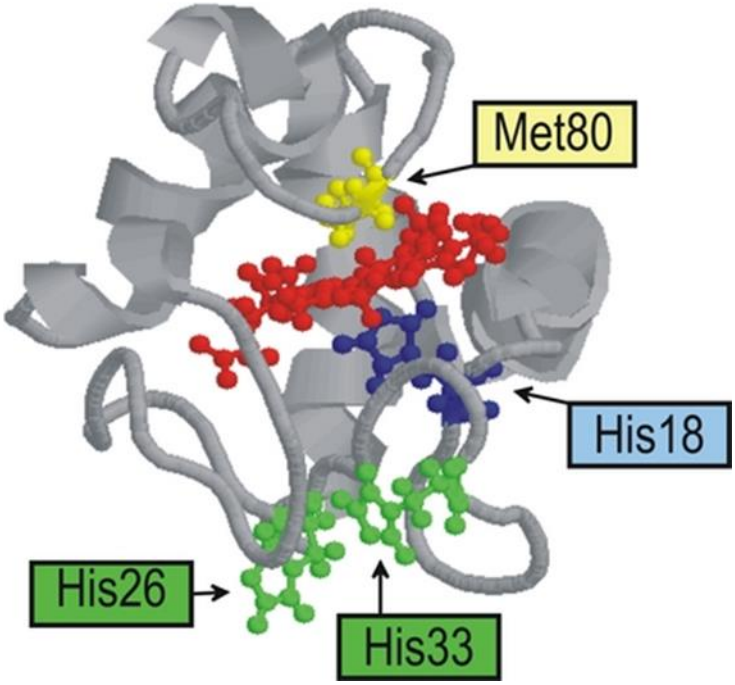


**Figure 2.2. Structure of the cytochrome c with native axial ligands.** Cytochrome c has two axial bonds, one with $His_{18}$ and the other with $Met_{80}$. Met, methionine; His, histidine [264].

The peroxidase function of cytochrome c requires direct physical interaction with cardiolipin. In general, >80% of the cardiolipin is localized to the inner mitochondrial membrane (IMM) wherein it is distributed at a ratio of 60:40 between the inner and the outer leaflets [276-280]. In addition to binding cytochrome c in the outer leaflet of the IMM, cardiolipin binds to other mitochondrial ETC proteins such as mitochondrial respiratory complexes I, III, and IV [281, 282]. However during apoptosis, cardiolipin content in the inner membrane decreases to 60% whereas its content in the outer mitochondrial membrane increases to 40%. In apoptotic cells, the decrease in the inner membrane cardiolipin levels is accompanied by changes in the intermembrane distribution of CL wherein approximately only 30-40% of the cardiolipin is confined to its inner leaflet [283, 284]. The mechanisms that are responsible for mitochondrial inter- and intramembrane cardiolipin translocation are not well understood. The transmigration of cardiolipin during apoptosis involves two proteins: tBid and phospholipid scramblase-3 (PLS-3) [284, 285]. Although, tBid is localized to the outer mitochondrial membrane, it inserts into the inner and outer membrane through its cardiolipin-binding domain at the contact and noncontact sites [286, 287]. t-Bid treated mitochondria undergo significant changes in the intra- and intermembrane distribution of cardiolipin [279, 284]. PLS-3 is another mitochondrial protein that plays a role in bidirectional translocation of cardiolipin during apoptosis and is activated by calcium [285, 288]. During apoptosis, PLS-3 undergoes posttranslational modification, phosphorylation of a specific Thr21 residue by protein kinase Cδ [289] leading to cardiolipin translocation through an unknown mechanism. Thus, during apoptosis, phosphorylation and activation of PLS-3 and tBid-

dependent pathway causes transmembrane redistribution of cardiolipin which is a critical step for the mitochondria to initiate the apoptotic program [264].

### II. 1. 4. Peroxidation of cardiolipin by cytochrome c

The peroxidase activity of cytochrome c utilizes cardiolipin as the substrate and is mainly associated with participation in the execution of apoptosis [264]. The cytochrome c-catalyzed peroxidation has substrate specificity and the preferred oxidation substrates are polyunsaturated anionic phospholipids, particularly cardiolipin, phosphatidylserine, and phosphatidyl-inositol's. Another study showed that saturated and monounsaturated cardiolipin molecules do not undergo peroxidation [224, 290-292]. Apoptosis induced by γ-irradiation, exposure to staurosporine or actinomycin D in cultured cells, showed accumulation of cardiolipin hydroperoxides [292-296]. Coinciding with this observation, exposure of mice to total body irradiation, formed cardiolipin hydroperoxy derivatives comprising $(C18:2)_3/(C18:2\text{-}OOH)_1$, $(C18:2)_2/(C18:2\text{-}OOH)_2$, $(C18:2)_1/(C18:2\text{-}OOH)_3$, $(C18:2\text{-}OOH)_4$ which are detected via mass spectrometry [292]. Interestingly, other abundant phospholipids with polyunsaturated acyl chains phosphatidylcholines, phosphatidylethanolamine, and phosphatidylinositol are not oxidized [292]. This emphasizes the role of cytochrome c/cardiolipin peroxidase in determining the substrate specificity for cardiolipin oxidation [264].

Lipid peroxides are highly unstable and they decompose rapidly leading to direct depletion of cardiolipin from the inner membrane [223]. Alternatively, the peroxy-acyl groups can form complexes with proteins that cause depletion of cardiolipin from the membrane [221]. Depletion of cardiolipin results in translocation of cytochrome c from

the inner membrane into the inter-membrane space [227]. In normal conditions the outer membrane is impermeable to cytochrome c, however during pathological situations; the integrity of the outer membrane lipid bilayer is disrupted by the activation of cytosolic/mitochondrial phospholipases or insertion of pro-apoptotic proteins into the outer membrane [149, 220, 297]. This leads to an increase in the permeability of the outer membrane allowing release of cytochrome c and pro-apoptotic proteins (like Aif, SMAC/DIALBO) from the inter-membrane space into the cytosol **(Figure 2.3)**. In the cytosol, cytochrome c binds to Apaf-I protein which activates caspase-9. Activated caspase-9 in turn activates caspase-3 which is the “executioner” of the apoptotic pathway [298]. Hence, the oxidation of cardiolipin, if not counteracted by synthesis of new cardiolipin activates apoptosis leading to cell death. The remaining cardiolipin in the inner membrane that did not delocalize showed no signs of modification [224, 225].

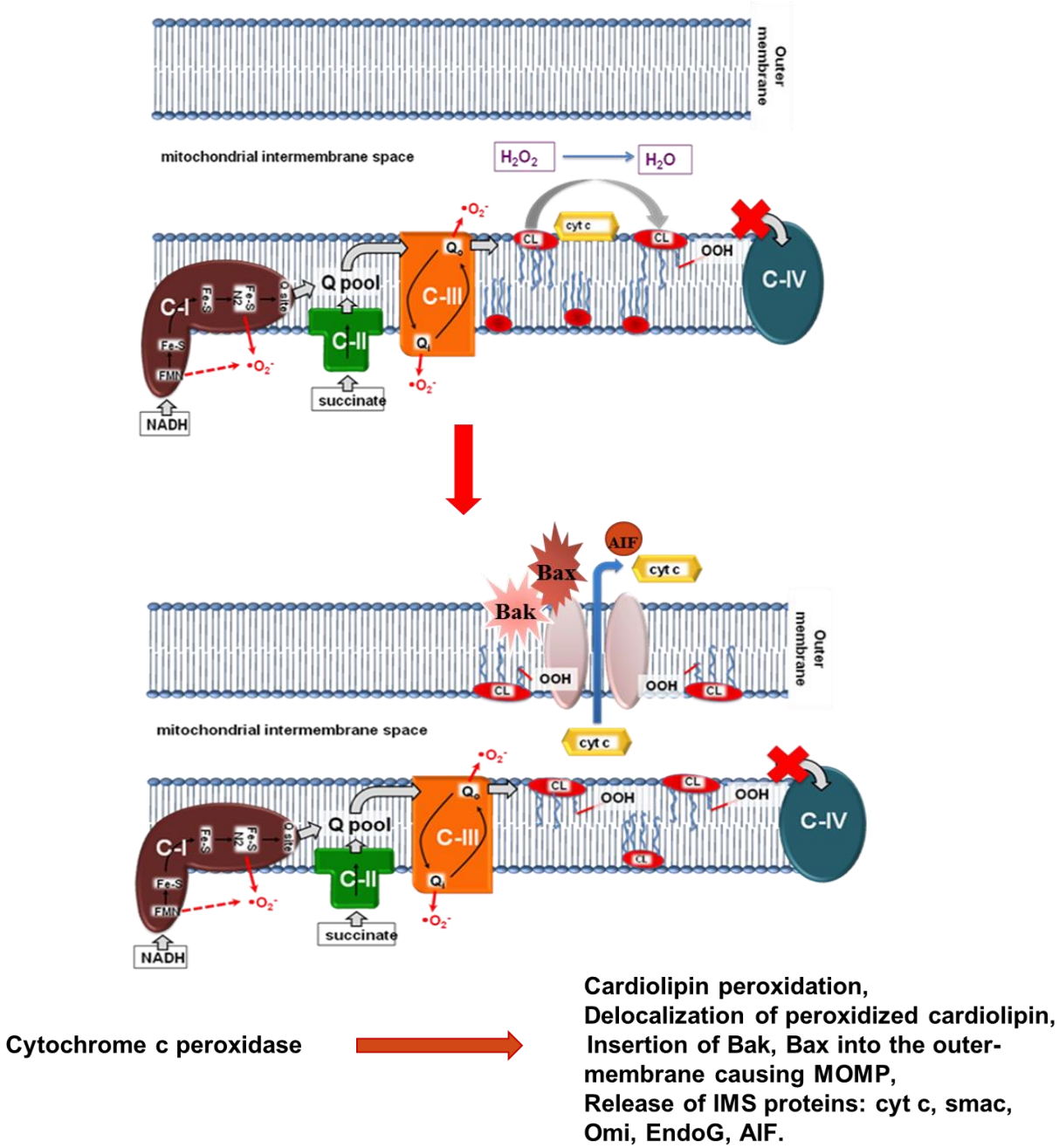


**Figure 2.3. Cartoon depicting consequences of cytochrome c peroxidase.** Cyt c; cytochrome c; CL, cardiolipin, AIF, apoptosis inducing factor

In a study by Kagan et al., actinomycin D induced apoptosis in different cell models, have shown that cytochrome c bound to cardiolipin acts as a peroxidase that selectively oxidizes cardiolipin. Peroxidation of cardiolipin increases outer mitochondrial membrane permeability, releasing of cytochrome c into the cytosol and thereby initiating the apoptotic program by activating caspase 3/7 [276]. Also, in-vitro direct measurements of peroxidase activity during induced oxidative stress in the liposomes are measured using chemiluminescence and fluorescence based assays with luminol and Amplex Red respectively. In addition, electron spin resonance spectroscopy of the EPE phenoxyl radical also confirmed the formation of cytochrome c peroxidase [276]. In addition, work by Vlasova et al. demonstrated that nitric oxide nitrosylates the heme of cytochrome c and blocks the cytochrome c peroxidase activity thereby preventing oxidation of cardiolipin [299].

Under physiological conditions, complex III reduces cytochrome c while complex IV oxidizes it [6, 67]. Cytochrome c accepts electrons from complex III at a redox potential of +250 mV (vs SHE) while it donates electrons to the CuA site in complex IV at a redox potential of +285 mV (vs SHE) [300]. Any significant change of the redox potential of cytochrome c disrupts the electron transfer between the complexes [300, 301]. However, under $H_2O_2$-induced oxidative stress in cardiolipin liposomes, the redox potential of cytochrome c shifts negatively by 350-400 mV. This shift in redox potential, switches off the cytochrome c function as an electron transporter. This alteration inhibits the reduction of complex III by cytochrome c [301]. The peroxidase activity of cytochrome is functionally well characterized in *in-vitro* and in non-physiological cell death models [276, 301]. Although, its physiological relevance during diseased

conditions is still unknown. To understand the mechanistic importance of cytochrome c peroxidase formation and its ability to trigger apoptosis would be a great interest with respect to disease models.

Hence, we intend to study the role of cardiolipin-cytochrome c peroxidase in ischemia, which is unknown and is the focus of my research. During ischemia, we hypothesize that excessive generation of ROS may oxidize the methionine residue ($Met_{81}$) switching on its peroxidase activity ultimately oxidizing the linoleic fatty acyl chains of cardiolipin. This hypothesis is supported by experimental evidence (mass spectrometric data) which showed an increase in the amount of the monolysocardiolipin (degradation product of cardiolipin) in the samples generated following 30 min of ischemia when compared to the control non-ischemic hearts [302].

## RESEARCH AIMS

Mitochondrial electron transport chain (ETC) contributes to its own damage during ISC. Blocking ETC with inhibitors that disrupt electron flow through the respiratory complexes have shown that the locus of ischemic damage is between complexes III and IV. One key component of this site is the cytochrome c which interacts with cardiolipin. Cardiolipin is an oxidatively sensitive phospholipid that is unique to mitochondria and is modified during ischemia-reperfusion (ISC-REP) in the heart. Studies in non-physiological cell stress models have shown that cytochrome c in its peroxidase mode catalyzes oxidation of cardiolipin during oxidative stress. However, the role of cytochrome c peroxidase in ischemia is not yet known and is the focus of my research. This project proposes to identify cytochrome c peroxidase as a key contributor to mitochondrial driven ischemic injury which oxidizes cardiolipin resulting in cardiac injury.

As depicted in **Figure 2.4**, we hypothesize that during ISC, oxidants from complex I and complex III modify cytochrome c and it creates an alternate route for electron transport. Oxidation of the cytochrome c at the methionine-81 residue serves as the marker for the peroxidase formation. As mentioned earlier, there is an increase in ROS production during ischemia which is converted to $H_2O_2$. $H_2O_2$ acts as a substrate for cytochrome c peroxidase or modified cytochrome c which causes the oxidation of cardiolipin to the peroxidized form. Modification and depletion of cardiolipin disrupts normal physiology, impairs electron transport, disrupts membrane integrity and augments cell death via the release of cytochrome c from mitochondria. Identification of this innovative pathobiology

during ISC-REP recognizes a novel therapeutic target, cytochrome c peroxidase, which can be a focal point for new therapeutic interventions to decrease cardiac injury.

## Specific aims:

1. Identify the oxidation of cytochrome c at the methionine-81 residue, a marker for cytochrome c peroxidase, during ischemia-reperfusion.
2. Determine the contribution of ROS and electron flow through cytochrome c in oxidizing cytochrome c at the methionine residue.

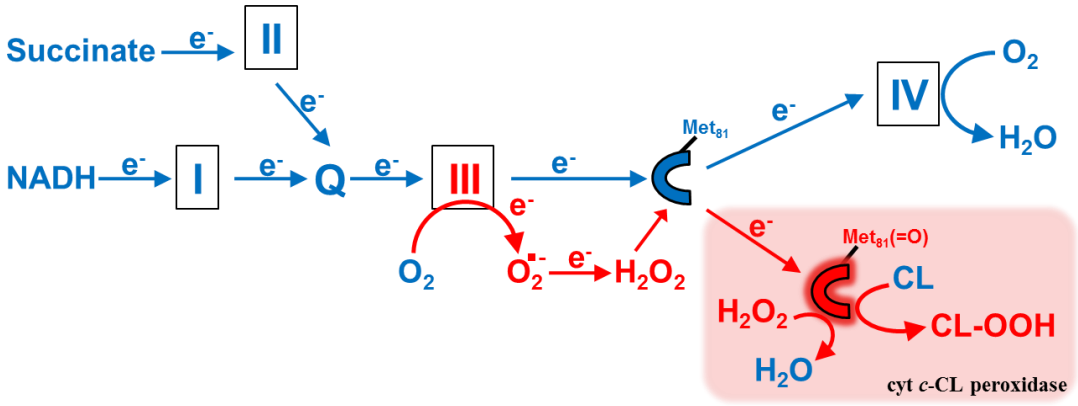


**Figure 2.4. Schematic of alternate route for electron transport by cyt c-CL peroxidase during ISC-REP.** ISC, ischemia; REP, reperfusion; Met, methionine; cyt c, cytochrome c; CL, cardiolipin; CL-OOH, peroxidized cardiolipin.

## II. 2. Materials and Methods

### II. 2. 1. Materials

All chemicals and reagents were purchased from Fisher Scientific, Pittsburgh, PA, or stated otherwise, except the ones used in mitochondria isolation and mitochondria-related functional assays, which were purchased from Sigma-Aldrich, Saint Louis, MO.

**Animals**

Animals were housed in the fully AAALAC-accredited Animal Research Facility at the Virginia Commonwealth University. Experimental animals were purchased through, and maintained by the Animal Research Facility (ARF) of Virginia Commonwealth University. C57BL6 mice were obtained from the Jackson Laboratory (Bar Harbor, ME). Mice were given heparin (1000 U/kg; i.p.) followed by deep anesthesia with pentobarbital (90 mg/kg; i.p.). Only mice which were 8-10 weeks old were used for the experiments. All animal experiments were conducted under the guidelines on humane use and care of laboratory animals for biomedical research published by the National Institutes of Health (revised 2011).

### II. 2. 2. Methods

#### II. 2. 2. 1. Preparation of mouse heart for perfusion

Male C57BL/6 mice (24.6 ± 0.9 g) were anesthetized with pentobarbital sodium (0.1 mg/g i.p.) and anti-coagulated with heparin (1000 U/g i.p.). Hearts were excised and immediately immersed in a petri dish containing ice-cold (4°C) modified Krebs-Henseleit

buffer solution (composition, in mM: 115 NaCl, 4.0 KCl, 2.0 $CaCl_2$, 25 $NaHCO_3$, 1.1 $MgSO_4 \cdot H_2O$, 0.9 $KH_2PO_4$, and 5.5 glucose; pH 7.4) oxygenated with 95% $O_2$/5% $CO_2$. Any attached connective tissue was carefully removed using fine surgical scissors. The heart was transferred to the perfusion apparatus and the aorta was carefully slipped onto the grooved tip of the perfusion cannula and secured in place with a ligature. Hearts were retrograde perfused via the aorta in the Langendorff mode with modified Krebs-Henseleit buffer. The temperature of the perfusate and the heart were rnaintained at 37 °C using a water jacket wamed by a water bath. Cardiac function was monitored with a balloon inserted into the left ventricle, and data were recorded digitally using the Powerlab recording system (AD Instruments, Colorado Springs, CO). Hearts mounted on the Langendorff system were stabilized for 15 min by buffer perfusion after which coronary flow, heart rate and perfusion pressure was recorded. After stabilization, experimental hearts were either subjected to 45 min control perfusion (TC), or 25 min global ischemia (ISC) by stopping the coronary flow at 37 $^oC$ followed by 30 min reperfusion. Hearts were paced at 420 beats per min during the 15-min equilibration period and after 10 min of reperfusion. Throughout the reperfusion period, continuous timed samples of the coronary effluent were collected and kept on ice.

**II. 2. 2. 2. Isolation of mitochondria, cytosol, and heart tissue homogenates**

Adult male mice (body weight ~30 gram) were anesthetized by an intraperitoneal (i.p.) injection of pentobarbital (90 mg/kg), followed by rapid removal of the heart for the experiment. The heart was washed and placed in pre-chilled modified Chappell-Perry 1 (CP1) buffer (pH 7.4) with the following composition: 100 mM KCl, 50 mM 3-(N-morpholino) propanesulfonic acid (MOPS), 1 mM ethylene glycol-bis(2-

aminoethylether)-N,N,N′,N′-tetraacetic acid (EGTA), 5 mM $MgSO_4 \cdot 7H_2O$, and 1 mM adenosine 5′-triphosphate disodium (ATP).

A single, combined population of total cardiac mitochondria was isolated using the procedure described below. The entire mitochondrial isolation process was performed on ice with chilled buffers and equipment. Hearts were excised and only ventricles were used. Heart tissue was washed in the modified CP1 buffer. Further, the heart tissue was dried with Whatman filter paper, weighed, and then thoroughly minced in a glass beaker. The minced heart tissue was transferred to a glass tube for homogenization. Next, the cardiac tissue was homogenized in 3 ml of CP1 buffer using a polytron tissue blender (Kinematica, Bohemia, NY) for 2.5 s at a rheostat setting of 10,000 rpm. 50 µl of the homogenate was saved as the heart tissue extract. The polytron homogenate was centrifuged at 6,000 x g for 10 min at 4$^{o}$C and supernatant was saved as a crude cytosol for further purification. The homogenate pellet was re-suspended in 3 ml of CP1 buffer and incubated with 5 mg/g (wet weight) trypsin (#T0303, Sigma-Aldrich, Saint Louis, MO) for 15 min at 4$^{o}$C. Next, 3 ml of CP2 buffer [CP1 buffer containing 0.2% bovine serum albumin (BSA) (#A7030, Sigma-Aldrich, Saint Louis, MO)] was added to decrease the trypsin digestion. Digested tissue was then homogenized (two strokes) with a tight Teflon pestle/glass tube homogenizer set at steady stirring speed of 600 rpm. From the remaining homogenate, the undigested tissue and heavier cell fractions were separated by centrifugation at low speed 500 x g for 10 min at 4$^{o}$C. The supernatant that contains the mitochondria was then transferred to a new tube and centrifuged at 3000 x g for 10 min at 4$^{o}$C. The pellet containing the mitochondria was washed with 2 ml of KME buffer [100 mM KCl, 50 mM MOPS, and 0.5 mM EGTA] and

centrifuged at 3000 x g for 10 min. Lastly, the mitochondrial pellet was re-suspended in 80-100 µl of KME and the protein concentration was measured by Lowry method using BSA as a standard and sodium deoxycholate (Sigma-Aldrich, Saint Louis, MO) as a detergent to solubilize the mitochondria.

Crude cytosolic fraction was supplemented with protease and phosphatase inhibitor cocktails (Roche, Indianapolis, IN) and was further purified to separate any low-weight cell fraction by ultra-centrifugation at 100,000 x g for 30 min at 4$^{o}$C. Also, heart tissue homogenate was supplemented with protease and phospatase inhibitor cocktails and further lysed in a whole cell extraction buffer (WCE buffer: 20 mM Hepes pH 7.0, 300 mM NaCl, 10 mM KCl, 1 mM $MgCl_2$, 20% glycerol, 1% Triton X-100) for 30 min at 4$^{o}$C. Cell debris was then removed from the lysates by centrifugation at 20,000 x g for 15 min at 4$^{o}$C. The protein concentrations of the cytosols and whole cell extracts were determined using Bio-Rad protein assay (Bio-Rad, Hercules, CA) based on Bradford dye-binding method.

### II. 2. 2. 3. Measurement of oxidative phosphorylation in intact mitochondria

Polarographic measurement of oxygen consumption by intact mitochondria was performed in a glass chamber equipped with a Clark-type oxygen electrode (Strathkelvin Instruments, Glasgow, Scotland) as described below. The measurements were performed at 30$^{o}$C in 500 µl of a respiration buffer (80 mM KCl, 50 mM MOPS, 1 mM EGTA, 5 mM $KH_2PO_4$ and 1 mg/ml defatted BSA, at pH 7.4). For glutamate/malate-dependent respiration (complex I) and succinate-dependent respiration (complex II), 150 µg of mitochondrial protein was used, and for TMPD (N,N,N′,N′-tetramethyl-p-

phenylenediamine)/ascorbate (complex IV), 50 µg of protein was used. Next, the selected substrates for complex I (20 mM glutamate+5 mM malate), complex II (20 mM succinate with 7.5 µM rotenone), or complex IV (1 mM TMPD/20 mM L- ascorbate with 7.5 µM rotenone) of the respiratory chain were added to the chamber. State 3 respiration was measured by the addition of 0.2 mM ADP (final concentration) followed by state 4 respiration. After state 4 was attained, 2 mM ADP (final concentration) was added to the chambers to measure the maximum rate of state 3 respiration. Finally, 0.04 mM uncoupler DNP (2, 4-dinitrophenol) was used to measure the uncoupled respiration rate. In case of TMPD/ascorbate, only maximum rate of state 3 (2 mM ADP) was measured. At the end of that measurement, 2 mM azide was added to determine the specificity of complex IV-dependent oxygen consumption.

ADP-stimulated (state 3) and ADP-limited (state 4) respiration rates were defined and calculated according to the method of Chance and Williams [303, 304]. Respiratory control ratios (RCR) were calculated as a ratio of stimulated state 3 to state 4 respiration according to Estabrook [305].

**II. 2. 2. 4. In-vitro modulation of electron transport chain**

Isolated mitochondria were incubated with succinate and rotenone in the presence of azide (to establish a distal block at complex IV) and compared with incubations from succinate and rotenone with or without antimycin A (A.A) or thenoyltrifluoroacetone (TTFA). 1 mg of isolated mitochondria was incubated with 20 mM succinate + 7.5 µM rotenone with or without 10 mM TTFA or 10 mM antimycin A or 2 mM azide. Incubation studies of mitochondria were carried out in MSM buffer for 50 min at 37$^{o}$C with gentle

rotation. Then, the mitochondrial protein was spun down at 3000 g for 15 min and the pellet was re-suspended in immunoprecipitation buffer (Invitrogen).

Following incubations, cytochrome c was isolated from mitochondria using Dynabeads® Protein G immunoprecipitation kit (Invitrogen) with cytochrome c primary antibody (BD Biosciences). Immunocaptured cytochrome c was separated using SDS/PAGE electrophoresis system, transferred to the PVDF membrane and blotted for Met(O) [Cayman Chemical] and cytochrome c [BD Biosciences] (control for equal mitochondrial protein loading) as explained later in Materials and Methods II. 2. 2. 6.

### II. 2. 2. 5. Immunoprecipitation of cytochrome c

Cytochrome c was immunoprecipitated from isolated mitochondria using Dynabeads® Protein G immunoprecipitation (IP) kit (Invitrogen). Initially, Dynabeads® were completely resuspended by pipetting or by rotating on a roller for 5 minutes. Later, 50 µl (1.5 mg) of Dynabeads® were transferred to an eppendorf tube. Next, the supernatant was removed after immobilizing the beads on the magnet. To the Dynabeads®, 8 µg anti-mouse cytochrome c antibody (BD Biosciences), diluted in antibody binding and washing buffer [PBS buffer (Invitrogen)+0.02% Tween-20], was added and incubated with antibody at RT for 120 min. by rotation. After incubation with the antibody, the supernatant was removed after immobilizing beads with a magnet. The beads were washed 2X with washing buffer. After removing the the final wash, 0.5 mg mitochondrial protein suspended in IP buffer (Invitrogen) (20 µl saved as “Before IP”) was added to the Dynabeads®-antibody complex and was incubated with rotation for 120 min. at RT which allowed the antigen (Ag) to bind to the Dynabeads®-antibody complex. In the

next step, the supernatant was recovered by immobilizing beads on the magnet and transferred to a clean tube for further analysis ("After IP"). Following, the Dynabeads®-Ab-Ag complex was then washed three times using washing buffer [PBS buffer, pH 7.4, Invitrogen; catalog # 10010-023]. In order to avoid co-elution of the proteins bound to the eppendorf tube wall along with the protein of interest, the Dynabeads®-Ab-Ag complex was resuspended in washing buffer and transferred to a clean tube. Again, the supernatant was removed and the elution buffer [50 mM glycine, pH 2.8] was added to resuspend the Dynabeads®-Ab-Ag complex and incubated with rotation for 5 min. at RT which dissociated the Ab-Ag complex. Finally, the supernatant containing eluted antibody and antigen was transferred to a clean tube. For the eluted protein to be used for Western Blotting, the pH of the eluate was adjusted by adding 1 µl of 2.8 M Tris pH 8.5 for 45 µl of eluate.

### II. 2. 2. 6. Western blot analysis

Samples containing an equal amount of protein samples were mixed with Lammelli sample buffer (Invitrogen, Carlsbad, CA) containing DTT (dithiotreitol) (Invitrogen, Carlsbad, CA) and incubated at 95$^{o}$C for 5 min. Immediately after, samples were loaded on the gel. Proteins were separated using SDS/PAGE electrophoresis system consisting of 4-20% gradient Tris-glycine pre-cast gels (Invitrogen, Carlsbad, CA). After separation, gels were transferred to Immobilon-P PVDF (polyvinyldifluoridine) membrane (Millipore) using transfer buffer with 10% methanol and a semi-dry transfer apparatus (Bio-Rad). The blots were then incubated for 1 h at RT with 5% (w/v) non fat dry milk (Bio-Rad) in TBS-Tween20 buffer (10 mM Tris, pH 7.5, 150 mM NaCl, and 0.1% Tween20). Next, the membranes were incubated overnight at 4$^{o}$C with the primary

antibody prepared in 5% BSA or 1% (w/v) non-fat dried milk in TBS-Tween buffer. Next day, the blots were washed three times, 15 min each, with TBS-Tween buffer and were incubated with a 1:50,000 dilution of anti-mouse or anti-rabbit IgG $F(ab)_2$ fragments conjugated with Horse Radish Peroxidase (HRP) in 5% BSA/TBS-Tween buffer for 1 hr. Lastly, blots were washed three times, 15 min each, with TBS-Tween. The immunoreactive proteins were visualized using Amersham ECL Plus western blotting detection reagents (GE Healthcare Lifesciences, Piscataway, NJ) or SuperSignal Femto maximum sensitivity substrate kit (Pierce). Protein bands on western blot were quantified by densitometric analysis by the using ImageJ software (NIH, Bethesda).

### II. 2. 2. 7. In solution enzymatic digestion of proteins

In-solution digestion of immunoprecipitated cytochrome c or commercial cytochrome c (Sigma) was done using the trypsin or chymotrypsin enzyme. Initially, 5 µl of 0.5 M tris(2-carboxyethyl)phosphine (TCEP) was added to the sample protein mixture which was incubated at 37$^{o}$C for 1 hr with shaking. Following 15 µl of 55 mM iodoacetamide (IAM) was added to the protein mixture and incubated for 1 hr at 37$^{o}$C with rotating in the dark. Further the trypsin digestion buffer was prepared by adding 990 µl of 100 mM ammonium bicarbonate ($NH_4HCO_3$) (pH 7.8) and 10 µl of 100 mM $CaCl_2$ which activates the enzyme to a 20 µg vial of sequencing Grade trypsin (Promega, #V511). Chymotrypsin digestion buffer was prepared by adding 500 µl of 1 mM HCl, 495 µl of 100 mM $NH_4HCO_3$ (pH 7.8) and 5 µl of 100 mM $CaCl_2$ to a 25 µg vial of Chymotrypsin Sequencing Grade (Roche, No. 11418467001). Then 100 µl of trypsin/chymotrypsin digestion buffer was added and the reaction was carried out at 37$^{o}$C for one day with shaking. Next day, 200 µl of 10% TFA and 50 µl of 5% acetonitrile were added to stop

the reaction and the solution was subjected to reverse phase chromatography solid-phase extraction of peptides. The resulting peptide mixture was evaporated to dryness using a speedvac and then re-suspended in 30 µl of 95/5 0.1% TFA (aq)/acetonitrile. The samples were stored at -80$^{o}$C until given for mass spectrometric analysis.

### II. 2. 2. 8. Mass spectrometry analysis of immunoprecipitated cytochrome c

Peptide identification was performed using a Thermo (San Jose, CA) LTQ XL linear ion trap mass spectrometer in Dr. Scott Gronert's laboratory, Department of Chemistry, Virginia Commonwealth University. The LTQ XL was interfaced with a Thermo Surveyor capillary HPLC system. Peptides were separated on a reversed-phase, C18 column (150 µm × 10 cm, 5 µm particles, 300 A$^{o}$ pores; Column Technology, Fremont, CA) at a flow rate of ~1 µl min$^{-1}$ using 0.1% formic acid in water as mobile phase A and 0.1% formic acid in methanol as mobile phase B. Peptides were injected and a Michrom (Auburn, CA) CapTrap trapping column was used for rapid sample injection. The gradient started from 2% B, then increased to 15% B over 5 min, then increased to 80% B over 70 min, and finally increased to 95% B over 15 min. The eluted peptides were introduced into the LTQ XL with a nanospray source operating at a spray voltage of 2.1 kV, a capillary voltage of 21 V, and a capillary temperature of 200°C. A full scan in the m/z range 300-2000 was performed to obtain precursor ions, followed by four data-dependent CID MS/MS scans for the four most abundant precursor ions in the full scan. Dynamic exclusion was used, that is, if the same precursor ion was picked for fragmentation twice within a 30 s window, it was excluded from further analysis for 180 s.

**Database searching and data processing**

Peptide sequences and modifications were identified using the BioWorks version 3.3.1, SP1 implementation of Sequest (Thermo). No scan grouping was performed in preparing peak lists for database searching. The protein sequence database used consisted of the NCBI RefSeq version of the complete mouse proteome and reversed versions of all sequences. Reversed sequences permit false discovery rate estimation. Sequences were downloaded on June 27, 2011, and the final database contained 70499 entries. Only fully-tryptic and chymotryptic peptides were considered and up to three missed cleavage sites were allowed. Fixed mass shifts were applied for alkylated cysteines (+57 Da) and oxidized methionines (+16 Da). Sequest output was refined using the Trans-Proteomic Pipeline (version 4.4; Institute for Systems Biology, Seattle, WA) software package. Specifically, PeptideProphet was used, in semi-supervised mode, to improve identification confidence. A PeptideProphet score threshold of 0.9 was applied.

**II. 2. 2. 9. LC-MS/MS of cardiolipins**

Isolated mitochondria (1 mg) in 50 µL of 100 mM potassium phosphate buffer were mixed with 1,2-dipalmitoyl-sn-glycero-3-phospho-N-methylethanolamine (internal standard) and extracted with 1 mL of chloroform:methanol, 2:1 containing 2 mM butylated hydroxytoluene as an antioxidant. The lipids were given for mass spectrometric analysis to the VCU Lipidomics Core, Department of Biochemistry and Molecular Biology, Virginia Commonwealth University.

For LC-MS/MS analyses, a Shimadzu LC-30 AD binary pump system coupled to a SIL-30AC autoinjector and DGU20A3 degasser coupled to an ABI 4000 quadrupole/linear ion trap (QTrap) (Applied Biosystems, Foster City, CA) operating in a triple quadrupole mode was used. Q1 and Q3 were set to pass molecularly distinctive precursor and product ions (or a scan across multiple m/z in Q1 or Q3), using N2 to collisionally induce dissociations in Q2; the ion source temperature was 50°C. The lipids were separated by reverse phase LC using a Supelco 2.1 (i.d.) x 150 mm Ascentis C18 column (Sigma, St. Louis, MO) and a binary solvent system at a flow rate of 0.3 mL/min with a column temperature of 60°C. Prior to injection of the sample, the column was equilibrated for 0.5 min with a solvent mixture of 30% mobile phase A ($CH_3OH/H_2O$, 50/50, v/v, with 2.5 mL triethylamine and 2.5 mL glacial acetic acid) and 70% mobile phase B (IPA/ $H_2O$), 90/10, v/v, with 2.5 mL triethylamine and 2.5 mL glacial acetic acid). After sample injection (typically 40 µL), the A/B ratio was maintained at 30/70 for 2.0 min, followed by a linear gradient to 100% B over 7.0 min, which was held at 100% B1 for 4.3 min, followed by a 0.6 min gradient return to 30/70 A/B. The column was re-equilibrated with 30:70 A/B for 1.0 min before the next run. Each cardiolipin was quantified during each run by MRM analysis, and in addition, the structure was confirmed via a MS2 scan within the linear ion trap during the elution of each peak.

### II. 2. 3. Statistical analysis

Parameters were expressed as mean±standard error of the mean (SEM). The data consisting of two groups were analyzed by two-tailed Student's t-test. Differences among multiple groups were compared by one-way analysis of variance with post hoc comparisons performed using the Student-Newman-Keuls test. All analysis was

executed using SigmaPlot ver.11 software (Systat Software Inc., Chicago, IL). A $p<0.05$ was considered statistically significant.

## II. 3. RESULTS

During ischemia, the ETC is a major target of ROS produced by specific sites of ETC itself [5, 222]. As described in the background, previous work in the lab has shown that the locus of ischemic damage is between complex III and IV [254]. One of the key components of this site is the cytochrome c-cardiolipin complex which can potentially convert to a peroxidase during pathological conditions. Cytochrome c is a small heme protein located in the inner membrane of mitochondria that transfers electrons between electron transport chain (ETC) complexes III and IV [30, 43]. Excessive generation of reactive oxygen species (ROS) can oxidize a key methionine residue ($Met_{81}$) of mouse cytochrome c, disrupting the Fe-$Met_{81}$ bond [264]. Oxidized cytochrome c attains peroxidase activity as the heme catalytic center can now access $H_2O_2$, thereby catalyzing the oxidation of the unsaturated linoleic (C18:2) acyl chains in cardiolipin to form peroxy-groups [264, 276]. Hence, we propose that the oxidative stress condition of ischemia-reperfusion results in the formation of oxidized cytochrome c. Secondly; we will test the hypothesis that intra-mitochondrial ROS generation coupled with the electron flow into the cytochrome c segment of the ETC is required to oxidize cytochrome c.

To test this hypothesis, we used a Langendorff mouse model of ischemia and reperfusion established in the laboratory [306]. In this model of ischemia-reperfusion, the isolated, buffer perfused C57BL6 mouse hearts underwent either 45 min of buffer perfusion or 25 min of ischemia and 30 min of reperfusion followed by isolation of mitochondria. Cytochrome c was immunocaptured from the isolated mitochondria and

the formation of methionine sulfoxide [Met(O)], a marker for cytochrome c peroxidase formation, was assessed via semiquantitative immunoblotting. To test the second hypothesis, mitochondria were incubated with specific substrates and inhibitors to isolate particular segments of the ETC. Following incubations, cytochrome c was immunocaptured and methionine sulfoxide [Met(O)] formation, was confirmed via immunoblotting and mass spectrometry.

### II. 3. 1. Immunoprecipitation of cytochrome c from isolated mitochondria.

To establish the formation of cytochrome c peroxidase activity in oxidative stress conditions like ischemia-reperfusion, we have utilized immunoprecipitation as a technique to specifically pull down cytochrome c from a complex mixture of proteins in isolated mouse mitochondria. To confirm the specificity of the immunoprecipitation, freeze-thawed, buffer-solubilized whole isolated mitochondria were probed with the cytochrome c antibody immobilized on the Dynabeads® while negative control experiments were performed with mouse IgG antibody and no antibody. Immunocaptured cytochrome c from all the samples (cytochrome c antibody, IgG, no antibody) was subjected to SDS-PAGE followed by immunoblotting with anti-cytochrome c antibody.

The specificity of immunocapture antibody to cytochrome c in the isolated mitochondria was confirmed by comparing its immunodetection signal to the negative controls (mouse IgG, and no IP antibody). As shown in **Figure 2.5**, cytochrome c bands were absent in the negative controls whereas signal for cytochrome c was observed with cytochrome c antibody used during immunoprecipitation. Also, the cytochrome c signal was much enriched in the eluate containing immunocaptured cytochrome c when

compared to supernatants collected “before IP” and “after IP”. This result demonstrates that the immunocapture technique was successful to separate cytochrome c and the cytochrome c antibody used for immunoprecipitation has high specificity to pull down cytochrome c from complex mixtures of proteins (e.g. isolated mitochondria).

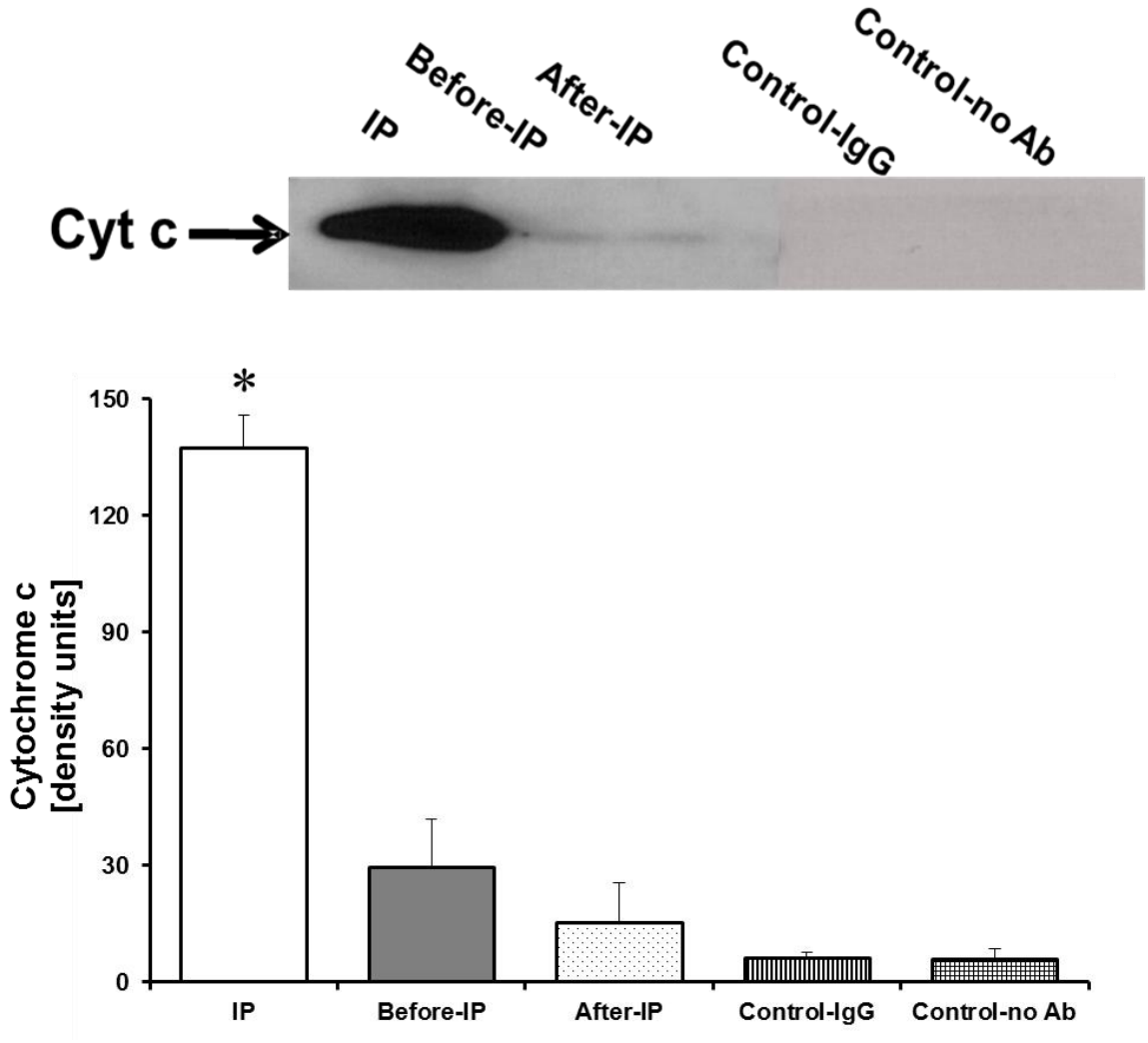


**Figure 2.5. Immunoprecipitation of cytochrome c from mitochondria.** Western blot showing detection of cytochrome c. Cytochrome c content in samples before-IP, after-IP, mouse IgG and no IP-cytochrome c antibody. Densitometry was measured using ImageJ (NIH, Bethesda). Results were mean±SE. All results were compared using one-way ANOVA test. *$p<0.05$ vs. control-no Ab. n= 4 in all groups. One representative blot out of four independent experiments was shown.

### II. 3. 2. Quantification of immunoprecipitated cytochrome c using Dynabeads®.

Spectrophotometric analysis of cytochrome c content in the mitochondria revealed that there is approximately 0.4 nmoles of cytochrome c/mg of isolated mitochondria [107, 203] which is equivalent to 4.8 µg of cytochrome c/mg of isolated mitochondria. In order to determine the amount of immunocaptured cytochrome c from 0.5 mg of isolated mitochondria, we have run a SDS-PAGE with the 5 µl of immunocaptured cytochrome c (from total of 50 µl cytochrome c) along with known concentrations of commercial equine cytochrome c (25ng, 50ng, 100ng, 500ng, 750ng, 1000ng, 2500ng).

From the semiquantitative calibration **(Figure 2.6)**, the concentration of immunocaptured cytochrome c was projected to be approximately 40 ng from 5 µl of immunocaptured cytochrome c. Hence, from 50 µl of immunocaptured cytochrome c, a total of 400 ng/0.4 µg of cytochrome c was separated from 0.5 mg of isolated mitochondria. Thus, the amount of successfully immunocaptured cytochrome c from 0.5 mg mitochondria was equivalent to 33.33 picomoles. However, the efficiency of the immunocapture protocol depends upon the amount of isolated mitochondria, cytochrome c antibody and the Dynabeads® utilized for the experiment.

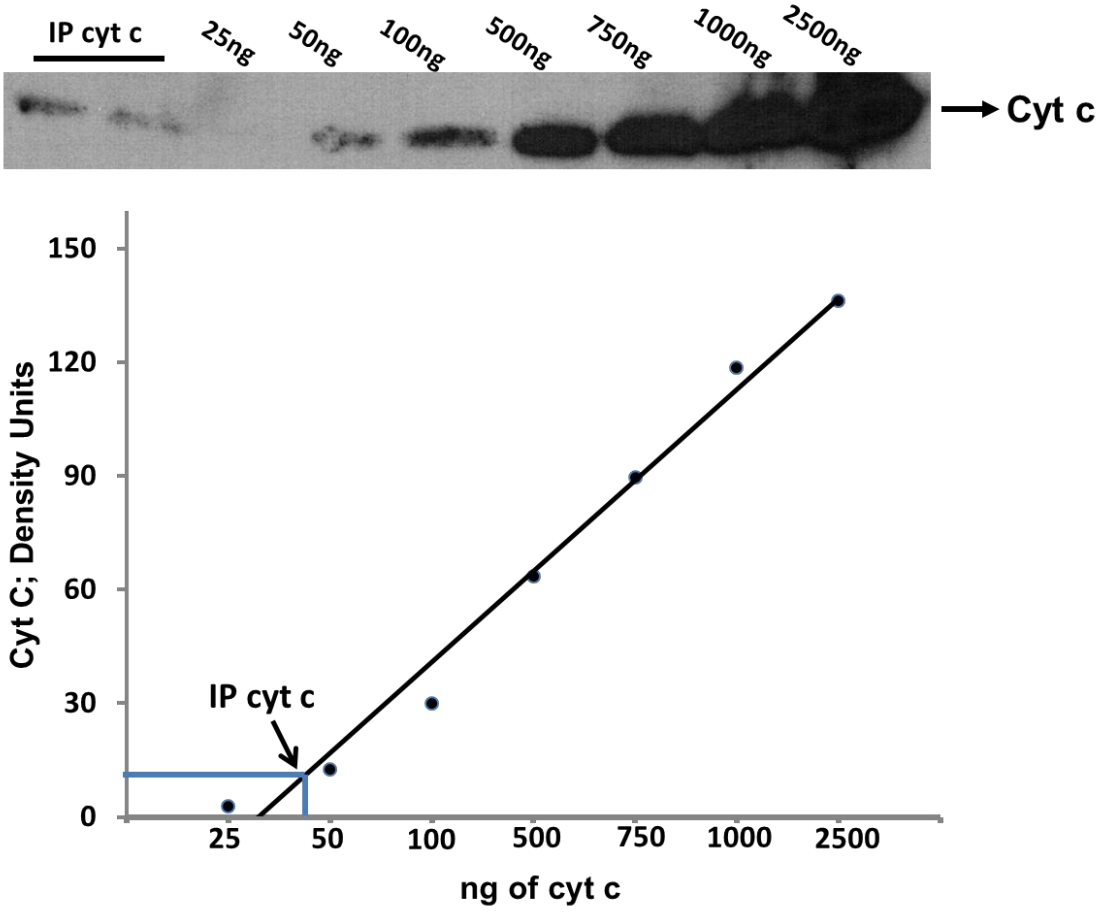


**Figure 2.6. Semi-quantification of immunoprecipitated cytochrome c using Dynabeads®.** Western blot showing detection of cytochrome c. Immunocaptured cytochrome c content in samples was determined by establishing a semiquantitative range with known concentrations of commercial cytochrome c. Densitometry was measured using ImageJ (NIH, Bethesda).

**II. 3. 3. Mass spectrometric analysis of cytochrome c containing the oxidized methionine residue.**

Murine cytochrome c has two methionines, one at 66 and the other at position 81. In order to confirm the specific oxidation of $Met_{81}$ which indicates formation of cytochrome c peroxidase in a physiological model of isolated mouse mitochondria, we have used the mass spectrometric approach to detect methionine sulfoxide modification.

As an initial control isolated mitochondria from mouse hearts were exposed to the oxidant, hypochlorous acid (10 nM HOCl for 15 min). Cytochrome c was immunocaptured and methionine sulfoxide [Met(O)] modification was determined. Isolated mitochondria from mouse were exposed to HOCl after which cytochrome c was immunocaptured and analyzed for oxidation of the Met-81 residue (axial ligand to the heme group) using mass spectrometry and western blotting.

As shown in **Figure 2.8A**, western blotting of immunocaptured cytochrome c from mitochondria exposed to HOCl show greater methionine sulfoxide formation compared to control mitochondria. Recovery of peptides containing the key Met-residue has been achieved with cytochrome c from the mouse species. Peptide fragment ions were indicated by a, b, or c if the charge was retained on the N-terminus and by x, y or z if the charge was maintained on the C-terminus. As shown in **Figure 2.7**, tryptic digest of murine cytochrome c using collision-induced dissociation as the fragmentation method yielded a short peptide MIFAGIK containing Met-81 (AA 81-87; MW 778.44) at the N-terminal end. The combined sequence coverage with trypsin proteolysis is around 58% for the LTQ analysis. Previous studies have shown that $b_1$ fragments cannot be

detected using collision-induced dissociation [307]. Hence MIFAGIK containing a +16 mass shift associated with methionine oxidation was not detected because of the lack of carbonyl group to initiate the nucleophilic attack on the carbonyl carbon located between the first two aminoacids, as a result of which the cyclic intermediate cannot be formed and thus cannot be identified [307].

In order, to generate a fragment ion encompassing Met-81, trypsin was replaced by chymotrypsin and the peptide IPGTKMIF (AA 76-83; MW 906.51) was generated. With the help of Dr. David Simpson from Dr. Scott Gronert's lab, we have confidently identified the peptide IPGTKMIF **(Figure 2.8B)**, oxidized at methionine, using linear ion trap mass spectrometer, with good coverage of fragment ions around Met-81. The combined sequence coverage with chymotrypsin proteolysis is around 32% for the LTQ analysis. As shown in the **Figure 2.8B**, the b-ions bracket the modification site for unambiguous localization. Identification was further supported by a characteristic peak for the neutral loss of methane sulfenic acid, which is common in peptides containing oxidized methionine residues. The numerous water losses were consistent with the presence of threonine and the most intense y-ion was consistent with the proline effect. This work demonstrates the feasibility of cytochrome c analysis to identify site specific oxidation of $Met_{81}$ using mass spectrometry.

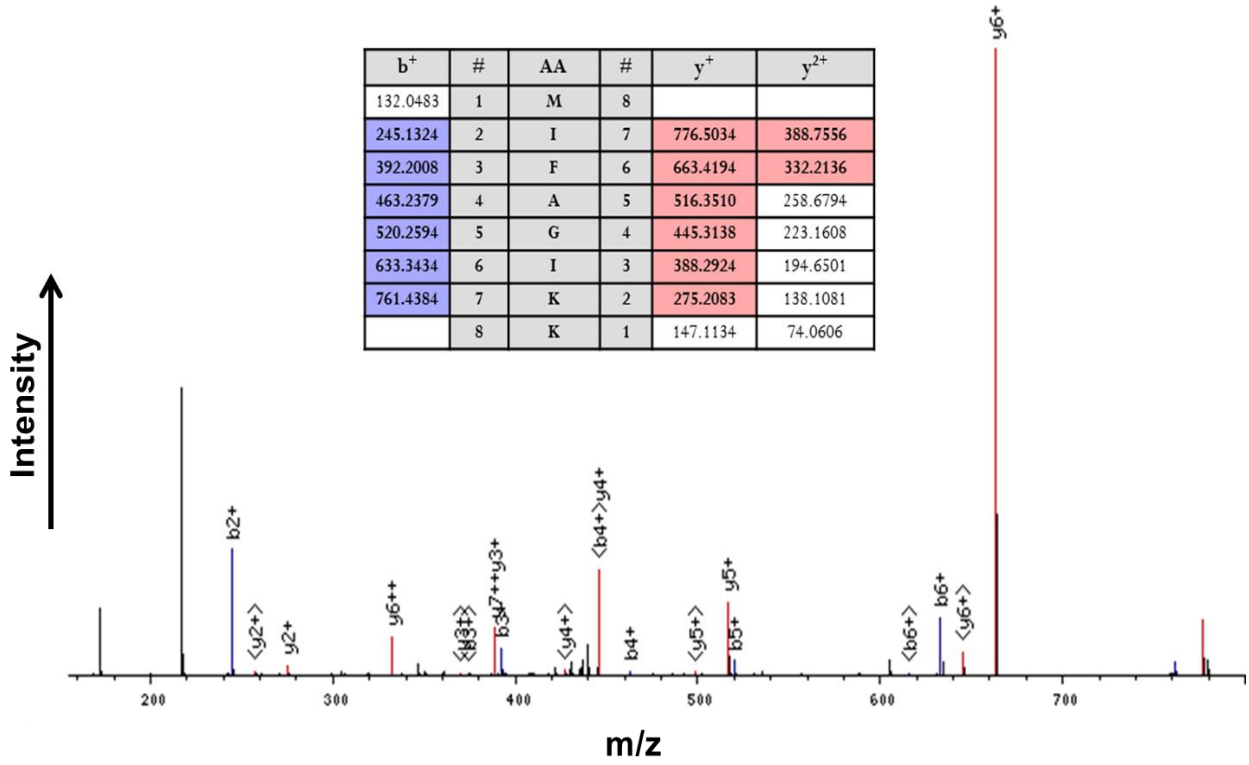


**Figure 2.7. Trypsin proteolysis results in "MIFAGIKK" with methionine at the terminal residue.** MS/MS spectrum of peptide containing residues 150-780 in the +1 or +2 charge state. Blue peaks are y ions and red peaks are b ions. Black peaks were not identified as b or as y ions.

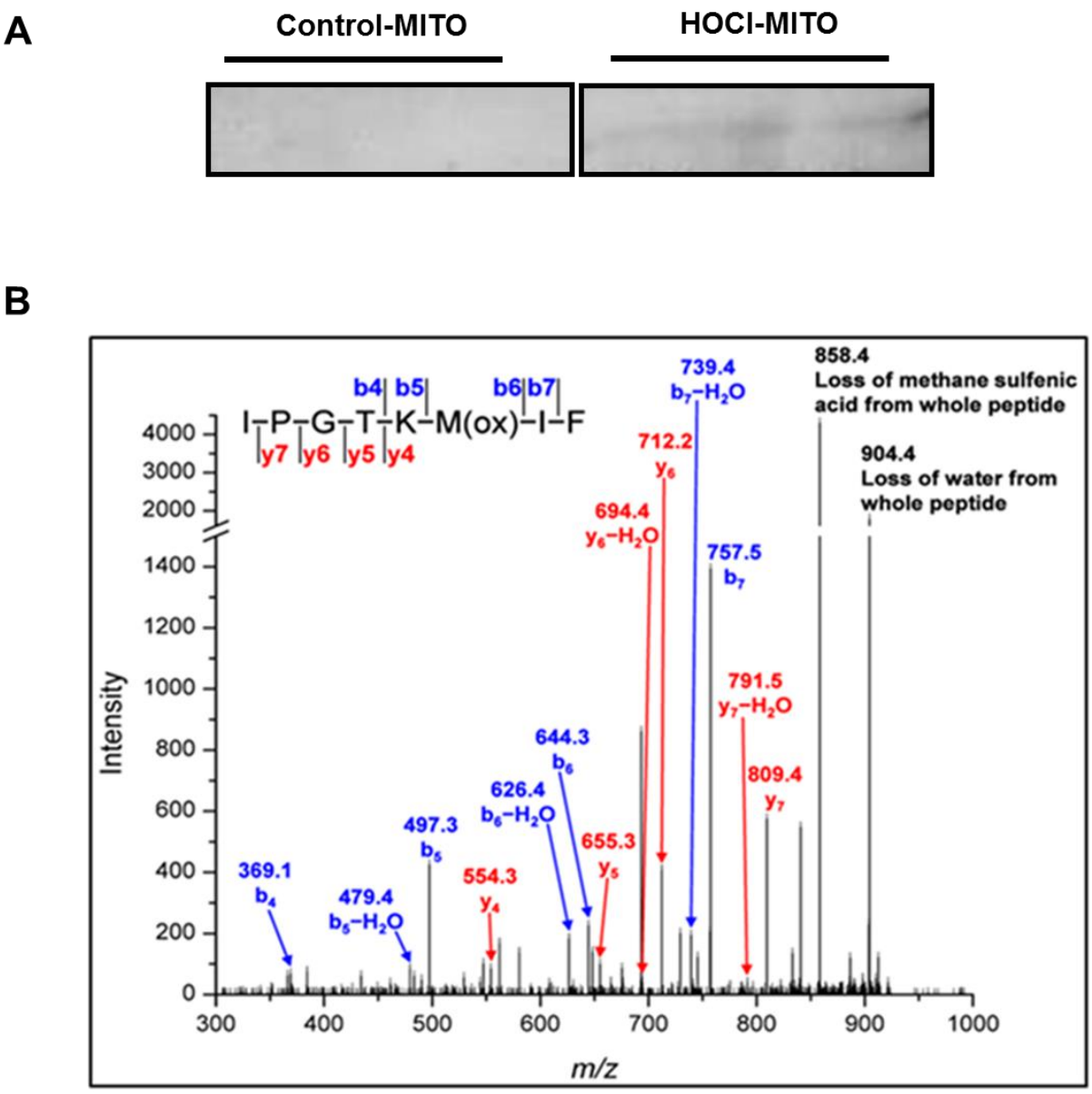


**Figure 2.8. Detection of IPGTKMIF containing oxidized methionine from the MITO treated with HOCl.** (A) Western blot showing detection of Met(O) isolated mitochondria treated with or without HOCl (B) Annotated tandem mass spectrum for chymotryptic peptide IPGTKMIF, oxidized at methionine (measured precursor ion m/z = 922.4; precursor ion determined to be singly charged).

### II. 3. 4. Cardiac function was decreased in mouse hearts following ischemia-reperfusion

Next, we examined if ischemia-reperfusion oxidizes cytochrome c immunocaptured from isolated from mouse hearts. To test this, the isolated, buffer perfused C57BL6 mouse hearts either underwent 45 min of buffer perfusion (TC perfusion) or 25 min of ischemia and 30 min of reperfusion (ISC-REP) following which the cardiac function, protein yield and the mitochondrial function was measured.

During the entire perfusion on the Langendorff system, the cardiac function was monitored in mouse hearts which underwent TC perfusion and ISC-REP. The left ventricular developed pressure (LVDP) was recorded in both the groups. In the two groups, LVDP was similar in each group at the end of equilibration perfusion, before ISC-REP [TC perfusion: 84±4 mm Hg; ISC-REP: 86±12; $p<0.05$]. In ISC-REP hearts, LVDP was markedly decreased during reperfusion compared with the pre-ischemic value [TC perfusion: 74±7 mm Hg; ISC-REP: 26±7; $p<0.05$]. Thus, as shown in **Figure 2.9**, the % LVDP recovery during reperfusion was decreased to approximately 31±6% in ischemia-reperfusion group. From the data it was clear that cardiac function was substantially decreased during ischemia-reperfusion.

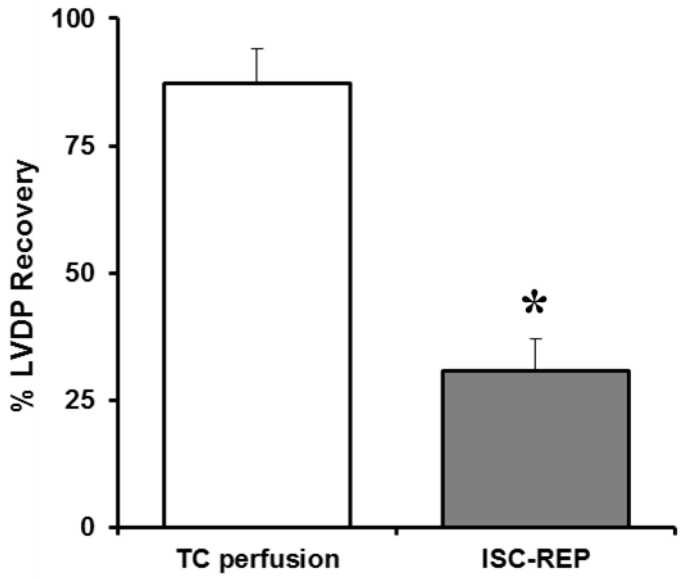


**Figure 2.9. Cardiac function was decreased in mouse hearts following ischemia-reperfusion.** Left ventricular developed pressure (LVDP) was recorded (as mm Hg) in TC perfusion and ischemia (ISC)-reperfusion (REP) groups. Ischemia decreases the recovery of LVDP during reperfusion compared with untreated hearts (A). Results were presented as mean±SE. A difference of $p<0.05$ was considered significant. Results were compared using t-test. *$p<0.05$ vs.TC perfusion. n=5 in all groups.

### II. 3. 5. Recovery of mitochondria from heart tissue was similar following ischemia-reperfusion.

Following mitochondrial isolation, protein concentration was measured by the the Lowry method using BSA as a standard and sodium deoxycholate as a detergent to solubilize the mitochondria. The protein yield of isolated mitochondria following 25 min of untreated ischemia and 30 min of reperfusion was similar to the protein yield in the time control perfusion group **(Figure 2.10)**. The protein yield averaged 21.0±2.0 mg/g wet weight in TC perfusion vs. 24.7±0.7 mg/g in ISC-REP hearts (p=ns). Thus, any differences between TC perfusion and ISC-REP (e.g. OXPHOS) were not due to a preferential selection of “good” or “bad” mitochondria during the isolation process. This was confirmed by the protein content between the two groups which provided a strong evidence of a similar recovery of mitochondria following isolation from heart tissue.

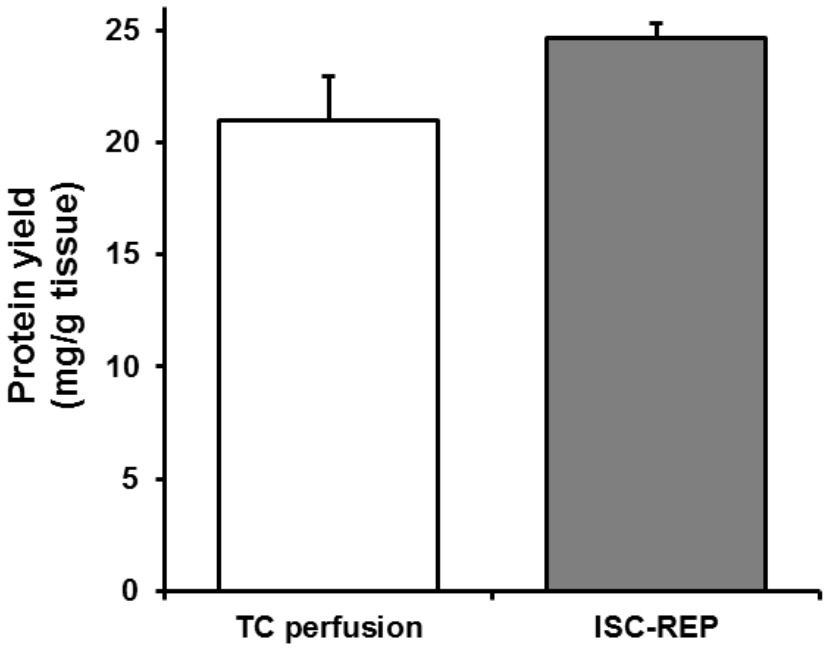


**Figure 2.10. Ischemia-reperfusion did not alter the mitochondrial protein yield.** The protein content of the one population mitochondria isolated from C57BL6 mice was unaltered in TC perfusion, ISC-REP groups (A). Results were presented as mean±SE. n= 5 in all groups.

### II. 3. 6. Glutamate+malate and TMPD+ascorbate dependent oxidative phosphorylation was decreased following ischemia-reperfusion.

The rates of oxidative phosphorylation were studied in mitochondria isolated from time control perfusion and ischemia-reperfusion groups using substrates that feed electrons to different entry points in the ETC. Glutamate+malate was used as the complex I substrate and TMPD/ascorbate (with rotenone) as electron donor to complex IV via cytochrome c. As shown in **Figure 2.11**, mitochondrial respiratory function was substantially decreased following ischemia and reperfusion. The maximal rates of oxidative phosphorylation were obtained by addition of saturating 2 mM ADP when glutamate+malate or TMPD/ascorbate were used as substrates. The maximal rate of respiration using a complex I substrate, glutamate+malate, (complex I→complex III→complex IV) was decreased by approximately 50% (TC: 438±36 nAO/min/mg protein; ISC-REP: 221±17, $p<0.05$). TMPD/ascorbate-dependent (complex IV) respiration was lowered by approximately 25% (TC: 1560±62 nAO/min/mg protein; ISC-REP: 1184±88, $p<0.05$) following ischemia-reperfusion. Respiratory control ratios (RCRs) were reduced after ISC-REP with glutamate+malate as a substrate **(Table 2.1)**. As a next step, the rates of uncoupled respiration by addition of 2, 4-ditrophenol (DNP) were measured. DNP is a protonophore that carries protons across the mitochondrial membrane. In its presence, the electron transport chain works independently from the phosphorylation apparatus. The use of DNP tests the relative contributions of the electron transport chain and ATP synthase/ANT/$P_i$ transporter to the decreased rate of oxidative phosphorylation. The DNP-uncoupled respiration with the glutamate+malate was reduced to a similar extent when compared to the respiration rates without the

uncoupling agent (2 mM ADP rates) **(Table 2.1)**. This observation suggests that the decrease in respiration was not caused by defects in ATP synthase, adenine nucleotide translocase (ANT) or phosphate ($P_i$) transporter, but was indeed localized to the electron transport chain.

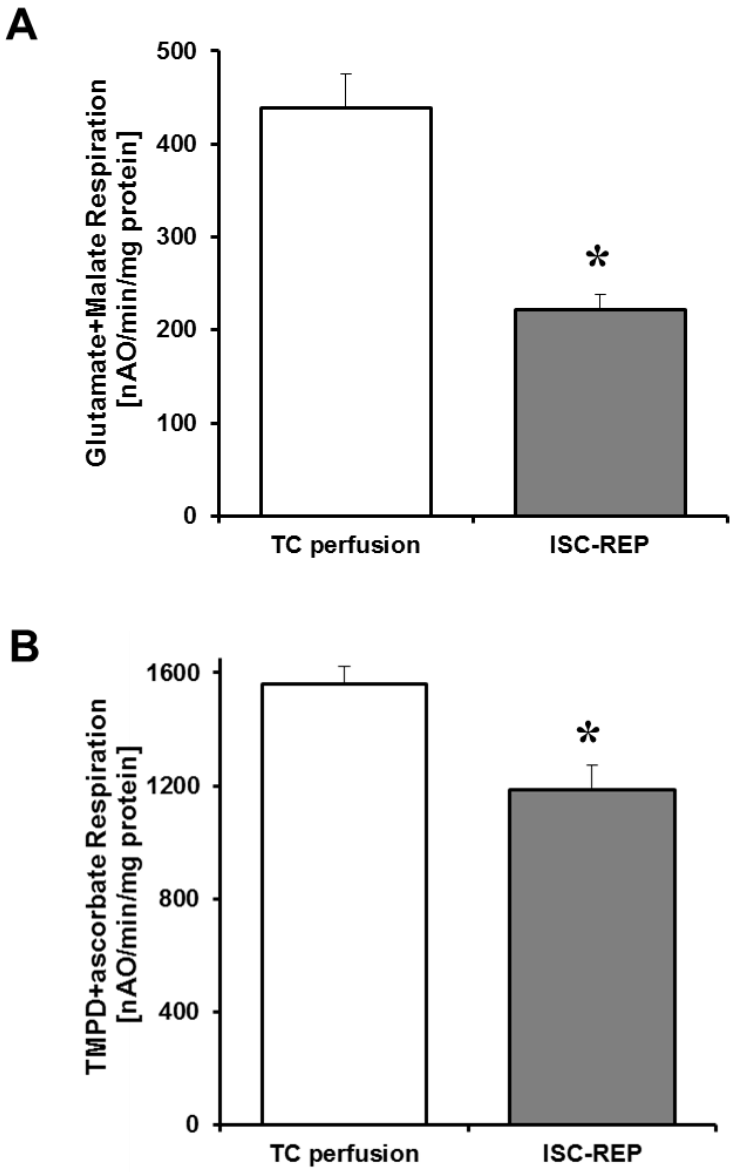


**Figure 2.11. Glutamate+malate and TMPD+ascorbate dependent oxidative phosphorylation was decreased following ischemia-reperfusion.** Oxygen consumption by intact mitochondria was measured by Clark-type electrode at 30 $^{o}$C as described in Materials and Methods. Incubations contained: 20 mM glutamate with 5 mM malate (A) or 1 mM TMPD/20 mM L-ascorbate with 7.5 µM rotenone (B). Maximum rates of state 3 respiration with 2 mM ADP were shown (A). For TMPD/Asc-dependent respiration azide-sensitive data were depicted (B). Results were expressed as nanoatoms of atomic oxygen/min/mg of mitochondrial protein and were presented as mean±SE. * $p<0.05$ vs. TC perfusion. All results were compared using t-test. n=5 in all groups.

**Table 2.1. Rates of oxidative phosphorylation in heart mitochondria isolated from TC perfusion and ISC-REP groups.**

| | TC perfusion | ISC-REP |
|---|---|---|
| | n=5 | n=5 |
| **Glutamate + Malate** | | |
| State3 | 346±20 | 198±9* |
| State 4 | 61±6 | 75±3 |
| RCR | 5.7±0.9 | 2.7±0.2* |
| 2mM ADP | 438±36 | 221±17* |
| DNP | 418±28 | 192±15* |
| **TMPD/ascorbate** | | |
| 2mM ADP | 1560±62 | 1184±88* |

**Table 2.1. Ischemia-reperfusion affects mitochondrial oxidative phosphorylation.** Mitochondria were isolated and rates of respiration were recorded. Based on state 3 and state 4 rates, respiratory control ratios (RCRs) were calculated. During recording of 2 mM ADP-dependent maximal state 3 rate, uncoupler 2,4-dinitrophenol (DNP) was added to establish relative contribution of phosphorylation apparatus to the observed defects in integral respiration. Results were presented as mean±SE. Values of state 3, state 4, 2 mM ADP and DNP rates are expressed in nanoatoms of atomic oxygen/min/mg of mitochondrial protein. A difference of $p<0.05$ was considered significant. All results were compared using t-test. *$p<0.05$ vs. TC perfusion. n=5 in all groups. ADP, adenosine di-phosphate; TMPD, N,N,N′,N′-tetramethyl-p phenylenediamine; RCR, respiratory control ratio; DNP, 2,4-dinitrophenol.

### II. 3. 7. Cytochrome c from ISC-REP hearts exhibit increased methionine modification

Mitochondria were isolated from the Langendorff perfused mouse hearts that underwent 45 min buffer perfusion (TC perfusion) or 25 min of ischemia and 30 min of reperfusion (ISC-REP). Isolated mitochondria from TC perfusion and ISC-REP hearts were subjected to immunoprecipitation to capture cytochrome c using Dynabeads® Protein G immunoprecipitation kit loaded with cytochrome c primary antibody. The immunocaptured cytochrome c was blotted for methionine sulfoxide [Met(O)] and cytochrome c (control for equal mitochondrial protein loading). Met(O) formation was the mechanistic indicator for cytochrome c peroxidase formation. As shown in **Figure 2.12**, the densitometry ratio of Met(O) to cytochrome c in ISC-REP hearts showed approximately 80% increase in the methionine sulfoxide formation when compared to TC perfusion [Ratio Met(O)/cyt c; normalized to TC perfusion; TC perfusion: 1.0±0.0; ISC-REP: 1.8±0.24; $p<0.05$]. This data supports the formation of cytochrome c peroxidase indicated by an increased Met(O) signal during pathological setting of ischemia-reperfusion.

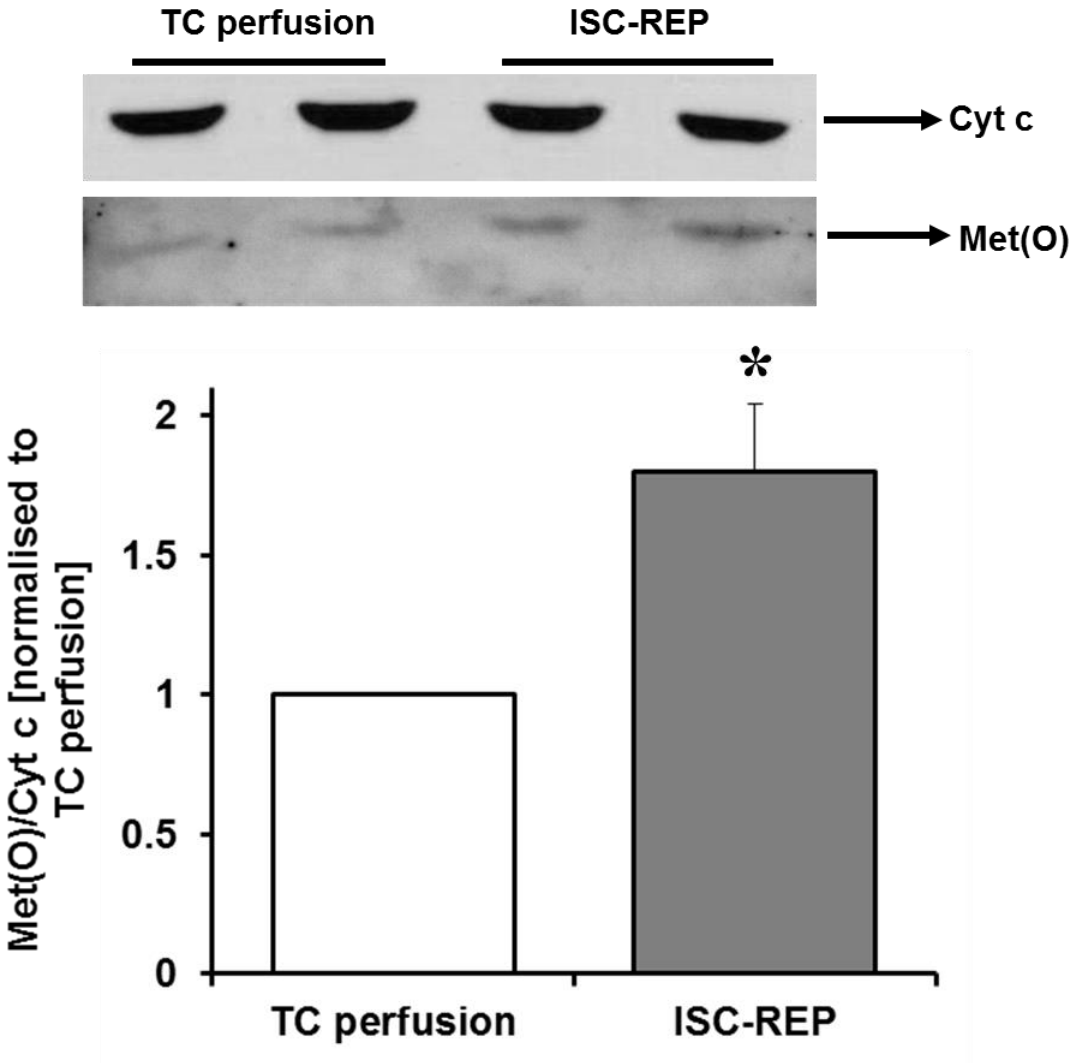


**Figure 2.12. Ischemia-reperfused hearts show increased Met(O) compared to buffer perfused hearts.** Western blot showing detection of Met(O) and cytochrome c at 12 kDa in buffer perfused (TC) and ischemia-reperfused (ISC-REP) hearts. MITO from buffer perfused (TC) and ischemia-reperfused (ISC-REP) hearts were subjected to IP and the eluate containing cytochrome c was subjected to SDS-PAGE and immunoblotted for Met(O) and cytochrome c (control for equal mitochondrial protein loading). Densitometry was measured using ImageJ (NIH, Bethesda) and expressed as ratio of Met(O) signal to cytochrome c signal. Results were expressed as mean±SE.* $p<0.05$ vs. TC perfusion. All results were compared using one-way ANOVA test. n=5 in all groups. Met(O), methionine sulfoxide.

### II. 3. 8. Mass spectrometric analysis to detect oxidized $Met_{81}$ in control and ischemia-reperfused samples

Studies to identify and analyze IPGTKMIF peptide in cytochrome c immunocaptured from control and ischemia-reperfused were carried out using mass spectrometry. However, basal oxidation of methionine in IPGTKMIF peptide was observed even in the control samples. A quantification approach with Tandem Mass Tag (TMT) labeling that irreversibly reacts with the primary amines (-NH2) groups was used to label the peptides of immunocaptured cytochrome c from control and ischemia-reperfused samples. Moreover, isobaric labeling with TMT tag was not compatible with immunocapture technique as the cytochrome c separated through this procedure is in the glycine solution which is a primary amine and thus will provide a lot of background signal. The approach to separate glycine from cytochrome using 5KDa filters was unsuccessful as the peptides were no longer detectable via mass spectrometry probably due to considerable loss of protein. In addition, thioglycolate and $N_2$ bubbling of the solutions used for immunocapture were also tested to reduce artifactual oxidation which might have occurred through sample handling. However, all these approaches could not prevent basal oxidation of methionine in control samples. One alternative, to quantify oxidation of methionine between control and ischemia-reperfused samples is to do an on-bead digestion of cytochrome c with chymotrypsin which will eliminate the problem of glycine for TMT-labeling.

### II. 3. 9. Distal blockade of electron transport chain increases formation of cytochrome c peroxidase

Given the importance of ETC as a source of ischemic damage, blocking it with inhibitors that manipulate electron flow through the respiratory complexes has shown that the segment located between complex III and complex IV is responsible for the ischemic damage [254]. One of key components of this site is the cytochrome c and cardiolipin complex located between complex III and complex IV which most likely plays an important role in ischemia mediated cardiac injury [254]. Hence, we hypothesize that during ischemia-reperfusion, an increase in intra-mitochondrial ROS generation coupled with the electron flow into the cytochrome c segment of the ETC is required to oxidize cytochrome c at the methionine residue converting to a peroxidase. To test this hypothesis, isolated mitochondria from C57BL6 mice were incubated with specific substrates and inhibitors to isolate particular segments of the ETC in such a way that the cytochrome c segment has access either to the ROS or electron flux or both.

For the experiment, mitochondria were incubated with succinate and blockers including rotenone, theonyl trifluoroacetic acid (TTFA), antimycin A and azide. Succinate feeds electrons into the ETC through complex II. Rotenone binds to the CoQ-binding site of complex I and prevents reverse electron transfer from complex II to complex I. TTFA blocks complex II at the distal portion of the compex and increases ROS from complex II. Antimycin A, inhibits the $Q_i$ center of complex III thereby causing a net increase in ROS production from the $Q_o$ site. The ROS generated from the $Q_o$ site in complex III is released into the intermembrane space (IMS). Azide inhibits electron transport in

complex IV by binding tightly with the iron coordinated in Cyt $a_3$ thereby increasing ROS release from upstream complex I and complex III.

The isolated mitochondria from C57BL6 mice hearts were incubated with the following combinations of substrate and inhibitors in order to test the importance of ROS and electron flux into cytochrome c in generating modified cytochrome c. As shown in **Figure 2.13**, **(A)** succinate + rotenone: Rotenone inhibits reverse electron transfer to complex I. This group was the control incubation **(B)** succinate + rotenone + TTFA: TTFA blocks at complex II. Here, in this group there would be increase in ROS from complex II and electron flux is blocked prior to complex III **(C)** succinate + rotenone + antimycin A: Antimycin A inhibits the $Q_i$ center of complex III. Therefore, in this group there would be an increase in ROS from complex III but no electron flux into cytochrome c **(D)** succinate + rotenone + azide: Azide inhibits electron transport in complex IV. From this group there would be an increase in ROS from complex III along with electron flux through cytochrome c. Following incubations, cytochrome c was immunocaptured using Dynabeads® Protein G immunoprecipitation kit. Cytochrome c and methionine sulfoxide [Met(O)], a marker for cytochrome c peroxidase formation, were immunoblotted.

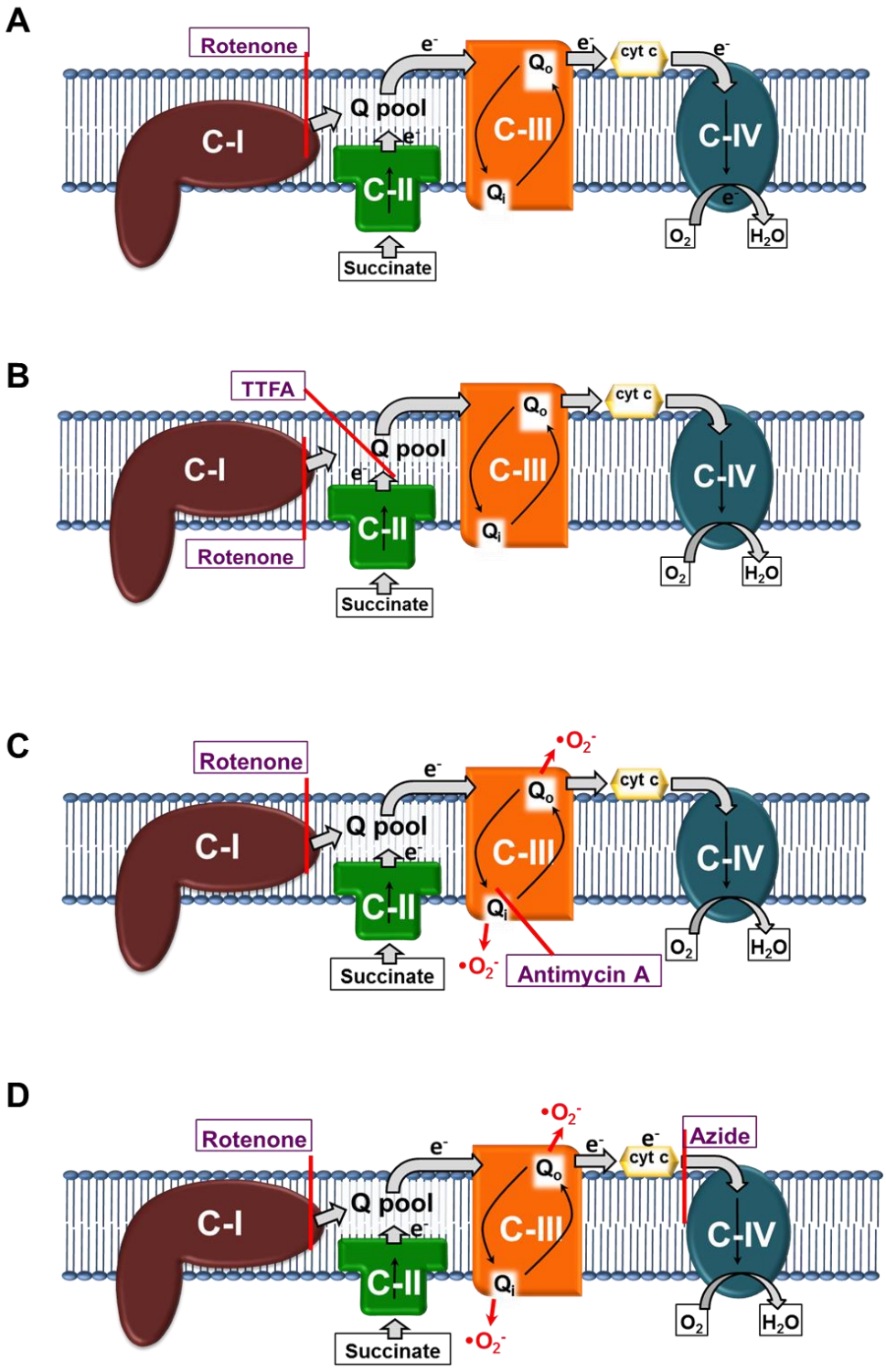


**Figure 2.13. Schematic of mitochondrial incubations with substrates to test the contribution of ROS and electron flow to oxidize cytochrome c:** Isolated mitochondria were incubated for 50 min with succinate+rotenone, succinate+rotenone+TTFA, succinate+rotenone+A.A, succinate+rotenone+azide. TTFA, Thenoyltrifluoroacetone; A.A, Antimycin A; cyt c, cytochrome c; Met(O), methionine sulfoxide.

Incubation of isolated mitochondria with the ETC blockers antimycin A and azide, blocks electron flow at complex III and complex IV respectively, causing increase in ROS production from complex I and complex III. However, distal blockade of complex IV with azide showed approximately 200% increase in the signal as a result of Met(O) formation compared to TTFA (blocks complex II) or A.A (blocks complex III) [Ratio Met(O)/cyt c; normalized to succ+rot; succ+rot+TTFA: 1.04±0.38; succ+rot+A.A: 0.87±0.16; succ+rot+azide: 3.46±1.10 $p<0.05$ vs. succ+rot+TTFA or succ+rot+A.A]. Azide not only increases ROS from complex III but also allows electron flow to cytochrome c as shown in **Figure 2.14**. This data suggests that both ROS and the electron flux into cytochrome c were needed to increase the formation of Met(O), which is the marker for cytochrome c peroxidase formation.

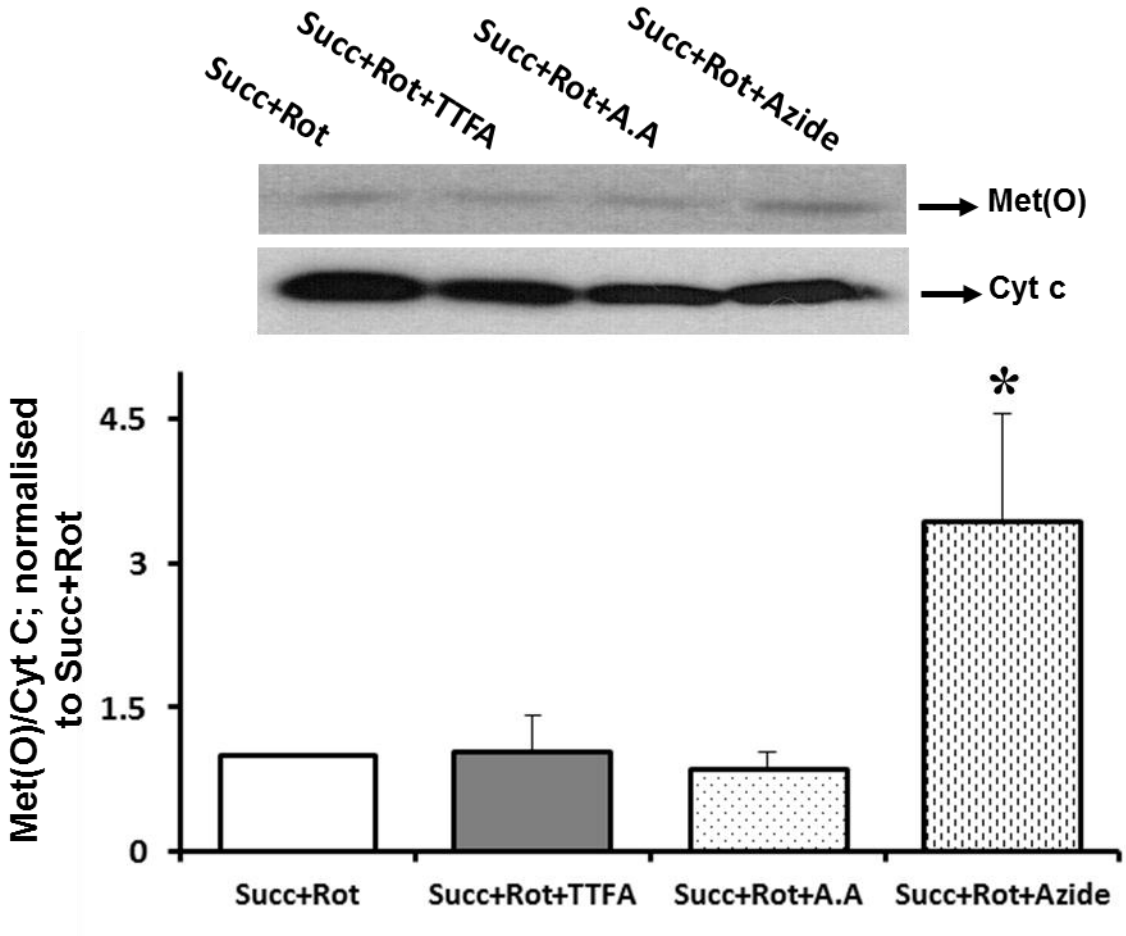


**Figure 2.14. ROS and electron flow into cytochrome c was essential for its modification.** Western blot showing detection of methionine sulfoxide [Met(O)] and cytochrome c at 12 kDa. Isolated mitochondria were incubated for 50 min with succinate+rotenone, succinate+rotenone+TTFA, succinate+rotenone+A.A, succinate+rotenone+azide and then subjected to IP. The eluate containing immunoprecipitated cytochrome c was subjected to SDS-PAGE and immunoblotted for Met(O) and cytochrome c (control for equal mitochondrial protein loading). Densitometry was measured using ImageJ (NIH, Bethesda) and expressed as ratio of Met(O) signal to cytochrome c signal (lower panel). Results were expressed as mean±SE, n=5-7 for each group. All results were compared using one-way ANOVA test. *$p<0.05$ vs. Succ+Rot. One representative blot out of seven independent experiments is shown. Succ, succinate; Rot, rotenone; TTFA, Thenoyltrifluoroacetone; A.A, Antimycin A; cyt c, cytochrome c; Met(O), methionine sulfoxide.

**II. 3. 10. Cardiolipin content was decreased following distal blockade of electron transport chain.**

Cardiolipin, a key mitochondrial inner membrane phospholipid, plays a crucial role in ischemia mediated cardiac injury [5, 216]. Experiments performed with different animal models using global ischemia showed an overall decrease in the cardiolipin content [203, 216, 302, 308]. Ischemia increases ROS production resulting in cytochrome c peroxidase formation which causes the oxidation and depletion of cardiolipin. Depletion of cardiolipin delocalizes cytochrome c from the inner mitochondrial membrane into the cytosol thereby activating cell death [264, 276].

As shown in **Figure 2.13**, blockade at cytochrome oxidase of the ETC allows cytochrome c to have access to both ROS and electron flux which results in the oxidation of methionine residue of cytochrome c turning it to a peroxidase. Further, we asked if the formation of cytochrome c peroxidase as a result of distal blockade of ETC in isolated mitochondria consequently altered the content or composition of cardiolipin. Isolated mitochondria were incubated in KME buffer containing succinate and rotenone with or without azide for 90 min. Phospholipids from the mitochondrial incubations were extracted and quantified using LC/MS/MS analysis.

As shown in **Figure 2.15**, the content of cardiolipin was significantly decreased, by approximately 20%, in incubations containing succinate+rotenone+azide when compared to incubations containing succinate+rotenone [succ+rot: 48±1 nmol/mg protein; succ+rot+azide: 39±2; $p<0.05$ vs. succ+rot]. This data suggests that the formation of cytochrome c peroxidase ultimately results in loss of cardiolipin in isolated mitochondria.

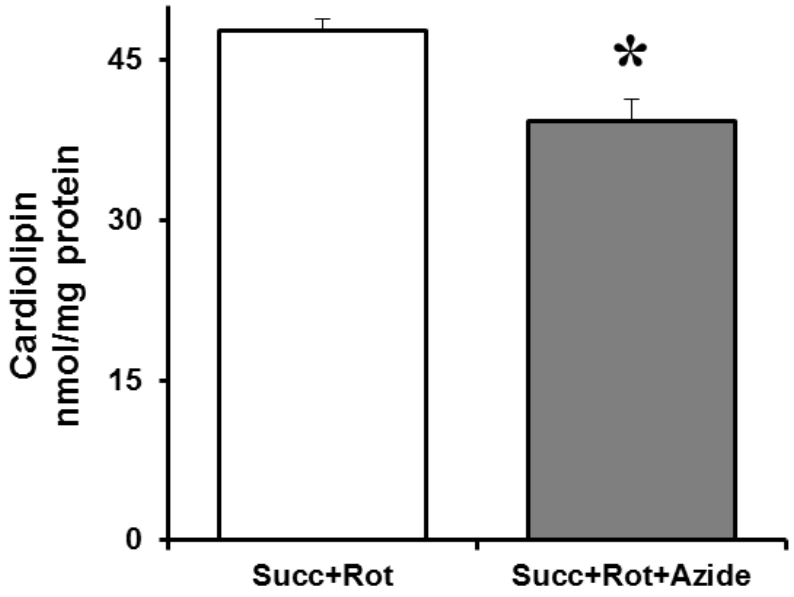


**Figure 2.15. Content of cardiolipin was decreased following incubation of mitochondria with succinate+roteonone+azide.** Quantification of cardiolipin content by phosphate measurement per mg mitochondrial protein (nmol/mg protein) in isolated mitochondria incubated with Succ+Rot and Succ+Rot+Azide for 90min. Results were expressed as mean±SE, n=3 for each group. All results were compared using t-test. *p<0.05 vs. Succ+Rot. Succ, succinate; Rot, rotenone.

## II. 4. SUMMARY

- Ischemia-reperfusion increases the formation of methionine sulfoxide, a mechanistic indicator for cytochrome c peroxidase formation.

- Increase in ROS generation along with electron flow through cytochrome c is essential to convert cytochrome c to a peroxidase.

- As a result of increase in cytochrome c peroxidase activity with distal blockade of ETC, cardiolipin is selectively depleted from the mitochondrial membrane.

## II. 5. DISCUSSION

Cell culture and *in-vitro* studies identified a novel function of cytochrome c during non-physiological stress conditions [264, 276, 301]. During oxidative stress, cytochrome c converts to a peroxidase and specifically oxidizes the polyunsaturated molecular species of cardiolipin. As a result cardiolipin oxidation and depletion, pro-apoptotic proteins, including cytochrome c and Smac/Dialbo are released into the cytosol both of which cause cell death via the caspase dependent pathways [276]. Inhibition of cytochrome c peroxidase by nitric oxide prevents cardiolipin oxidation and cytochrome c loss [299], suggesting that the peroxidase is a potential site that generates mitochondrial damage. However, the molecular switch that disrupts the electron shuttling function of cytochrome c and converts it to a peroxidase was not identified. In addition, the physiological relevance of the cytochrome c peroxidase is unknown. Thus, the focus of this study was to identify the role of cytochrome c peroxidase during a pathological condition such as ischemia-reperfusion. This work demonstrates that during ischemia-reperfusion, an increase in intra-mitochondrial ROS generation coupled with the electron flow through the cytochrome c segment of the ETC oxidizes cytochrome c at the methionine residue which confers peroxidase activity, resulting in depletion of cardiolipin.

Cardiolipin, a phospholipid unique to mitochondria, is located in the inner membrane and is required for the optimal activity of ETC complexes [264]. The close proximity to the ETC makes cardiolipin, containing highly enriched oxidatively sensitive linoleic acid (C18:2) groups, a prime target for ROS generated during ischemia [309]. During

ischemia, ROS from complex III along with electron flow through cytochrome c depletes cardiolipin leading to a decrease in complex IV activity [203, 216, 310]. In addition, cardiolipin depletion results in the loss of cytochrome c from the inner membrane which in turn enhances ROS production from the ETC after ischemic damage. Under normal physiologic conditions, cytochrome c shuttles electrons from complex III to complex IV. However, under pathological oxidative stress conditions, methionine is oxidized disrupting the binding of $Met_{81}$ to the heme of cytochrome c resulting in the formation of cytochrome c peroxidase [264, 271].

The changes in the cytochrome c heme environment were detected in *in-vitro* studies by CD spectra shifts in the 375-425 nm region (heme moiety), changes in the UV region (250-280 nm) as well as the quenching of the $Trp_{59}$ fluorescence due to the closely located heme group [264, 271]. In addition, the disruption of the Fe-$Met_{81}$ bond can be detected by measuring its characteristic absorbance at 695 nm [264, 271]. Yet, the cause for the changes in absorbance or fluorescence cannot be confidently attributed to cytochrome c oxidation. For example, the loss of the 695-nm absorption in cytochrome c may also be due to the nitration of tyrosine residues, which is not a consequence of sulfhydryl oxidation in $Met_{81}$ [273]. However, the changes in absorbance/fluorescence can only indicate oxidation of the sixth heme ligand at $Met_{81}$ but there is no direct evidence supporting this speculation. Moreover, the sphectrophotometric approaches were used mainly for *in-vitro* studies wherein cytochrome c was the only protein present and so any changes in absorbance/fluorescence can only be attributed to the alterations in cytochrome c. However, these approaches cannot be used at a tissue level for characterizing cytochrome c peroxidase due to the complex mixture of proteins involved

which would make it impractical to attribute the changes in absorbance/fluorescence specifically to cytochrome c.

Murine cytochrome c has two methionines, one at position 66 and the other at position 81, whereas in the equine cytochrome c, methionines are located at positions 65 and 80. Oxidation of $Met_{81}$ (in mouse) or $Met_{80}$ (in horse) results in formation of cytochrome c peroxidase. *In-vitro* radiolysis of equine cytochrome c showed that $Met_{80}$ is the prime target for oxidation [311]. *In-vitro* studies using HOCl to oxidize cytochrome c were shown to disrupt the Fe-$Met_{80}$ bond of equine cytochrome c mainly by oxidation of $Met_{80}$. Oxidation of $Met_{80}$ facilitates the reactivity of heme center to $H_2O_2$ thereby inducing the peroxidase activity [272]. The mass spectrometry approach provided direct evidence that methionine residues are oxidized to methionine sulfoxide and that $Met_{80}$ oxidation was more favored than $Met_{66}$ (72% $Met_{80}$ vs. 23% $Met_{65}$) [272]. This suggests that methionine 80 (the heme ligand) in cytochrome c is the preferred site of oxidation. In addition, the HOCl oxidized cytochrome c exhibited an increase in peroxidase activity as seen by an increase in ability to oxidize tyrosine to tyrosyl radical (measured by EPR spectroscopy) [272] .

Though, the immunoblotting for methionine sulfoxide from HOCl- treated mitochondria supports the formation of cytochrome c peroxidase **(Figure 2.8A)**, identification of site specific oxidation of $Met_{81}$ from mouse hearts would unequivocally confirm the cytochrome c peroxidase formation. Hence, in order to confirm the specific oxidation of $Met_{81}$, we have utilized the mass spectrometric approach. In our study, we have shown at a tissue level that the cytochrome c immunocaptured from HOCl treated mitochondria showed site

specific oxidation of $Met_{81}$ which is inline with the earlier observation with *in-vitro* HOCl oxidation of commercial cytochrome c **(Figure 2.8A)**.

Actinomycin D or staurosporine induced apoptosis in cell culture models showed that cytochrome c bound to cardiolipin acts as a peroxidase that resulted in cardiolipin peroxidation and apoptosis [276]. Also, *in-vitro* direct measurements of peroxidase activity in the liposomes was measured using chemiluminescence, fluorescence and electron paramagnetic resonance based assays which determine cytochrome c peroxidase activity in the presence of $H_2O_2$ [276]. However, these studies functionally measure cytochrome peroxidase activity but could not characterize the cytochrome c peroxidase formed as a result of oxidative stress. Also, the role of $Met_{81}$ oxidation in cytochrome c peroxidase formation was unclear in these studies. Moreover, the cytochrome c peroxidase activity was well characterized in *in-vitro* liposomal systems [271, 276, 299, 312] or non-physiological cell stress models [276] and its physiological relevance is still unknown. Thus, the main objective of the present study was to identify the cytochrome c peroxidase formation at a tissue level during pathological condition such as ischemia-reperfusion.

Myocardial ischemia damages the mitochondrial electron transport chain resulting in decreased rates of mitochondrial respiration [5, 102, 203, 204, 222]. In our study, 25-min ischemia followed by 30-min reperfusion led to a significant decrease in glutamate+malate- and TMPD-dependent respiration **(Figure 2.11)** which was consistent with previous studies [102, 201, 206]. During ischemia, mitochondria are the major contributors of ROS production [5, 222]. Complex I and complex III are the major sites for ROS generation during ischemia. Antimycin A, given immediately before

ischemia, preserved complex IV respiration, cytochrome c content whereas treatment with azide did not protect the ischemia-mediated decrease in respiration and loss of cytochrome c [254]. This allows us to speculate that the locus of ischemic damage is located between complex III and complex IV and that increased ROS and electron flow to this segment both contribute to the ischemic damage. Key component of this locus is the cytochrome c which can potentially convert into the peroxidase during ischemia-reperfusion.

To identify the formation of cytochrome c peroxidase during ischemia-reperfusion, the immunocapture approach was used to specifically separate cytochrome c **(Figure 2.5)** from isolated mitochondria and asess the methionine sulfoxide formation. Oxidation of $Met_{81}$, loosens the iron coordination of cytochrome c providing access of the heme catalytic center to small molecules like $H_2O_2$. As a result, cytochrome c converts to a peroxidase which will reduce $H_2O_2$ to $H_2O$ and simultaneously generate peroxidized cardiolipin. Hence, Met(O) formation is the mechanistic indicator for cytochrome c peroxidase formation. In this study, we have demonstrated that ischemia-reperfused hearts show an approximate 80% increase in the methionine sulfoxide formation **(Figure 2.12)** which supports the role of cytochrome c peroxidase during physiological oxidative stress conditions. Further studies will be required to study the contribution of cytochrome c peroxidase during ischemia or during early reperfusion.

Blockade of the ETC at complex I decreases ROS generation and prevents cardiolipin depletion [210] which suggests that when electron flow into the cytochrome c-cardiolipin segment is limited it may inhibit peroxidase activity of cytochrome. In the present study, mitochondrial incubation with succinate+rotenone+TTFA did not increase the formation

of cytochrome c peroxidase. This observation suggests that the complex II generated ROS did not contribute to the peroxidase formation. The mitochondrial incubation with succinate+rotenone+antimycin A also did not increase peroxidase formation which suggests that the increase in ROS due to complex III blockade was not sufficient to convert cytochrome c to a peroxidase. Interestingly, incubation of mitochondria with succinate+rotenone+azide significantly increased the methionine sulfoxide signal as a result of cytochrome c peroxidase formation. This observation suggests that along with the increase in ROS from complex III, electron flow into cytochrome c was essential for oxidizing cytochrome c at the methionine residue resulting in formation of cytochrome peroxidase. Thus, from this study we have demonstrated that distal blockade of cytochrome c-cardiolipin segment with azide showed increase methionine sulfoxide formation when compared to proximal blockade of ETC with TTFA or Antimycin A **(Figure 2.14)**. This highlights the importance of electron flow through the cytochrome c segment as a key factor which influences peroxidase formation along with increased ROS during ischemia-reperfusion.

Experiments performed with different animal models using global ischemia or *in-vivo* ischemia showed an overall decrease in cardiolipin content [203, 216, 302]. The increase in ROS production during ischemia is converted to $H_2O_2$ which acts as a substrate for cytochrome c peroxidase causing the oxidation of cardiolipin to the peroxidized form. Cardiolipin can undergo oxidation at the unsaturated cis double bonds of the linoleic (C18:2) fatty acyl chains that will give rise to peroxy-groups: $(C18:2)_3/(C18:2\text{-}OOH)_1$, $(C18:2)_2/(C18:2\text{-}OOH)_2$, $(C18:2)_1/(C18:2\text{-}OOH)_3$, $(C18:2\text{-}OOH)_4$ [292]. Furthermore, hydrolysis of the peroxidized cardiolipin results in formation of

monolysocardiolipin (degradation product) [229]. Alternatively, the peroxy-acyl groups can interact directly with proteins leading to covalent cardiolipin-protein complexes. Also, inter-molecular dimerization of cardiolipin by peroxyl bond formation undergoes decomposition and finally generates a secondary peroxidation product, 4-hydroxy-2-nonenal (HNE) [313]. In addition, HNE forms Michael adducts by interacting with the nucleophilic groups in cysteine, histidine or lysine residues of the proteins. Also, HNE can interact with ε-$NH_2$ groups of Lys residues forming Schiff-bases [314]. The decomposed cardiolipin or cardiolipin interacting with proteins is no longer extractable by organic solvents and thus cannot be detected [308].

In this study, we have shown that incubation of isolated mitochondria for 50 min with succinate+rotenone+azide enhanced peroxidase formation as detected by increase in Met(O) signal but did not alter cardiolipin content (data not shown). Further mitochondrial incubation with succinate+rotenone+azide for 90 min resulted in depletion of cardiolipin **(Figure 2.15)**. This suggests that peroxidase formation occurs earlier than peroxidation of cardiolipin. In addition, the data confirms that the increase in ROS generation along with the electron flow through cytochrome c enhanced the peroxidase activity of cytochrome c leading to the depletion of cardiolipin from the mitochondria **(Figure 2.15)**. Moreover, we were not able to detect any monolysocardiolipin, a degradation product of cardiolipin. So, it is possible that the oxidized cardiolipin is degraded via hydrolysis or modified to form Michael adducts or Schiff's bases. Future studies to support the depletion of cardiolipin via degradation will include blotting for HNE in the mitochondrial incubations.

Ischemia decreased cardiolipin content in rabbit heart mitochondria whereas the content of other phospholipids was preserved [203]. Also, ischemia did not alter the composition of cardiolipin that remained in the mitochondrial membrane [203]. This is consistent with our study using distal blockade of ETC wherein cardiolipin content was decreased but the remaining cardiolipin composition was not altered **(Figure 2.15)**. In our study, the cytochrome c peroxidase formation was increased during ischemia-reperfusion **(Figure 2.12)** that recapitulates the role of cytochrome c peroxidase in the depletion of cardiolipin in rabbit mitochondria [203]. Rotenone or amobarbital treatment immediately before *in-situ* ischemia markedly improved respiration and attenuated the loss of cardiolipin and cytochrome c from the mitochondria [230, 255]. Antimycin A, given before ischemia, preserved complex IV respiration and cytochrome c content [254]. On the other hand, azide treatment before ischemia resulted in decreased respiration and cytochrome c content [254]. These observations from *ex-vivo* ischemia-reperfusion studies strongly supports that the blockade of electron flow into cytochrome c protects mitochondria and preserves cardioipin content which conceptually correlates to the observations from the *in-vitro* mitochondrial incubations from our study.

In summary, the present study showed that cytochrome c converts to cytochrome c peroxidase during ischemia-reperfusion. The increase in ROS generation and electron flow through the cytochrome c segment were required for the cytochrome c peroxidase activity that results in depletion of cardiolipin from the mitochondria **(Figure 2.16)**.

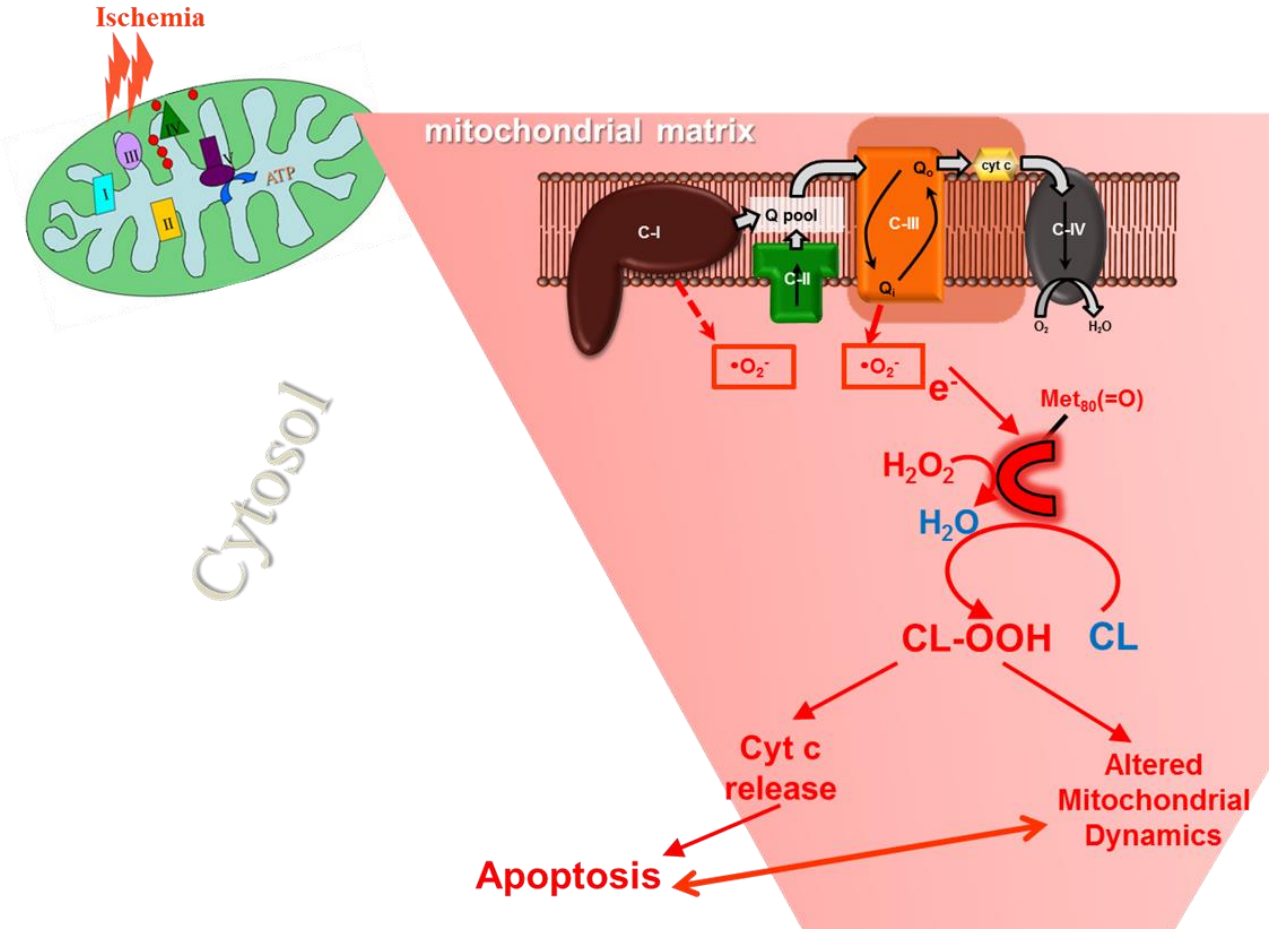


**Figure 2.16. Schematic showing the formation of cytochrome c peroxidase during ischemia-reperfusion.** Electron flow into cytochrome c and reactive oxygen species from electron transport chain oxidize cytochrome c during ischemia-reperfusion converting it into a peroxidase. Cytochrome c peroxidase, converts $H_2O_2$ to $H_2O$ inturn peroxidising cardiolipin thereby depleting it from the mitochondrial membrane. Depletion of cardiolipin delocalizes cytochrome c into the cytosol activating apoptotic cascades. The peroxidized cardiolipin also alters the mitochondrial dynamics thereby triggering cell death.

# CHAPTER III: Apoptosis signaling kinase-1 inhibitor decreases mitochondrial damage during ischemia-reperfusion

## III. 1. Introduction

Living organisms, during their lifetime, are exposed to ROS which is released as a consequence of several physico-chemical stressors. While small amounts of ROS have an important function as signal mediators, their overproduction in cells causes pathological redox signaling which induces oxidative stress ultimately leading to cell death [315-317]. In order to maintain homeostasis, cells have defense mechanisms to counteract the excessive production of ROS. One of the major intracellular defense mechanisms against the oxidative stress is the thioredoxin (Trx) system [318].

### III. 1. 1. Thioredoxin/ Thioredoxin reductase system

Thioredoxin system contains thioredoxin, NADP (H) and thioredoxin reductase; together they maintain a reduced intracellular redox state by the reduction of protein thiols. Cytosolic thioredoxin-1 (Trx1) and mitochondrial Trx2 are the two major isoforms of thioredoxin encoded by two distinct genes. Trx, an antioxidant protein, contains an

active site with two cysteine residues which under reduced conditions exist as thiols. However, during oxidative stress conditions, the thiols are reversibly oxidized to form an intramolecular disulfide bond [319, 320]. Studies from thioredoxin genetic mouse models suggest that thioredoxin is essential for survival. Thioredoxin-knockout mice have shown that Trx is essential for the early development and morphogenesis of the mouse embryo [321]. Thioredoxin-overexpressor transgenic mice are more resistant to oxidative stress with longer life spans, compared to the wild-type mice [322].

The thioredoxin-interacting protein TXNIP, also known as VDUP1 (vitaminD3 up-regulatedprotein-1) or TBP-2 (thioredoxin-binding protein-2), binds to both thioredoxin isoforms (Trx1, Trx2) and negatively regulates Trx ability to scavenge ROS **(Figure 3.1)** [323-325]. On the other hand, Trx is bound directly to apoptosis signal-regulating kinase 1 (ASK1) that inhibits ASK1 kinase activity [319, 326, 327]. Under oxidative stress conditions, TXNIP localized primarily in the nucleus, translocates to cytosol and mitochondria where it binds to and oxidizes Trx1 and Trx2, thereby reducing Trx1/Trx2 binding to ASK1 and allowing for ASK1 phosphorylation/activation **(Figure 3.1)** [324, 328, 329]. The interaction between Trx and ASK1 depends on the redox state of Trx, which is supported by experimental studies wherein ASK1 fails to interact with the oxidized form of Trx or with a Trx mutant in which both active site cysteines are replaced with serine residues [330].

ASK1 belongs to the mitogen-activated protein kinase (MAPK) kinase kinase family that activates the MAPK kinase 4 (MKK4)/MKK7-JNK and MKK3/6-p38 pathways through a ROS-dependent mechanism in response to various stress conditions including ischemia-reperfusion injury, oxidative stress, tumor necrosis factor-α (TNF-α),

lipopolysaccharide (LPS), endoplasmic reticulum stress and calcium overload [331-336]. Activation of these pathways induces cellular responses such as apoptosis, differentiation, cell survival, and production of inflammatory cytokines [337, 338]. Sustained activation of ASK1 induces apoptosis mainly through mitochondria-dependent caspase activation [330, 339, 340]. TNFα-induced apoptosis in mouse embryonic fibroblasts (MEFS) from ASK1 deficient mice demonstrated that ASK1 is required for the execution of ROS-induced apoptosis through JNK/p38 pathways [337].

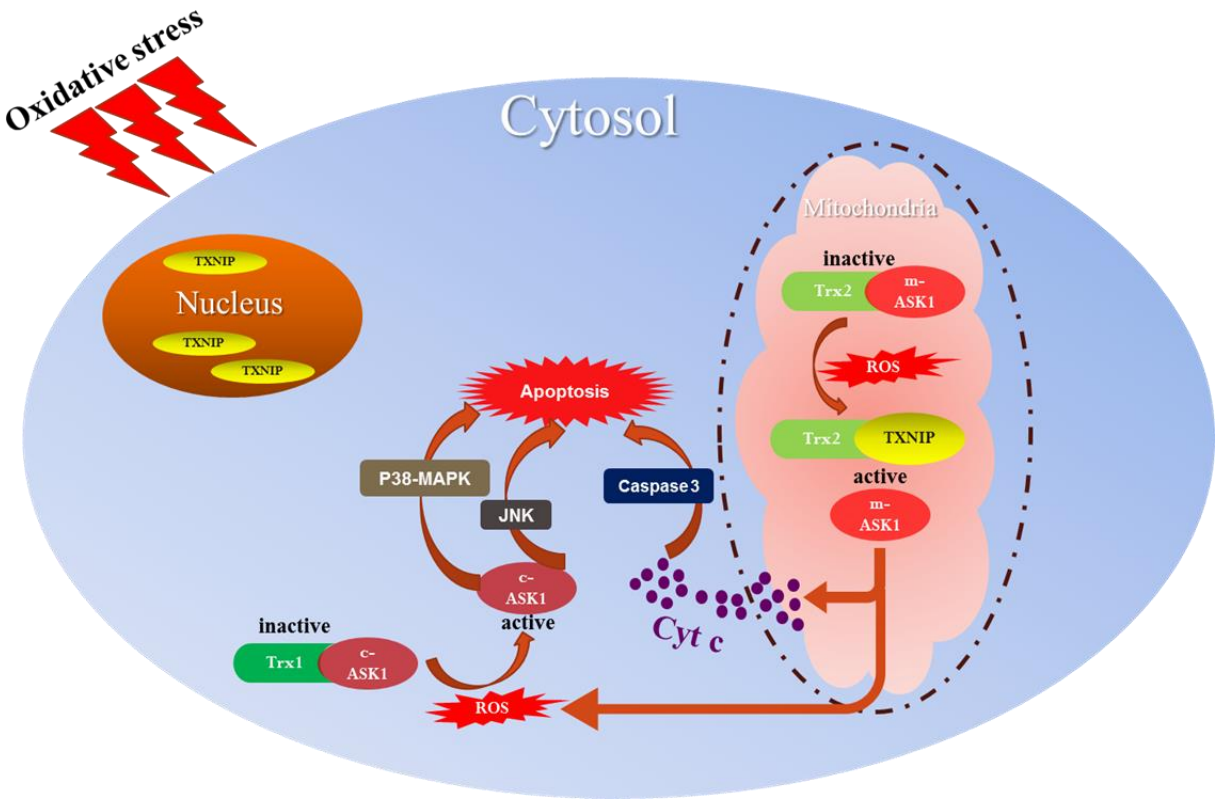


**Figure 3.1. Schematic depicting the activation of ASK1 signaling cascade during oxidative stress conditions.** TXNIP localized primarily in the nucleus, translocates to cytosol and mitochondria where it binds to and oxidizes Trx1 and Trx2, thereby reducing Trx1/Trx2 binding to ASK1 and allowing for ASK1 phosphorylation/activation. ASK1 activation leads to cell death via p38, JNK or mitochondrial dependent pathways.

ASK1 is constitutively oligomerized through its C-terminal coiled-coil (CCC) domain, which is necessary for its basal activity [341, 342]. Under physiological conditions, Trx inhibits the homo-oligomeric interactions through the N-terminal coiled-coil (NCC) domain of ASK1 [343]. However, during oxidative stress conditions, Trx dissociates from ASK1. ASK1 activates itself by homo-oligomerization of ASK1 through its NCC domain thereby resulting in autophosphorylation at the threonine 845 residue (**Figure 3.2)** [342]. Post-translational modification of ASK1, including phosphorylation, regulates ASK1 activity. Akt directly phosphorylates ASK1 at Ser83 and negatively regulates ASK1 [344, 345]. Moreover, calcium/calmodulin-dependent protein kinase type II (CaMKII), in response to calcium influx, also phosphorylates ASK1 and activates the ASK1-p38 pathway [336]. In addition to phosphorylation, ubiquitination is shown to stabilize ASK1 and is important for the net activation of ASK1 and ROS-induced cell death [346]. On the other hand, two protein phosphatases, protein phosphatase 5 and serine/threonine protein phosphatase (PP2Cε) inactivate ASK1 by directly dephosphorylating Thr845 residue [347, 348].

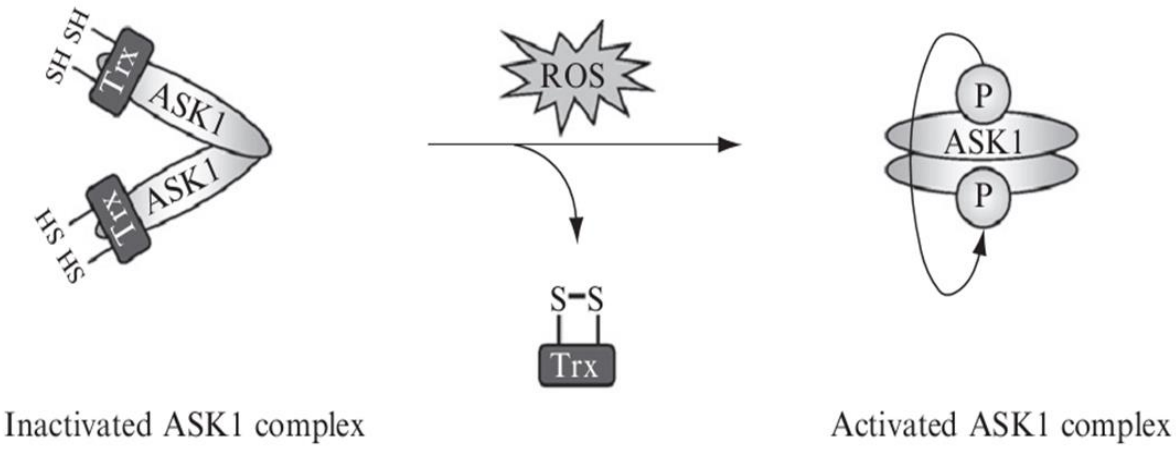


**Figure 3.2. Schematic model of ROS-induced activation of ASK1 regulated by Trx.** ASK1 is constitutively oligomerized through its C-terminal coiled-coil (CCC) domain. Trx inhibits the homo-oligomeric interactions through the N-terminal coiled-coil (NCC) domain of ASK1. During oxidative stress conditions, Trx dissociates from ASK1. ASK1 activates itself by homo-oligomerization of ASK1 through its NCC domain thereby resulting in autophosphorylation at the threonine 845 residue [319]. Trx, thioredoxin; ASK1, Apoptosis signaling kinase 1.

### III. 1. 2. ASK/p38/JNK activation during ischemia reperfusion injury

It is well understood that increased ROS production during ischemia-reperfusion contributes to cardiac injury. One of the mechanisms through which ischemia-reperfusion contributes to cell death is via the ROS-dependent activation of JNK/p38 pathways [349, 350] . JNK and p38 are differentially activated during ischemia-reperfusion. The p38 pathway is rapidly activated during ischemia and remains active during reperfusion whereas JNK is activated only during reperfusion [351-353]. Cloning and transfection experiments using cell culture and mouse gene knockout experiments have shown that ASK1 is the upstream regulator for JNK and p38 [354, 355]. Downstream to ASK1, MKK4 and MKK7 regulate JNK [356-358], while MKK3 and MKK6 regulate p38 [356, 359].

Recent studies in cardiac myocytes have confirmed that ischemia preferentially activates ASK1 and thereby MKK6-p38 pathway but does not activate JNK [360]. ASK1-deficient cardiomyocytes are resistant to $H_2O_2$- or calcium-induced cell death [361]. Also, ASK1 overexpression negatively regulates heat shock transcription factor-1 (HSF-1) [362]. In turn, HSF-1 protects heart against ischemia-reperfusion injury [363, 364] by inhibiting $H_2O_2$-induced JNK activation and apoptosis [365]. Compared to young animals, cardiomyocyte apoptosis and infarct size during ischemia-reperfusion is increased in aging animals due to inhibition of Trx activity and subsequent disruption of Trx-ASK1 interactions [366]. As a result of increased afterload in chronic models of heart failure, as in transverse aortic constriction [367] or altered regional mechanical stress [368], the effects of increased ASK1 are observed weeks after the insult. However, following increased ROS generation and intense neurohormonal activation as

a result of cardiac decompensation, the protection of ASK1 deletion against adverse cardiac remodeling is evident 2 to 4 weeks after transverse aortic constriction or non-reperfused acute myocardial infarction [367, 368]. In the cardiomyopathic hamster model, adenovirus transfection of a dominant-negative ASK1 mutant gene suppressed heart failure progression by preventing cardiomyocyte apoptosis [369]. Together, all these studies suggest that ASK1 couples increase in ROS production to induction of cell death pathways.

A study by Watanabe et al., with $ASK1^{-/-}$ (knock-out) mice has shown a >50% decrease in infarct size following ischemia-reperfusion [361]. Another study by Liu et al., showed that cardiac-specific and inducible overexpression of ASK1 in the heart led to a 2-fold increase in infarct size after 60 minutes of regional myocardial ischemia and reperfusion [367]. Interestingly, in the absence of ischemia, cardiac specific overexpression of ASK1 had no baseline effects in the mice [367]. This observation highlights the role of ASK1 as a cellular redox sensor that is activated by ROS rather than a simple chemical mediator of cardiac injury. All the above studies suggest that ASK1 activation through p38/JNK pathways contributes to the pathogenesis of myocardial ischemia-reperfusion injury. Thus, any manipulations to inhibit ASK1/p38/JNK pathways should provide cardioprotection against ischemia-reperfusion injury.

### III. 1. 3. Pharmacological inhibitors of ASK/p38/JNK pathway

Many recent studies using inhibitor molecules have shown that the components of the ASK1-MAPK are potential therapeutic targets for decreasing cardiac injury during ischemia-reperfusion [351, 370, 371]. Among such compounds, p38 inhibitors have

been extensively studied. *In-vitro* treatment with a p38 inhibitor prior to ischemia protected the cardiac cells from ischemia/reperfusion injury [372-374]. *Ex-vivo* [375-377] and *in-vivo* studies [378-380] with p38 inhibitor treatment during pre-ischemia reduced infarct size and improved left ventricular (LV) function. However, inconsistent findings are also reported in which inhibitor treatment prior to ischemia failed to reduce the infarct size [381, 382]. Although p38 inhibitors are efficient in reducing cardiac injury in animal models, the outcomes from clinical use are disappointing due to their toxicity [383-386]. Recently, pre-treatment with an inhibitor of JNK, D-JNKI-1, at the time of left coronary artery occlusion was shown to markedly decrease infarct size after reperfusion [370]. In addition, an upstream kinase such as ASK1 is an alternative therapeutic target which regulates the stress responses through the JNK and p38 pathways and may provide less toxic pharmaceutical treatment options [387]. In a very recent study by Toldo et al., treatment with ASK1-inhibitor (ASK1-i), GS-459679, at reperfusion led to a significant dose-related reduction in infarct size, inhibition of apoptotic cell death, and preservation of left ventricular dimension and systolic function at both 24 hours and 7 days [388].

Mitochondria are both the targets and sources of damage during cardiac ischemia and reperfusion [5, 222]. Myocardial ischemia disrupts the electron transport chain that results in decrease in the rate of the integrated respiration and increase in ROS generation [5, 222]. This in turn predisposes mitochondria to MPTP opening, cytochrome c release and activation of apoptosis [147, 154, 228]. In view of the substantial reduction in cardiac injury observed in the *in-vivo* model with ASK1-i

treatment [388], it is of great interest to understand the potential role of mitochondria in the observed cardioprotection during ischemia-reperfusion.

## RESEARCH AIMS

ASK1 (apoptosis signal regulating kinase 1) is a MAPK (mitogen-activated protein kinase) kinase kinase, and its activation during ischemia (ISC)-reperfusion (REP) increases cardiac injury through p38 and JNK pathways [320, 360]. ASK1 is considered as a cytosolic protein (c-ASK1) [320]. Mitochondrial localized ASK1 (m-ASK1) has recently been identified [389]. ASK1 is deactivated when it is bound on its endogenous inhibitor, a reduced thioredoxin (Trx). ISC damages the ETC and increases the production of reactive oxygen species (ROS) which oxidizes Trx thereby activating ASK1 [319]. Earlier work showed that the selective small molecule inhibitor of ASK1 (ASK1-i) given at reperfusion led to a significant dose-related reduction in infarct size measured *in-vivo* at both 24 hours and 7 days [388].

Damage to the mitochondrial electron transport chain (ETC) from ischemia (ISC) increases oxidant production and favors mitochondrial permeability transition (MPTP) during REP [5, 222]. In view of the substantial reduction in cardiac injury observed in the in vivo model, the potential role of mitochondria in the protection from ASK1-i treatment was studied.

## Specific aim:

1. To identify whether mitochondria contribute to the cardioprotection confered by ASK1 inhibition at reperfusion in the *in-vivo* model of ischemia-reperfusion.

### III. 2. Materials and Methods

#### III. 2. 1. Materials

All chemicals and reagents were purchased from Fisher Scientific, Pittsburgh, PA, or stated otherwise, except the ones used in mitochondria isolation and mitochondria-related functional assays, which were purchased from Sigma-Aldrich, Saint Louis, MO.

**Animals**

Animals were purchased and housed as mentioned in Materials and Methods II. 2. 1.

**III. 2. 2. METHODS**

**III. 2. 2. 1. Preparation of mouse heart for perfusion**

Hearts from male C57BL/6 mice were excised and perfused using a Langendroff perfusion system as explained in Material and Methods II. 2. 2. 1.

**III. 2. 2. 2. Lactate dehydrogenase (LDH) assay**

Lactate dehydrogenase catalyzes the oxidation of lactate as shown in the following reaction:

$$\text{Lactate} + NAD^+ \leftrightarrow \text{pyruvate} + NADH + H^+$$

During ischemia, deficiency of oxygen and metabolic substrate depletes cellular ATP which leads to loss of cellular integrity. As a result, intracelluar enzymes such as LDH and creatine kinase were released into the extracellular space.

For the assay, the following solutions are made fresh and kept on ice until used: 100 mM phosphate (pH 7.5), 125.3 mM pyruvate and 11.3 mM NADH. Coronary effluent collected during 30 min of reperfusion was tested for LDH release. Reaction was started by adding 0.20 ml of effluent to 0.76 ml of 100 mM phosphate buffer which was

incubated for 5 min. Following 30 µl of 11.3 mM NADH was added and the baseline reading was recorded. Finally 10 µl of 125.3 mM pyruvate was added and the oxidation of NADH was monitored as a decrease in absorption at 340 nm.

### III. 2. 2. 3. Isolation of mitochondria, cytosol, and heart tissue homogenates

Following perfusion, mitochondria were isolated from the hearts as described in Materials and Methods II. 2. 2. 2.

### III. 2. 2. 4. Measurement of oxidative phosphorylation in intact mitochondria

Oxygen consumption in isolated mitochondria was measured using a Clark-type oxygen electrode at 30°C as explained in Materials and Methods II. 2. 2. 3.

### III. 2. 2. 5. Measurement of mitochondrial membrane potential

Membrane potential of intact mitochondria ($\Delta\Psi_m$) was measured using the fluorogenic indicator, tetramethylrhodamine methyl ester (TMRM) dye (Invitrogen, Carlsbad, CA) as described below. TMRM is a lipophilic cation which accumulates in the mitochondria in proportion with membrane potential according to the Nernst equation. As the dye accumulates in the mitochondria it exhibits a red shift in both its absorption and fluorescence emission spectra. When mitochondria were uncoupled, TMRM was mostly in the medium exhibiting excitation spectra at 546 nm whereas when mitochondria were coupled or polarized, TMRM accumulates inside the mitochondria exhibiting excitation spectra at 573 nm. These properties were used to dynamically monitor $\Delta\Psi_m$ of isolated mouse heart mitochondria using a ratio fluorescence approach (573/546). Emission intensity at 590 nm was recorded by LS55 Fluorescence Spectrometer (PerkinElmer,

Waltham, MA). Freshly isolated mitochondria (200 µg) were incubated in respiration buffer (100 mM KCl, 50 mM MOPS, 5 mM $KP_i$, 1 mM EGTA) with 0.1 µM TMRM with stirring at 30°C. Mitochondria were polarized and depolarized by sequential addition of 5 mM glutamate + 1.25 mM malate (state 2 respiration) and 0.5 mM ADP (state 3 respiration: uses protons to produce ATP from ADP by complex V). The membrane potential was re-generated by adding 1 nM oligomycin which inhibits complex V ($state4_{oligomycin}$) followed by titration with 25 µM DNP resulting in complete uncoupling of of the mitochondria ($\Delta\Psi_0$). The difference between state $4_{oligomycin}$ and $\Delta\Psi_0$ is termed $\Delta\Psi_{max}$ which should correspond to the the physiological $\Delta\Psi_m$ (theoretical value is -160 mV).

### III. 2. 2. 6. Mitochondrial $H_2O_2$ net production

Mitochondria-generated $H_2O_2$ was measured by the enzymatic oxidation of the fluorogenic indicator Amplex Red (10-acetyl-3,7-dihydroxyphenoxazine) (Invitrogen, Carlsbad, CA) in the presence of horseradish peroxidase (HRP) (Sigma-Aldrich, Saint Louis, MO) which produces the fluorescence product, resorufin as described below. The fluorescence of resorufin (Ex = 530 ± 25nm; Em = 585 ± 30nm) was measured by LS55 Fluorescence Spectrometer (PerkinElmer, Waltham, MA) with stirring at 30 $^oC$. Isolated mouse mitochondria (20µg) were incubated in buffer MMC (120 mM KCl, 5 mM $KH_2PO_4$, 1 mM EGTA; chelex treated buffer; (all from Sigma-Aldrich, Saint Louis, MO)) along with 25 µM Amplex Red and 0.25 units/ml HRP. Glutamate (6.67 mM) + Malate (3.33 mM) and succinate (6.67 mM) were used as complex I and complex II substrates along with their respective inhibitors rotenone (5 µM) and antimycin A (10 µM) to generate maximal complex I dependent and complex III dependent $H_2O_2$ production.

The amount of $H_2O_2$ generated was calculated based on the standard curve with known $H_2O_2$ concentrations. To show specificity of the assay, bovine liver-derived catalase (Sigma-Aldrich, Saint Louis, MO) was added to the reaction mixture incubated with succinate in the presence of antimycin A which quenches > 90% of the signal from $H_2O_2$ generation.

### III. 2. 2. 7. Determination of Calcium Retention Capacity

Calcium Retention Capacity (CRC) was defined as the amount of $Ca^{2+}$ required to trigger a massive $Ca^{2+}$ release by isolated cardiac mitochondria as described by Ichas *et al* [390]. Mitochondrial tolerance to calcium loading, CRC, is an indicator of the resistance of mitochondria to mitochondrial permeability transition pore opening (MPTP) following matrix $Ca^{2+}$ accumulation. Extra-mitochondrial $Ca^{2+}$ concentration was studied in the single-cell fluorimeter (LS 55; PerkinElmer, Waltham, MA) by monitoring the decrease in extra-mitochondrial $Ca^{2+}$ concentration using the fluorescent probe Calcium-Green 5N (Invitrogen, Carlsbad, CA) at excitation/emission wavelengths of 500/530 nm respectively. Calcium-Green fluorescence units were used to calculate the amount of mitochondrial $Ca^{2+}$ uptake by converting the signal to [$Ca^{2+}$], expressed as nmol $CaCl_2$/mg mitochondrial proteins, using an exponential standard curve established with increasing amounts of $Ca^{2+}$. Freshly isolated mitochondria (250 µg proteins) were incubated in CRC buffer (150 mM sucrose, 50 mM KCl, 2 mM $KH_2PO_4$ and 20 mM Tris/HCl, pH 7.4) along with 0.5 mM calcium green and 5 mM succinate for 60 sec with stirring at 30 °C. Pulses of calcium (20 nmoles) were added at 60 sec intervals and the progressive uptake of $Ca^{2+}$ by mitochondria was monitored until mitochondrial $Ca^{2+}$ release caused by MPTP opening was observed. CRC, an index of MPTP sensitivity,

was calculated as total amount of $Ca^{2+}$ taken up by mitochondria prior to triggering massive $Ca^{2+}$ release.

### III. 2. 2. 8. Spectrophotometric measurement of activity of mitochondrial enzymes

Enzyme activities of detergent-solubilized mitochondria were measured spectrophotometrically at 30 $^{o}$C as described below. Frozen mitochondria were thawed and solubilized in MSM/EDTA buffer (220 mM mannitol, 70 mM sucrose, 5 mM MOPS, 2 mM EDTA, pH 7.4) containing 0.5% cholate. The final protein concentration of solubilized mitochondria was 1 µg/µl. Calculated enzyme activities were expressed as nmol/min per mg of mitochondrial protein or 1/min/mg in case of complex IV.

### III. 2. 2. 8A. NADH-ubiquinone oxidoreductase (complex I)

Complex I activity was measured as a decrease in reduced nicotinamide adenine dinucleotide (NADH) added exogenously. Oxidation of NADH results in decreased absorbance at 340 nm which was monitored. Solubilized mitochondria (15 µg) were incubated in 1ml buffer containing 50 mM $KH_2PO_4$ pH 7.4, 0.1 mM EDTA, 0.2% de-fatted BSA (w/v), 0.015% sonicated asolectin, 0.2 mM NADH, 20 µg of antimycin A. After 2 min of equilibration, 0.05 mM oxidized decylubiquinone (DUQ) was added and the decrease in NADH concentration was monitored. Enzyme activities were calculated using an extinction coefficient of 6.22 $mM^{-1}cm^{-1}$ for NADH. Rotenone was used as a specific inhibitor of NADH-ubiquinone oxidoreductase activity. Thus, final rotenone-sensitive complex I activity was determined by subtracting the rate measured in the presence of 7.5 µM rotenone from the rate obtained without inhibitor.

### III. 2. 2. 8B. NADH-ferricyanide reductase (NFR)

NFR assay measures activity of the rotenone-insensitive proximal portion of complex I, which has a functional NADH dehydrogenase activity with non-covalently bound flavin-mononucleotide (FMN) molecule. NFR activity was recorded as a decrease in absorbance at 340 nm due to the oxidation of exogenously added NADH. The reaction is carried out in 1ml buffer at pH 7.4 containing 50 mM $KH_2PO_4$, 0.1 mM EDTA, 0.2% de-fatted BSA (w/v), 0.015% sonicated asolectin, 0.66 mM $K_3Fe(CN)_6$ (potassium ferricyanide, an artificial electron acceptor from FMN), 2 mM $NaN_3$ and 0.2 mM NADH. After the acquisition of a baseline reading, reaction was initiated by addition of 5 µg of mitochondrial protein and the NFR activities were calculated using an extinction coefficient of 6.22 $mM^{-1}cm^{-1}$ for NADH. Actual rates of NFR complex were obtained after substracting the baseline rates obtained in the absence of mitochondria.

### III. 2. 2. 8C. Succinate-decylubiquinone oxidoreductase (complex II)

Complex II activity was determined by monitoring the reduction of 2, 6-dichlorophenolindophenol (DCPIP), a potent acceptor of electrons from complex II-dependent reduced quinols. The reduction of DCPIP was measured sphectrophotometrically as a decrease in absorbance at 600 nm. Buffer at pH 7.4 containing 50 mM $KH_2PO_4$, 1 mM EDTA, 0.1% de-fatted BSA (w/v), 2 mM $NaN_3$, 30 µl of DCPIP (of OD of 30 µl in 1 ml of $H_2O$ being about 1.8), 0.05 mM oxidized DUQ (saturating amounts of exogenous ubiquinone), and 10 µg of mitochondrial protein in a total volume of 1ml was incubated for 3 min. After the equilibration period, reactions were started by the addition of 20 mM succinate, and the decrease in absorbance at

600 nm was monitored. Rates were calculated using DCPIP extinction coefficient of 21 $mM^{-1}cm^{-1}$. Theonyltrifluoroacetone (TTFA) was used as a specific inhibitor of succinate-ubiquinone oxidoreductase activity. TTFA-sensitive rates were calculated by subtracting the rate measured in the presence of 1 mM TTFA from the rate without the inhibitor.

**III. 2. 2. 8D. Ubiquinol: cytochrome c oxidoreductase (complex III)**

Complex III activity was measured as an increase in absorbance at 550 nm due to the reduction of cytochrome c. Reaction buffer (1 ml) at pH 7.4 containing 50 mM $KH_2PO_4$, 0.05 mM EDTA, 0.125% de-fatted BSA (w/v), 2 µg of mitochondrial protein extract, 3 mM $NaN_3$ and 0.06 mM cytochrome c was equilibrated for 1 min. After equilibration, the reaction was initiated by adding 0.1 mM reduced decylubiquinol (DUQ). Rates were calculated using an extinction coefficient of 19.1 $mM^{-1}cm^{-1}$ for reduced cytochrome c. Antimycin A-sensitive activity was measured by subtracting the rates measured in the presence antimycin A (20 mM) from the rate obtained without the inhibitor.

**III. 2. 2. 8E. Cytochrome c oxidase (complex IV)**

Complex IV activity was determined by monitoring the oxidation of exogenously added reduced cytochrome c which was measured as a decrease in absorbance at 550 nm. Reaction buffer at pH 7.4 containing 50 mM $KH_2PO_4$, 0.015% asolectin, 80 µl of 0.89 mM reduced cytochrome c in a final volume of 1 ml was incubated for 8 min. After the equilibration period, reactions were started by adding 2 µg of mitochondrial protein. The decrease in absorbance at 550 nm was monitored and the reaction follows substrate dependent first order kinetics. Rates were calculated and were expressed as 1/min/mg of mitochondrial protein.

Reduced cytochrome c was prepared by adding sodium dithionate ($Na_2S_2O_4$) to 5 ml of 3 mM oxidized cytochrome c followed by vigorous vortexing. The $Na_2S_2O_4$ treated cytochrome c solution was seperated on Amersham PD-10 column (GE Healthcare Life Sciences, Piscataway, NJ) to remove $Na_2S_2O_4$ from the solution. Collected 3 mM reduced cytochrome c was diluted with distilled $H_2O$ to a final volume of 10 ml. Reduced cytochrome c concentration was measured spectrophotometrically and calculated using its extinction coefficient 19.1 $mM^{-1}cm^{-1}$. One batch of the obtained reduced cytochrome c was used for all the samples assayed.

### III. 2. 2. 8F. Citrate synthase

In Krebs cycle, the formation of citrate from acetyl coenzyme A and oxaloacetate is catalyzed by citrate synthase which is an enzyme specific for the mitochondrial matrix. Citrate synthase activity assay measures of the rate of generation of mercaptide ion when citrate reacts with 5,5′-dithio-bis(2-nitrobenzoic acid) (DTNB, Ellman's reagent). The formation of yellow mercaptide ion was quantified spectrophotometrically by measuring the absorbance at 412 nm. Mitochondrial protein extracts (2 µg) were added to the reaction mixtures containing 0.1 mM DTNB and 0.34 mM acetyl CoA in a final volume of 1 ml, and the baseline reading was taken. Next, the reactions were started by adding 0.5 mM oxaloacetic acid (OAA) and the increase in absorbance at 412 nm was recorded. Activities were calculated using an extinction coefficient of 13.6 $mM^{-1}cm^{-1}$ for mercaptide ion, a result of a side reaction of DTNB with CoA-SH, a product of citrate synthase-mediated reaction.

### III. 2. 2. 9. Western blot analysis

Proteins were separated using SDS/PAGE electrophoresis system, transferred to the PVDF membrane as explained in Materials and Methods II. 2. 2. 6. The membrane is incubated with the cytochrome c (BD Biosciences) or α-Tubulin (Abcam) primary antibodies followed by Horse Radish Peroxidase (HRP) conjugated anti-mouse or anti-rabbit secondary antibody. The immunoreactive proteins were visualized using Amersham ECL Plus western blotting detection reagents (GE Healthcare Lifesciences, Piscataway, NJ) and measured as explained in Materials and Methods II. 2. 2. 6.

## III. 2. 3. STATISTICAL ANALYSIS

Data were expressed as the mean ± standard error of the mean and the statistical analysis were performed as mentioned in Materials and Methods II. 2. 3.

## III. 3. RESULTS

Studies from transgenic mouse models have shown that ASK1 is central to ischemia-reperfusion injury [361, 380]. Pharmacological treatment with ASK1-inhibitor (ASK1-i), GS-459679, at the onset of reperfusion decreases infarct size and improves cardiac function measured at 24 hr and 7 days [388]. Since cardiac mitochondria are both sources and targets of ischemic damage, we hypothesized that ASK1 inhibition would change the response of mitochondria to the ischemic insult resulting in cardioprotection observed *in-vivo.* Ischemic insult affects the electron transport chain, which in turn leads to decrease in the rate of integrated respiration [5].

In our experiments, we have used a Langendorff mouse model of ischemia and reperfusion that is established in our laboratory [306]. In this model of ischemia-reperfusion, the isolated, buffer perfused mouse hearts underwent 25 min of ischemia and 30 min of reperfusion followed by isolation of mitochondria. Four groups of mice were studied. Time control perfusion and untreated ischemia-reperfusion mice were control groups, and were treated with vehicle (DMSO). ASK1-i (10 µM final concentration) was given either before ischemia and during early reperfusion or during early reperfusion alone **(Figure 3.3)**. Cardiac function was monitored and lactate dehydrogenase (LDH) release during reperfusion was measured as the index of cell death in all the four groups. Mitochondria were isolated and oxidative-phosphorylation was measured using glutamate, succinate and TMPD/ascorbate as substrates. Mitochondrial susceptibility to MPTP opening was studied using the the calcium retention capacity (CRC) assay. Mitochondrial membrane potential was measured using the TMRM assay. The Amplex Red assay was used to measure $H_2O_2$ release from the

mitochondria. Spectrophotometric assays to determine changes in ETC complex activites were performed. Additonally, changes in specific protein levels were measured using Western blotting.

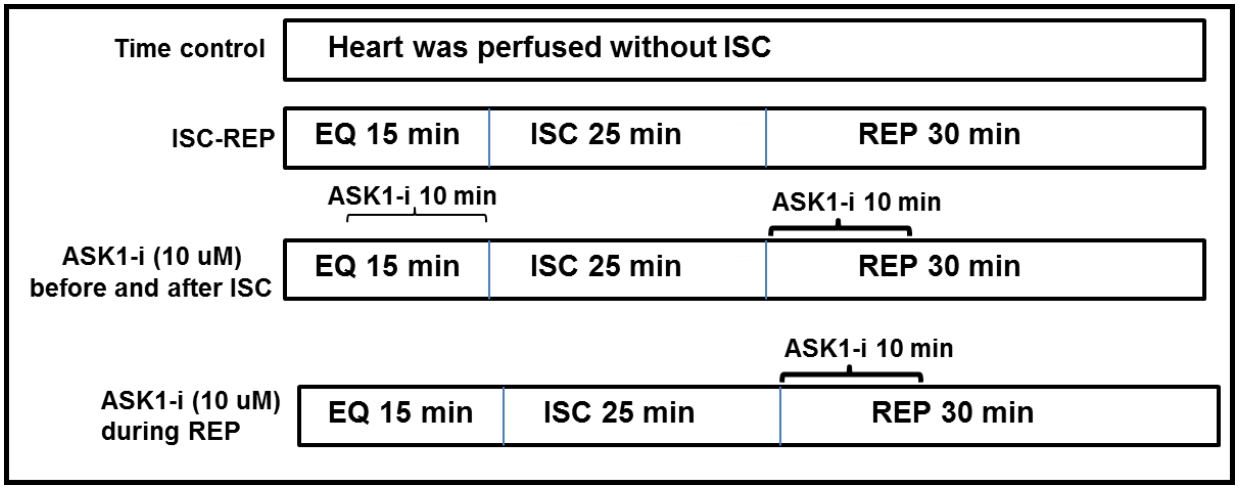


**Figure 3.3. Experimental Protocol.** ASK1-i was first dissolved in DMSO as vehicle, then diluted into Krebs-Henseleit (K-H) buffer to reach final concentration 10 uM. DMSO (0.001%) was added into K-H buffer for time control and ischemia-reperfusion hearts. EQ, equilibration; ISC-ischemia; REP- reperfusion.

### III. 3. 1. ASK1-i treatment improves cardiac function in mouse hearts following ischemia-reperfusion

Cardiac function was monitored in hearts that underwent TC perfusion, ISC-REP, ASK1-i before and after ISC, ASK1-i during reperfusion. The left ventricular developed pressure (LVDP) and diastolic pressure were recorded. In the four groups, the LVDP was similar in each group at the end of equilibration perfusion **(Figure 3.4)** [TC perfusion: 84±3 mm Hg; ISC-REP: 79±7; ASK1-i before and after ISC: 74±5; ASK1-i during reperfusion: 75±5; p=ns]. In untreated ISC-REP hearts and ASK1-i treatment before and after ISC, LVDP was markedly decreased during reperfusion compared with the pre-ischemic value [ISC-REP: 26±5 mm Hg; ASK1-i before and after ISC: 15±5; $p<0.05$ vs. TC perfusion]. In contrast, ASK1-i administration only during early reperfusion significantly increased LVDP during 60 min reperfusion compared with the untreated hearts or ASK1-i treatment before and after ISC [ASK1-i during reperfusion: 42±3 mm Hg; $p<0.05$ vs. ISC-REP] **(Figure 3.4)**.

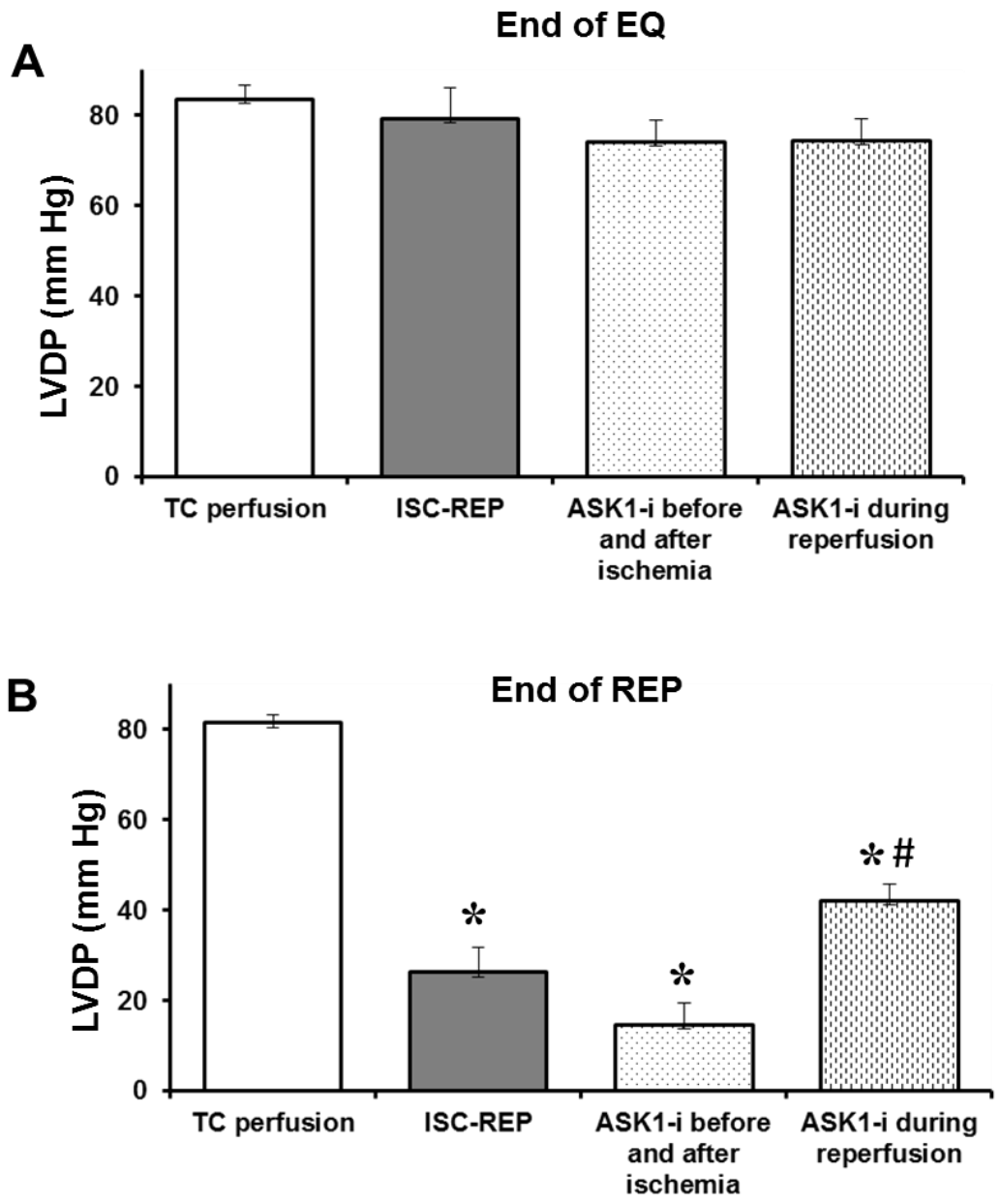


**Figure 3.4. ASK1-i treatment during reperfusion improves cardiac function in mouse hearts following ischemia-reperfusion.** Left ventricular developed pressure (LVDP) was recorded (as mm Hg) in TC perfusion, ISC-REP, ASK1-i before and after ischemia, ASK1-i during reperfusion groups. There were no differences in LVDP among the four groups at 15 minutes of equilibration (EQ) before the onset of ischemia (A). ASK1-i treatment during reperfusion improved the recovery of LVDP during reperfusion compared with untreated hearts (B). Results were presented as mean±SE. All results were compared using one-way ANOVA test. *p<0.05 vs. TC perfusion; #p<0.05 vs. ISC-REP. n= 6-7 in all groups.

There were no differences in diastolic pressure between groups (TC perfusion, ISC-REP, ASK1-i before and after ISC, ASK1-i during reperfusion) at the end of the 15 min equilibration perfusion (15 min) [TC perfusion: 9±2 mm Hg; ISC-REP: 9±1; ASK1-i before and after ISC: 9±1; ASK1-i during reperfusion: 8±1; p=ns] **(Figure 3.5)**. Ischemia-reperfusion markedly increased diastolic pressure in untreated hearts [ISC-REP: 31±8 mm Hg; $p<0.05$ vs. TC perfusion]. ASK1-i treatment before ischemia had no effect on the increased diastolic pressure [ASK1-i before and after ISC: 49±7 mm Hg; $p<0.05$ vs. TC perfusion] whereas ASK1-i administration during early reperfusion significantly decreased diastolic pressure during 60 min reperfusion compared with the untreated hearts or ASK1-i treatment before and after ISC [ASK1-i during reperfusion: 17±5 mm Hg; $p<0.05$ vs. ISC-REP] **(Figure 3.5)**. Thus, from the data it was clear that cardiac function following ischemia-reperfusion were substantially improved by ASK1-i given during early reperfusion.

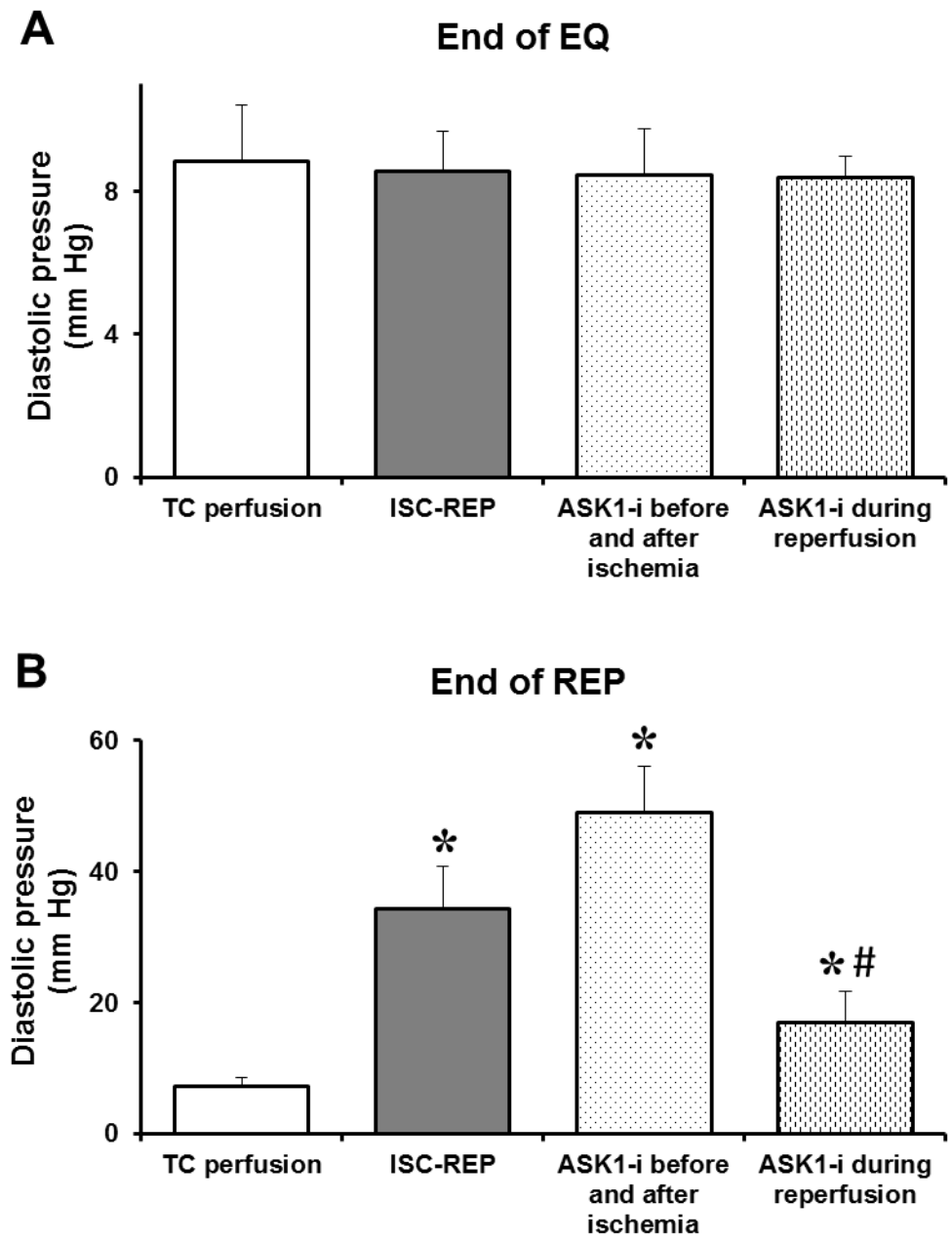


**Figure 3.5. ASK1-i treatment during reperfusion improves cardiac function in mouse hearts following ischemia-reperfusion.** Diastolic pressure was recorded (as mm Hg) in TC perfusion, ISC-REP, ASK1-i before and after ischemia, ASK1-i during reperfusion groups. There were no differences in diastolic pressure among the four groups at 15 minutes of equilibration (EQ) before the onset of ischemia (A). ASK1-i treatment during reperfusion lowered diastolic pressure during ischemia and reperfusion compared with untreated hearts (B). Results were presented as mean±SE. All results were compared using one-way ANOVA test. *$p<0.05$ vs. TC perfusion; #$p<0.05$ vs. ISC-REP. n= 6-7 in all groups.

### III. 3. 2. ASK1-i treatment decreases cardiac injury in mouse hearts following ischemia-reperfusion

To assess myocardial cell damage, we examined the lactate dehydrogenase (LDH) release into the coronary effluent during the 30 min reperfusion period. Ischemia-reperfusion increased total LDH release into the coronary effluent when compared to TC perfusion [TC perfusion: 198±89; ISC-REP: 890±65; $p<0.05$] **(Figure 3.6)**. ASK1-i given before ischemia and during the initial 10 minutes of reperfusion attenuated myocardial injury as observed from the decrease in LDH release during reperfusion [ASK1-i before and after ISC: 560±83; $p<0.05$ vs. ISC-REP]. Remarkably, treatment only during early reperfusion was as protective as given before ischemia as it decreased LDH release during reperfusion to a similar extent [ASK1-i before and after ISC: 533±61; $p<0.05$ vs. ISC-REP] **(Figure 3.6)**. Thus, the *in-vitro* model used for the study of mitochondrial function recapitulates the *in-vivo* observation of cardioprotection by treatment only during reperfusion.

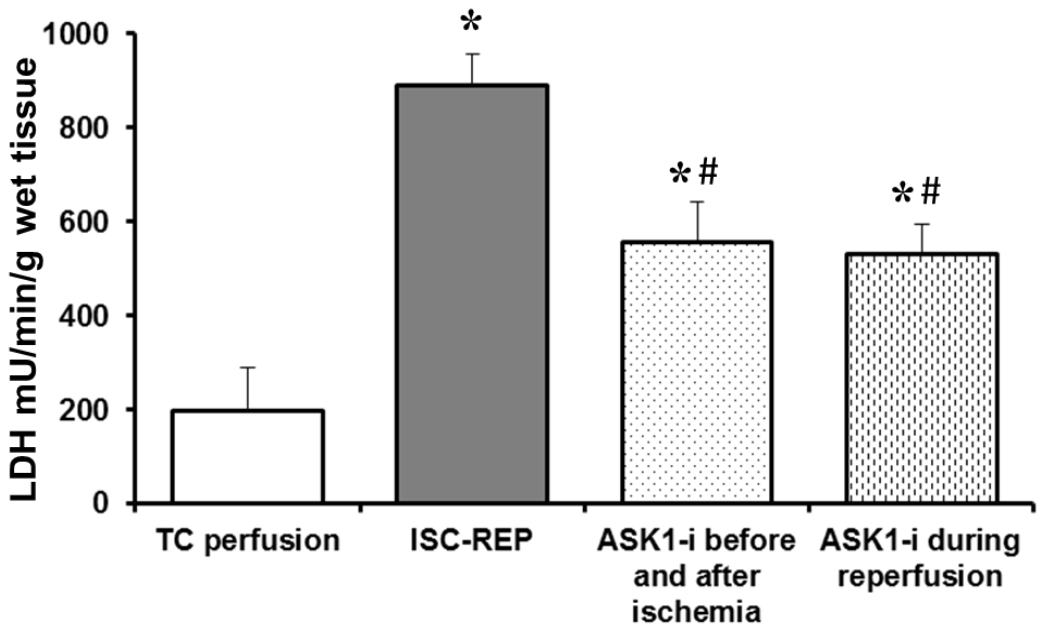


**Figure 3.6. ASK1-i treatment decreases cardiac injury in mouse hearts following ischemia-reperfusion.** LDH release, a marker for myocardial injury, was measured and expressed as mU/min/ g wet tissue. ASK1-i treatment decreased the amount of LDH release compared to untreated hearts. Results were presented as mean±SE. All results were compared using one-way ANOVA test. *p<0.05 vs. TC perfusion, #p<0.05 vs. ISC-REP. All results were compared using one-way ANOVA test. n=6-7 in all groups. LDH, lactate dehydrogenase.

### III. 3. 3. ASK1-i treatment during ischemia-reperfusion does not alter the protein yield or citrate synthase activity in the mitochondria.

Following, mitochondrial isolation, protein concentration was measured by Lowry method using BSA as a standard and sodium deoxycholate as a detergent to solubilize the mitochondria. Citrate synthase activity was quantified in cholate-solubilized frozen-thawed mitochondria by measuring the rate of 5,5′-dithiobis (nitrobenzoic acid)-reactive reduced coenzyme A (412 nm).

The protein yield of isolated mitochondria following 25 min of untreated ischemia and 30 min of reperfusion was similar to the protein yield in the time control perfusion group **(Figure 3.7A)**. The protein yield averaged 26.2±2.4 mg/g wet weight in TC perfusion vs. 25.0±1.5 mg/g in ISC-REP hearts respectively (p=ns). As shown in **Figure 3.7A**, the yields of mitochondria were also similar in ASK1-i treated groups [ASK1 before and after ISC: 21.9±1.5; ASK1 during reperfusion: 26.4±0.8; p=ns vs. ISC-REP].

To assess whether the relative purity of the mitochondria following isolation was similar in TC perfusion, ISC-REP and ASK1-i treated groups, activity of citrate synthase, the marker enzyme for mitochondrial matrix, was measured. From isolated mitochondria in all the four groups, the specific activity of citrate synthase was similar in all groups **(Figure 3.7B)** [TC perfusion: 3445±194; ISC-REP: 3277±232; ASK1-i before and after ISC: 3314±265; ASK1-i during reperfusion: 3239±183; p=ns].

Thus, following ischemia-reperfusion or ASK1-i treatment during ISC-REP, there is an unchanged protein yield of mitochondria along with similar marker enzyme activity. This confirms that neither ischemia-reperfusion nor the treatment with ASK1-i significantly

modified the recovery and purity of the mitochondria. In order to understand the role of ASK1 on mitochondrial functioning during ischemia reperfusion, we proceeded with the measurement of oxidative phosphorylation in untreated and ASK1-i treated groups.

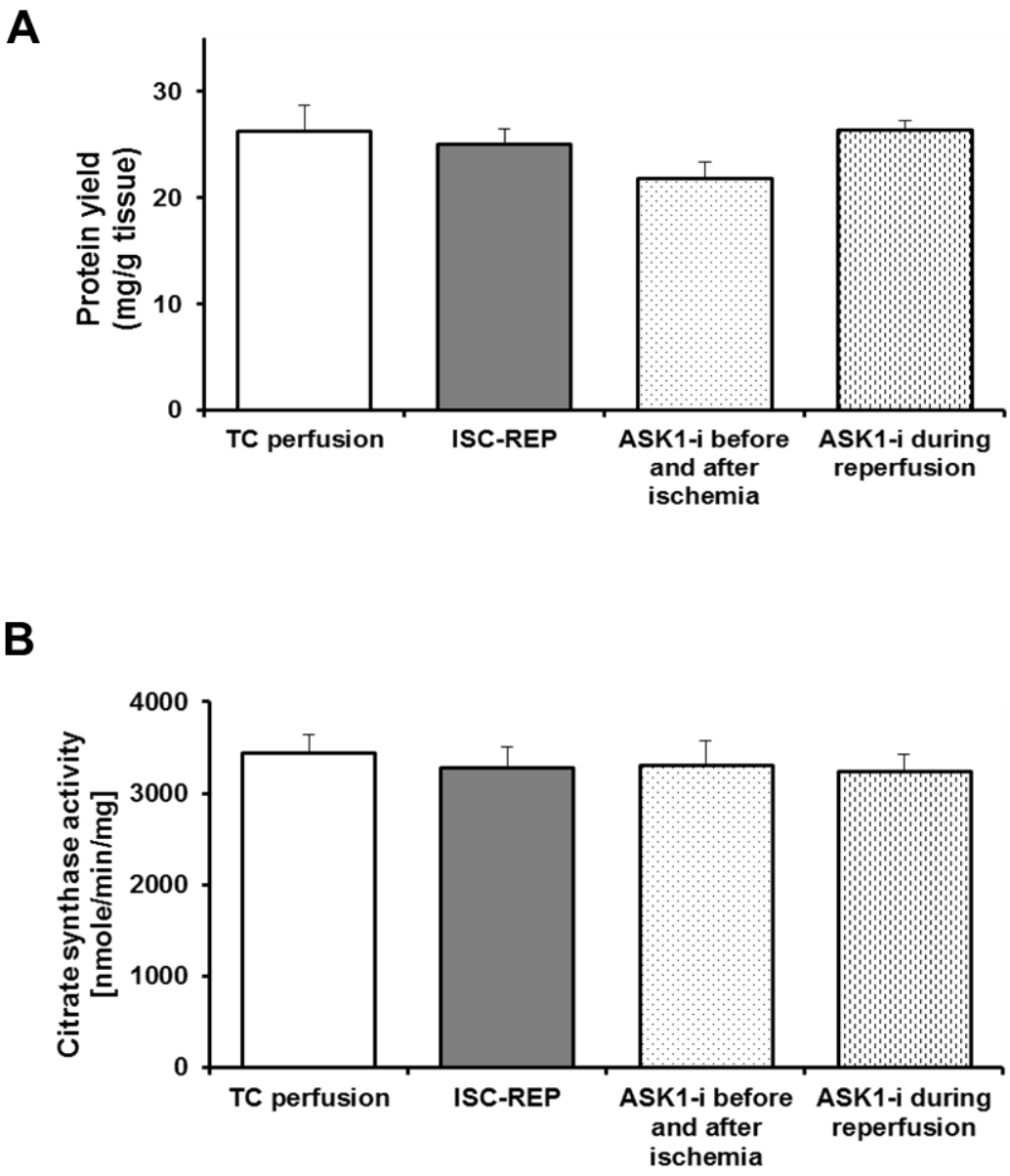


**Figure 3.7. ASK1-i treatment in mouse hearts following ischemia-reperfusion did not alter the mitochondrial protein yield and citrate synthase activity.** The protein content of the isolated mitochondria from C57BL6 mice was similar in TC perfusion, ISC-REP, ASK1-i before and after ischemia, ASK1-i during reperfusion groups (A). As a mitochondria-specific enzymatic marker, citrate synthase activity was measured in all samples tested (B). Results were presented as mean±SE. All results were compared using one-way ANOVA test. n= 6-7 in all groups.

### III. 3. 4. ASK1-i treatment improved oxidative phosphorylation following ischemia-reperfusion in heart mitochondria.

In order to investigate if ASK1 influences cardiac mitochondrial respiration, the rates of oxidative phosphorylation were studied in mitochondria isolated from four groups: time control perfusion, untreated ischemia-reperfusion, ASK1-i given either before ischemia and during early reperfusion or during early reperfusion alone using different substrates that donate electrons to the electron transport chain. Glutamate+malate was used as a complex I substrate, succinate (in the presence of rotenone) as a complex II substrate, and TMPD/ascorbate (with rotenone) as an electron donor to complex IV via cytochrome c. As shown in **Figure 3.8**, mitochondrial respiratory function was substantially decreased following ischemia and reperfusion. The maximal rates of oxidative phosphorylation were obtained by addition of saturating 2 mM ADP when glutamate+malate, succinate or TMPD/ascorbate was used as the substrate. The maximal rate of respiration using a complex I substrate, glutamate+malate, (complex I→complex III→complex IV) was decreased by approximately 50% (TC: 417±32 nAO/min/mg protein; ISC-REP: 202±12, $p<0.05$) **(Figure 3.8A)**. Succinate-dependent (complex II→complex III→complex IV) maximal integrated respiration rates showed a significant decrease, approximately 30% (TC: 617±65 nAO/min/mg protein; ISC-REP: 425±23, $p<0.05$) **(Figure 3.8B)** whereas TMPD/ascorbate-dependent (complex IV) respiration was lowered by approximately 30% (TC: 1776±167 nAO/min/mg protein; ISC-REP: 1275±43, $p<0.05$) **(Figure 3.8C)** following ischemia-reperfusion. Consistent with previously published data [102, 209], ISC-REP increased uncoupling of the mitochondria indicated by augmented state 4 rates when using different substrates

**(Table 3.1)**. Augmented uncoupling of respiration following ISC-REP is the result of increased permeability of the inner mitochondrial membrane. Respiratory control ratios (RCRs) were reduced after ISC-REP independently of the substrates used **(Table 3.1)**. As a next step, the rates of uncoupled respiration by addition of 2, 4-ditrophenol (DNP) were measured. DNP is a protonophore that carries protons across the mitochondrial membrane. In its presence, the electron transport chain works independently from the phosphorylation apparatus. Therefore, the use of DNP allows us to test the relative contributions of electron transport chain and ATP synthase/ANT/$P_i$ transporter to the decreased rates of oxidative phosphorylation. The DNP-uncoupled respiration with glutamate+malate and succinate was reduced to a similar extent when compared to the ADP stimulated maximal rates **(Table 3.1)**. This result suggests that the decrease in respiration was not caused by defects in ATP synthase, adenine nucleotide translocase (ANT) or phosphate ($P_i$) transporter, but was indeed localized to the electron transport chain.

Treatment with ASK1-i before ischemia and during reperfusion improved the maximal ADP-stimulated glutamate respiration rate by approximately 50% (300±21 nAO/min/mg protein, $p<0.05$) compared to ISC-REP **(Figure 3.8A)**. Furthermore, the maximum state 3 rates with glutamate+malate in the presence of DNP uncoupler were improved 55% (375±18 nAO/min/mg protein, $p<0.05$ vs. ISC-REP) which was comparable with the results without DNP **(Table 3.1)**. Apparently, the phosphorylation aparatus did not contribute to the improvement of complex I-dependent respiration. Also, succinate-and TMPD/ascorbate-dependent respiration rates were not significantly improved following ASK1-i treatment before ischemia and during early reperfusion **(Table 3.1)**.

Remarkably, administration of ASK1-i only during reperfusion was sufficient to protect the maximal complex I mitochondrial oxidative phosphorylation (381±13 nAO/min/mg protein, $p<0.05$) compared to ISC-REP **(Figure 3.8A)**. Respiratory control ratios (RCRs) were improved following ASK1-i treatment only during reperfusion independently of the type of substrates used **(Table 3.1)**. Furthermore, the DNP-uncoupled respiration on glutamate+malate and succinate was improved to the similar extent **(Table 3.1)** which suggests that the increase in respiration was due to protection of the electron transport chain. Remarkably, the ASK1-i treatment during early reperfusion alone was comparable to the regimen that included ASK1-i pre-treatment before ischemia.

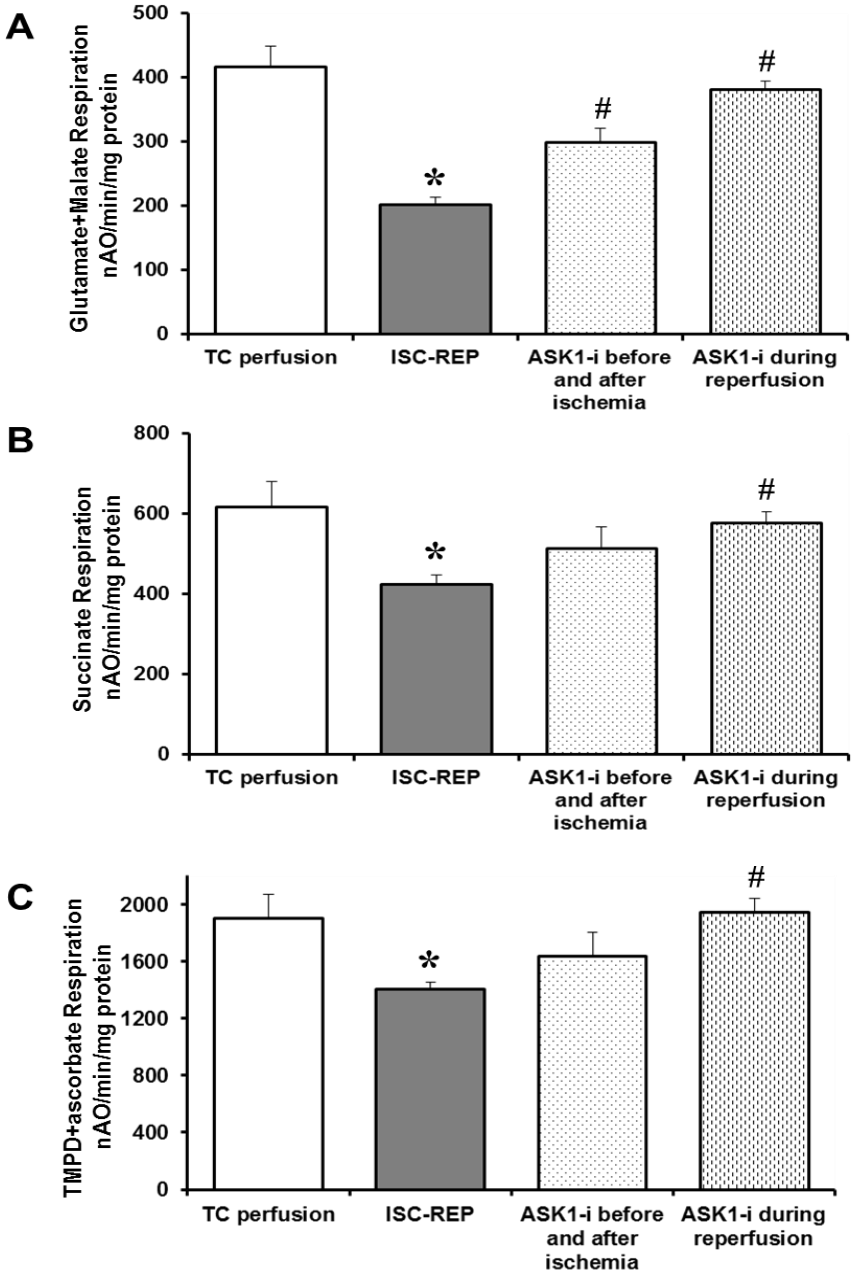


**Figure 3.8. ASK1-i treatment during reperfusion improves glutamate+malate, succinate and TMPD+ascorbate dependent oxidative phosphorylation following ischemia-reperfusion.** Oxygen consumption by intact mitochondria was measured by Clark-type electrode at 30 $^{o}$C as described in Materials and Methods. Incubations contained: 20 mM glutamate with 5 mM malate (A), 20 mM succinate with 7.5 μM rotenone (B), or 1 mM TMPD/20 mM L-ascorbate with 7.5 μM rotenone (C). Maximum rates of state 3 respiration with 2 mM ADP are shown (A and B). For TMPD/Asc-dependent respiration azide-sensitive data are depicted (C). Results were expressed as nanoatoms of atomic oxygen/min/mg of mitochondrial protein and were presented as mean±SE. * $p<0.05$ vs. TC perfusion, #$p<0.05$ vs. ISC-REP. All results were compared using one-way ANOVA test. n= 6-7 in all groups.

**Table 3.1. Rates of oxidative phosphorylation in heart mitochondria isolated from TC perfusion, ISC-REP and ASK1-i treated groups.**

| | TC perfusion | ISC-REP | ASK1-i before and after ischemia | ASK1-i during reperfusion |
|---|---|---|---|---|
| | n=7 | n=7 | n=6 | n=7 |
| **Glutamate + Malate** | | | | |
| State3 | 329±20 | 168±9* | 241±17# | 310±5# |
| State 4 | 81±5 | 69±5 | 91±5# | 90±6# |
| RCR | 4.1±0.4 | 2.5±0.1* | 2.7±0.2 | 3.5±0.2# |
| 2mM ADP | 417±32 | 202±12* | 300±21# | 381±13# |
| DNP | 408±30 | 187±14* | 289±22# | 375±18# |
| **Succinate** | | | | |
| State 3 | 643±65 | 374±28* | 449±26 | 542±32# |
| State 4 | 195±18 | 156±4* | 185±15 | 196±7# |
| RCR | 3.3±0.1 | 2.4±0.1* | 2.4±0.1 | 2.8±0.1# |
| 2mM ADP | 617±65 | 425±23* | 514±53 | 579±27# |
| DNP | 559±57 | 396±20* | 480±47 | 542±28# |
| **TMPD/ascorbate** | | | | |
| 2mM ADP | 1776±167 | 1275±43* | 1571±155 | 1799±97# |

**ASK1-i treatment during ischemia-reperfusion affects mitochondrial oxidative phosphorylation.** Mitochondria were isolated and rates of respiration were recorded. Based on state 3 and state 4 rates, respiratory control ratios (RCRs) were calculated. During recording of 2 mM ADP-dependent maximal state 3 rate, uncoupler 2,4-dinitrophenol (DNP) was added to establish relative contribution of phosphorylation apparatus and the ETC. Results were presented as mean±SE. Values of state 3, state 4, 2 mM ADP and DNP rates were expressed in nanoatoms of atomic oxygen/min/mg of mitochondrial protein. All results were compared using one-way ANOVA test. *$p<0.05$ vs. TC perfusion; #$p<0.05$ vs. ISC-REP. n=6-7 in all groups. ADP, adenosine di-phosphate; TMPD, N,N,N′,N′-tetramethyl-p phenylenediamine; RCR, respiratory control ratio; DNP, 2,4-dinitrophenol.

### III. 3. 5. Mitochondrial membrane potential was similar/unaffected by ASK1-i treatment during ischemia-reperfusion.

Mitochondrial membrane potential ($\Delta\Psi_m$) is an integral component of cellular energy homeostasis and normal cellular function. It is a major indicator of mitochondrial membrane intactness which reflects the pumping of protons across the inner membrane during the process of electron transport and oxidative phosphorylation [36]. TMRM (tetramethylrhodamine methyl ester) is a permeant cationic fluorescent probe whose accumulation in the mitochondria depends on high trans-membrane potential (the matrix being negative) maintained by functional mitochondria [36]. However, dissipation of the mitochondrial transmembrane potential by protonophores (DNP) or inhibitors of electron transport chain eliminates the selective mitochondrial association with TMRM dye. Therefore, the intactness of the inner mitochondrial membrane was measured by dynamic changes in the TMRM fluorescence signal in mitochondria isolated from ASK1-i treated and untreated groups [36].

The maximum membrane potential that the mitochondria could generate ($\Delta\Psi_{max}$), was expressed as a difference between fully polarized mitochondria in the presence of 1 nM oligomycin (state $4_{oligomycin}$) and fully uncoupled mitochondria following addition of 25 µM DNP ($\Psi_0$). Addition of oligomycin inhibits proton translocation through ATP synthase. Due to the activity of ETC in the presence of excess of substrates, the protons were still being moved from matrix to the intermembrane space. Therefore, the measured state $4_{oligomycin}$ represents the maximal inner membrane polarization state. Values of $\Delta\Psi_{max}$ from TC perfusion, ISC-REP and ASK1-i treatment groups **(Figure 3.9)** indicate that

even though ISC-REP and ASK1-i treatment altered glutamate+malate respiration, they did not affect the ability to generate normal proton motive force in mitochondria.

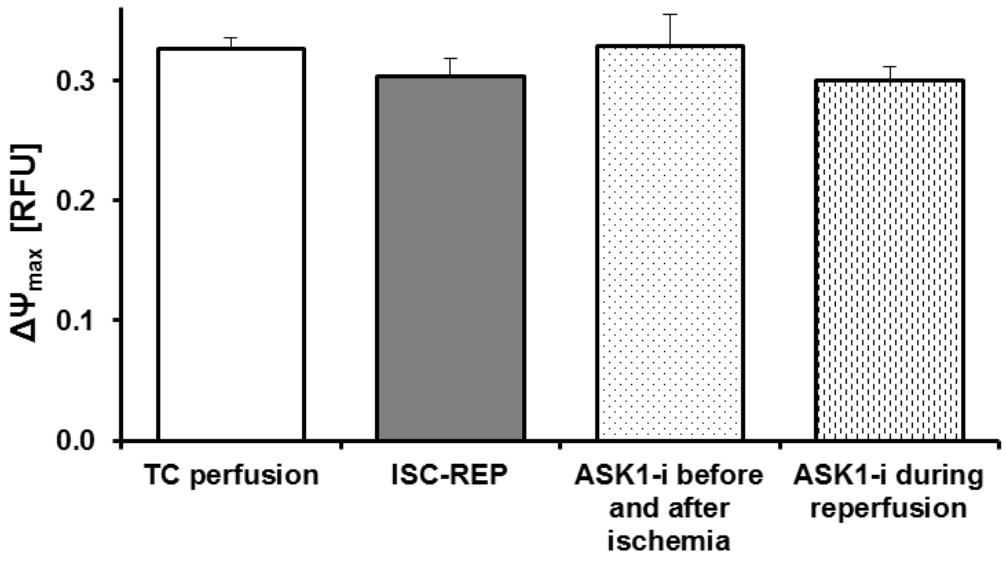


**Figure 3.9. ASK1-i treatment during ischemia-reperfusion did not alter the maximum mitochondrial potential, $\Delta\Psi_{max}$.** $\Delta\Psi_m$ was measured in 200 µg of intact mitochondria using 0.1 µM TMRM, a fluorescent dye that accumulates in polarized mitochondria. (A) $\Delta\Psi_{max}$, maximum potential that mitochondria were capable to generate defined as the difference in membrane potential between fully polarized mitochondria in the presence of 1 nM oligomycin (state $4_{oligomycin}$) and fully uncoupled mitochondria after sequential titration with 25 µM DNP ($\Psi_0$). All results were compared using one-way ANOVA test. *$p<0.05$ vs. TC perfusion. n=6-7 in all groups. RFU, relative fluorescence units.

### III. 3. 6. ASK1-i treatment does not decrease the net $H_2O_2$ release following ischemia-reperfusion

To assess ROS production in the isolated heart mitochondria, we measured net $H_2O_2$ release from these organelles. In normally respiring mitochondria superoxide generation from the electron transport chain is low [80]. Due to this reason, the isolated intact mitochondria were supplied with excess quantity of metabolic substrates which results in the depletion of ADP and establishment of higher ROS-generating state 4 of mitochondrial respiration.

The maximal capacity of complex I to produce $H_2O_2$ by inhibition of complex I with rotenone was studied. Specific inhibitors were present during the time of incubation of isolated mitochondria with respiration substrates. As shown in **Figure 3.10**, ischemia significantly increased the maximal capability of complex I to generate $H_2O_2$ [TC perfusion: 103±12 pmol/mg protein/30min; ISC-REP: 213±22; $p<0.05$]. On the other hand, ASK1-i treatment during ischemia and early reperfusion showed a trend towards increase in the maximal complex I $H_2O_2$ production which was not significant when compared to ISC-REP [ASK1-i before and after ISC: 275±37 pmol/mg protein/30min] **(Figure 3.10)**. However, this increasing trend was not observed in the mouse hearts which underwent ASK1-i treatment only during reperfusion [ASK1-i during reperfusion: 187±29 pmol/mg protein/30min; $p<0.05$ vs. ASK1-i before and after ISC] **(Figure 3.10)**.

The maximal capacity of complex III to generate $H_2O_2$ was determined using succinate in the presence of rotenone and antimycin A. From **Figure 3.11**, it is clear that ischemia-reperfusion increased the maximal capability of complex III to $H_2O_2$ net

release [TC perfusion: 654±62 pmol/mg protein/30min; ISC-REP: 1010±87; $p<0.05$]. On the other hand, ASK1-i treatment during ischemia and early reperfusion significantly increased the maximal complex III $H_2O_2$ production when compared to ISC-REP [ASK1-i before and after ISC: 1528±118 pmol/mg protein/30min] **(Figure 3.11)**. Conversely, mouse hearts which underwent ASK1-i treatment only during reperfusion did not additionally increase the ROS release from complex III when compared to ISC-REP group [ASK1-i during reperfusion: 1013±63 pmol/mg protein/30min; $p<0.05$ vs. ASK1-i before and after ISC] **(Figure 3.11)**.

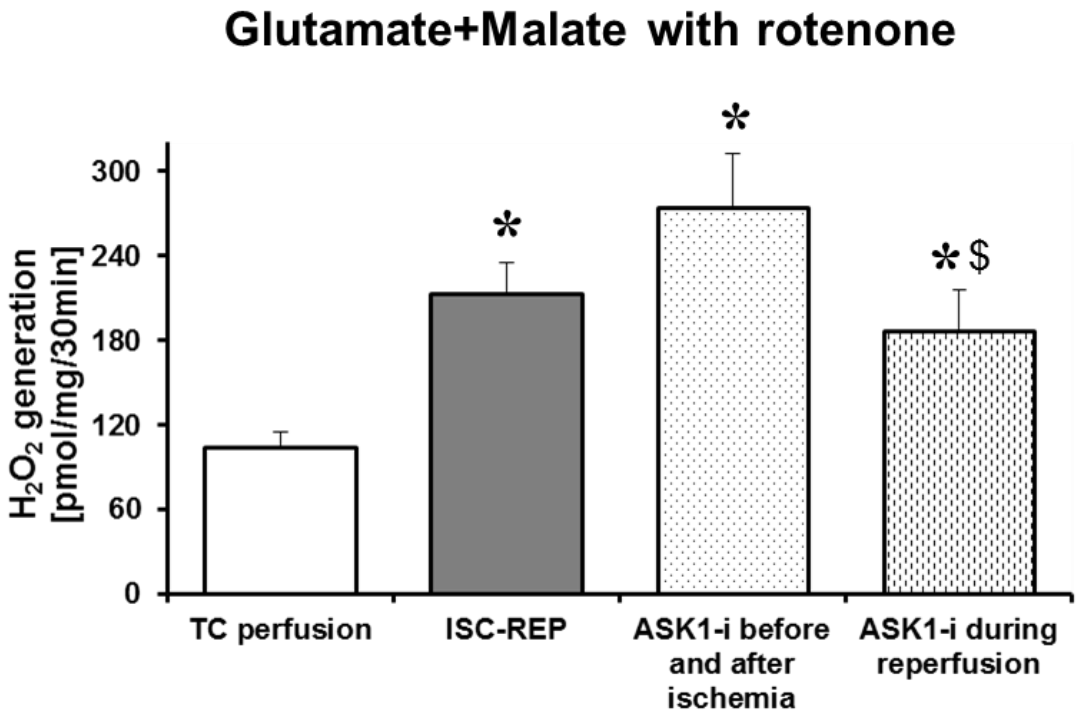


**Figure 3.10. ASK1-i treatment does not decrease the maximal net $H_2O_2$ production from complex I following ischemia-reperfusion.** Intact mitochondria were isolated and incubated with glutamate+malate+rotenone followed by measurement of $H_2O_2$ net production using Amplex Red and HRP. Results were expressed as pmol/mg/30min and were presented as mean±SE. All results were compared using one-way ANOVA test. *p<0.05 vs. TC perfusion; $p<0.05 vs. ASK1-i before and after ischemia. n=6-7 in all groups.

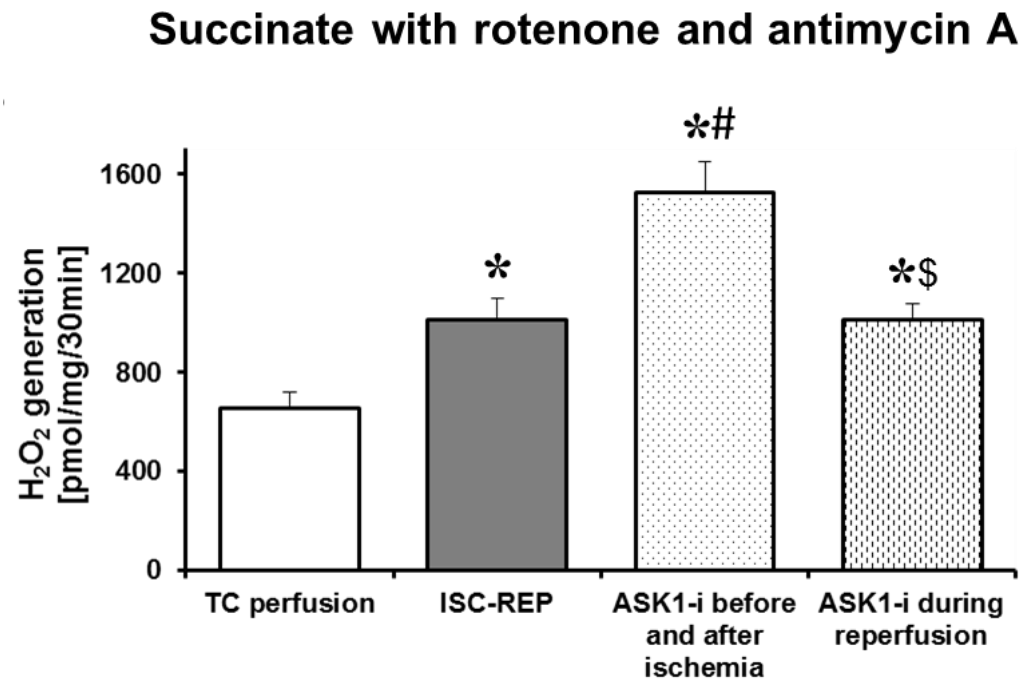


**Figure 3.11. ASK1-i treatment does not decrease the net $H_2O_2$ production from complex III following ischemia-reperfusion.** Intact mitochondria were isolated and incubated with succinate+rotenone+antimycin A followed by measurement of $H_2O_2$ net production using Amplex Red and HRP. Results were expressed as pmol/mg/30min and were presented as mean±SE. All results were compared using one-way ANOVA test. *p<0.05 vs. TC perfusion; #p<0.05 vs. ISC-REP; $p<0.05 vs. ASK1-i before and after ischemia. n=6-7 in all groups.

### III. 3. 7. ASK1-i treatment during ischemia-reperfusion decreases MPTP susceptibility in mitochondria.

Damage to the electron transport chain from ischemia increases the production of reactive oxygen species and predisposes to the onset of mitochondrial permeability transition (MPTP) [246]. As shown in **Figure 3.10 and 3.11**, the production of reactive oxygen species was not affected by ASK1-i treatment. MPTP is triggered during reperfusion by calcium overload leading to subsequent opening of the permeability transition pore followed by increased permeability of the inner and outer mitochondrial membranes. This increase in membrane permeability results in cellular necrosis (increased infarct size) as well as the release of mitochondrial proteins that activate programmed cell death pathways [246].

Calcium Retention Capacity (CRC) was used to assess the susceptibility to MPTP opening in isolated mitochondria. Representative original tracings of CRC are shown for TC perfusion and ISC-REP groups in the upper panel of **Figure 3.12A**. From the tracings, it is clear that ischemia-reperfusion increases the mitochondrial susceptibility to undergo MPTP, manifest by a decreased tolerance of mitochondria to exogenous calcium before MPTP occurs. The release of calcium from the mitochondrial matrix indicated MPTP opening. In TC perfusion group, CRC averaged 640±32 nmol $CaCl_2$/mg protein which was markedly decreased during ISC-REP to 344±11 nmol $CaCl_2$/mg protein [$p<0.05$] **(Figure 3.12B)**. Remarkably, treatment with ASK1-i before ischemia and during reperfusion significantly decreased mitochondrial susceptibility to calcium-induced MPTP as shown by their improved CRC [ASK1-i before and after ISC: 480±16 nmol $CaCl_2$/mg protein; $p<0.05$ vs. ISC-REP] **(Figure 3.12B)**. However, treatment only

during reperfusion was as protective as treatment that was given before ischemia as noticed in the improved CRC indicating decreased sensitivity to MPTP opening [ASK1-i before and after ISC: 451±12 nmol $CaCl_2$/mg protein; $p<0.05$ vs. ISC-REP] **(Figure 3.12B)**.

Differences between TC perfusion, ISC-REP and ASK1-i treatment groups were not due to a preferential selection of “good” mitochondria in the ASK1-i treated groups during the isolation process. This was confirmed by the protein content or the citrate synthase activity between the three groups which provided a strong evidence of a similar recovery of mitochondria from all the four groups.

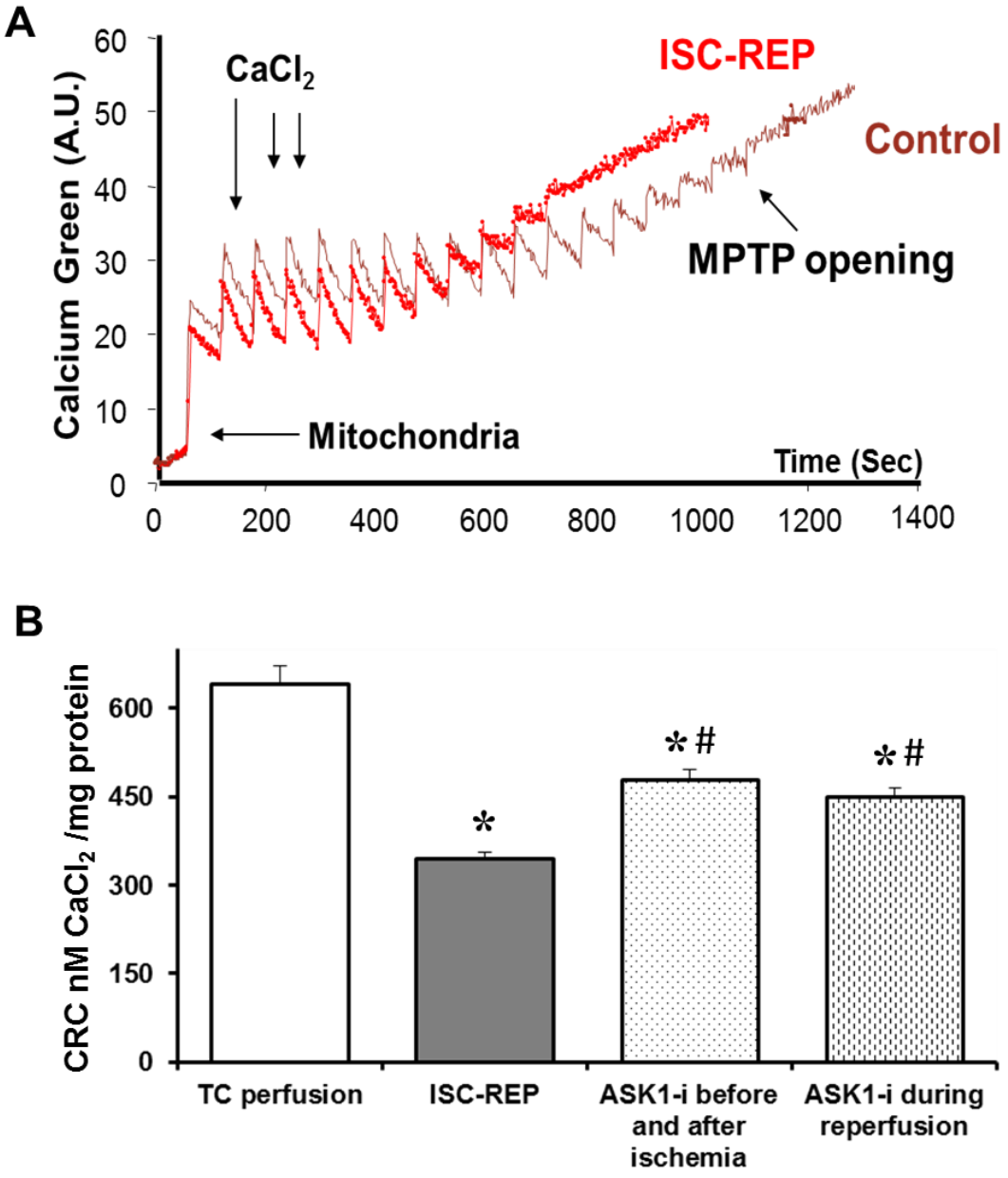


**Figure 3.12. ASK1-i treatment decreases MPTP susceptibility in mitochondria following ischemia-reperfusion.** The upper panel shows a representative original tracing of CRC measurement during time control (TC) perfusion and ischemia (ISC)-reperfusion (REP) (A). The number of calcium pulses to elicit MPTP opening was markedly decreased after ischemia-reperfusion compared with time control. ASK1-i treatment given before and after ischemia, during reperfusion alone improved CRC when compared with untreated hearts (B). Data were expressed as mean ± SE. All results were compared using one-way ANOVA test. * $p<0.05$ vs. TC perfusion, # $p<0.05$ vs. ISC-REP. N= 6-7 in all groups.

### III. 3. 8. ASK1-i treatment during ischemia-reperfusion decreases cytochrome c release from mitochondria into cytosol

Mitochondrial electron transport chain (ETC) is both the source and target for ischemic damage [5, 222]. The sequence of events leading to mitochondrial ischemic damage involves damage to ETC, increase in mitochondrial membrane permeability, depletion of cytochrome c and activation of apoptotic pathways [5, 79, 156, 222]. From the earlier data, it is clear that ASK1-i treatment improved oxidative phosphorylation through ETC **(Figure 3.8)** and decreased the susceptibility to MPTP opening **(Figure 3.12)**. As a next step, we would like to test whether the ASK1-i treatment has any effect on the cytochrome c release from the mitochondria into the cytosol. Therefore, we measured cytochrome c content in cytosols from hearts subjected to ISC-REP with or without ASK1-i treatment or TC perfusion.

Western blot analysis revealed a significant increase in release of cytochrome c into the cytosols of ISC-REP hearts **(Figure 3.13)** which is consistent with the earlier published data. ISC-REP enhanced the release of cytochrome c from the mitochondria when compared to TC perfusion [densitometric ratio of cyt c/α-tubulin; TC perfusion: 0.286±0.090; ISC-REP: 0.818±0.223; $p<0.05$]. In contrast, from the densitometric measurements, both ASK1-i treatment before and after ischemia [ratio of cyt c/α-tubulin; ASK1-i before and after ISC: 0.211±0.082; $p<0.05$] and during reperfusion alone [ratio of cyt c/α-tubulin; ASK1-i during reperfusion: 0.276±0.110; $p<0.05$] significantly reduced the cytochrome c release into the cytosol from the mitochondria when compared to ISC-REP **(Figure 3.13)**. Therefore, this data suggests that ASK1-i treatment improves

complex I, II and IV-dependent respiration in ischemic mitochondria by decreasing susceptibility to MPTP opening thereby retaining cytochrome c in the mitochondria.

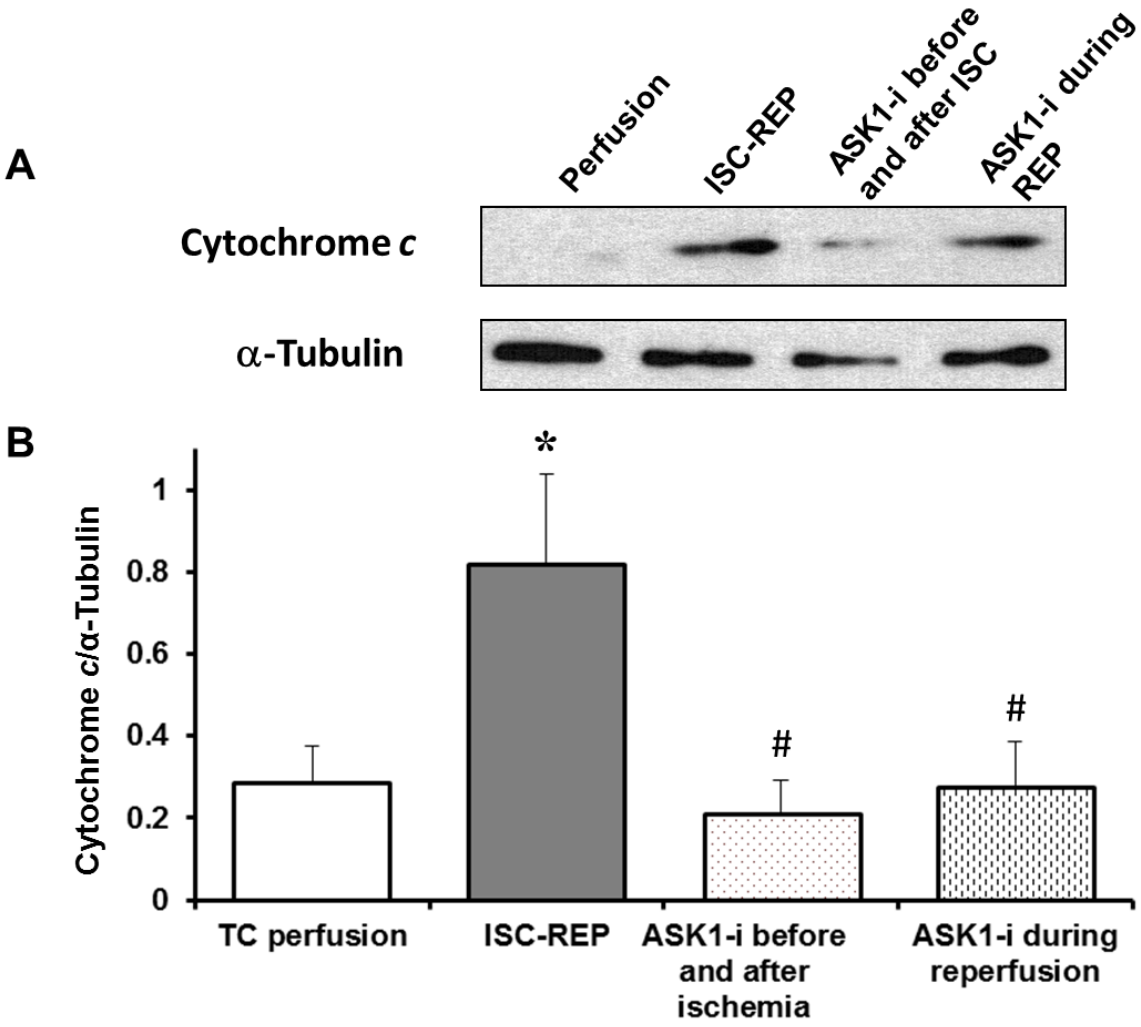


**Figure 3.13. ASK1-i decreases cytochrome c release from mitochondria into cytosol.** Mitochondrial protein extracts (10 µg) from TC perfusion, ISC-REP, ASK1-i treated groups were resolved by SDS-PAGE and immunoblotted against cytochrome c and porin (mitochondrial loading control). Data were expressed as mean±SE. All results were compared using one-way ANOVA test. *p<0.05 vs. TC perfusion, #p<0.05 vs. ISC-REP. A representative blot from six independent experiments is shown.

### III. 3. 9. Complex III maximal enzymatic activities were increased upon ASK1-i treatment during reperfusion

Various reports indicate that the initial site of ischemic damage to the ETC is complex I and with increasing duration of the insult, it progresses to complex III and IV [5, 222]. Therefore, as a next step, maximal activities of complex I, II and III were measured to investigate if ASK1-i treatment during ischemia and reperfusion or reperfusion alone protects against damages to complexes. As an internal 'loading' control, the activity of matrix-localized citrate synthase (one of the Kreb's cycle enzymes) was also assayed. Spectrophotometric analysis of individual respiratory chain complexes is achieved by total disruption of both mitochondrial membranes using freeze-and-thaw technique and additional solubilization with 0.5 % sodium cholate. This technique dissects the entire electron transport chain into single complexes therefore their maximum enzymatic activity (zero order) in the presence of excess substrates (electron donors and acceptors) was measured.

Citrate synthase rates were equal and within a normal range (2500-3000 nmol/min/mg) among all the four groups, indicating similar relative purity of mitochondria isolated from the heart tissue **(Table 3.2)**. Measurement of ubiquinol: cytochrome c oxidoreductase (complex III) activity has shown that ISC-REP decreased complex III enzymatic activity by approximately 30% (TC perfusion: 7403±335 nmol/min/mg protein; ISC-REP: 5385±392; $p<0.05$) when compared to the TC perfusion which localizes the defect within the electron transport chain **(Figure 3.14)**. This data along with OXPHOS data and Western blotting for cytochrome c suggests that the slower rates of glutamate+malate, succinate and TMPD/ascorbate respiration in ISC-REP mitochondria

were likely atleast in part due to the impaired enzymatic activity of complex III or cytochrome c loss. Interestingly, ASK1-i treatment during early reperfusion showed a significant improvement, approximately 30% (7892±341 nmol/min/mg protein; $p<0.05$), when compared to ISC-REP group **(Figure 3.14)**.

As depicted in **Table 3.2**, ischemia did not affect the maximal activity of complex I in mitochondria isolated from mice hearts with or without ASK1-i treatment during ischemia-reperfusion. Additionally, the rotenone-insensitive activity of NADH dehydrogenase (NFR), the proximal part of complex I was measured. ISC-REP did not decrease maximal enzymatic rates of NFR in ASK1-i treated and untreated groups. Complex II activity was not decreased by ischemia when compared to the TC perfusion and ASK1-i treatment has no effect on the basal enzymatic rates.

Decrease in ETC activities may be caused by changes in expression of particular subunits of respiratory complexes. ETC activity can also be affected by the loss, damage or functional inactivation of protein subunits [214]. ETC activities can also modulated by post-translational modifications, including S-nitrosylation or phosphorylation [22, 61, 208, 215]. Identification of the mechanistic reason for improvement in the complex III activity with ASK1-i treatment during reperfusion will be one of the future directions of this project.

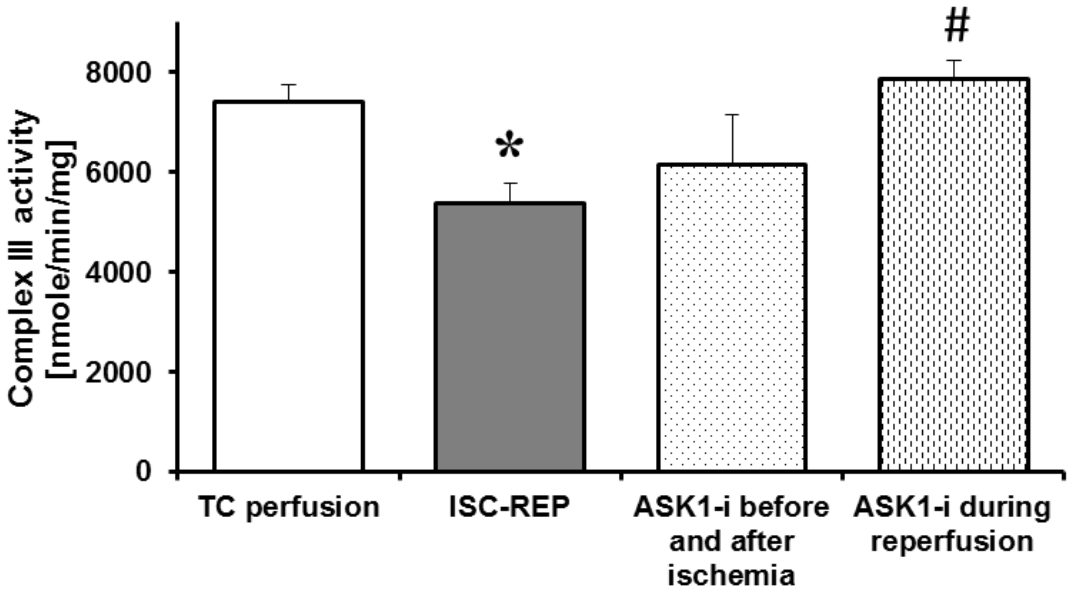


**Figure 3.14. ASK1-i treatment during reperfusion improves the maximal activity of complex III in heart mitochondria.** Integrity of isolated mouse heart mitochondria was disrupted by freeze-and-thaw procedure followed by solubilization with 0.5% (final v/v) cholate in MSM/EDTA buffer and adjusted to final protein concentration of 1 µg/ul. All enzymatic activities were measured spectrophotometrically using over-saturating amounts of specific substrates and inhibitors (zero rate kinetics) as outlined in Materials and Methods and expressed as nanomole of substrate decreased or product increased per minute per mg of mitochondrial protein [nmol/min/mg]. Data are presented as mean±SE. A difference of $p<0.05$ was considered significant. *$p<0.05$ vs. TC perfusion, #$p<0.05$ vs. ISC-REP. All results were compared using one-way ANOVA test. n=6-7 in all groups.

**Table 3.2. ETC-related enzyme activities of the isolated mitochondria from TC perfusion, ISC-REP, ASK1-i treated groups.**

| Mitochondria | Complex I | NFR | Complex II | Complex III | Complex IV | CS |
|---|---|---|---|---|---|---|
| TC perfusion | 665±22 | 3308±132 | 258±36 | 7403±335 | 403±112 | 3445±194 |
| ISC-REP | 620±24 | 3422±284 | 299±46 | 5385±392* | 334±44 | 3277±232 |
| ASK1-i before and after ISC | 613±39 | 3908±128 | 329±44 | 6168±993 | 333±55 | 3314±265 |
| ASK1-i during REP | 643±22 | 3273±95 | 270±17 | 7892±341# | 472±76 | 3239±183 |

**ASK1-i treatment during reperfusion increases maximum activity of complex III following ischemia-reperfusion.** Complex I, II and IV activities were not altered in all the four groups. Mitochondria were isolated, cholate-solubilized and enzymatic activities of individual ETC complex and of citrate synthase were determined spectrophotometrically as described in Materials and Methods. All results were expressed in nmol/min/mg or 1/min/mg in case of complex IV. Values were expressed as mean±SE (in $nmol.min^{-1}.mg\ protein^{-1}$); n=6-7 experiments. Complex I, NADH:decylubiquinone oxidoreductase; NFR, NADH:ferricyanide oxidoreductase; Complex II, succinate-ubiquinone oxidoreductase; Complex III, ubiquinol-cytochrome c oxidoreductase; Complex IV, cytochrome c oxidase; CS, citrate synthase. ISC-REP, ischemia-reperfusion; ASK1-i, apoptosis signaling kinase 1 inhibitor. All results were compared using one-way ANOVA test. *p<0.05 vs. TC perfusion; #p<0.05 vs. ISC-REP.

## III. 4. SUMMARY

- ASK1-i treatment during ISC-REP limits damage to mitochondria by:
  1. Preservation of oxidative phosphorylation
  2. Increased resistance to mitochondrial permeability transition.
  3. Attenuation of damage to the respiratory chain.
  4. Decrease in release of cytochrome c from mitochondria.

- Interestingly, treatment at the onset of REP with a cell-permeable small molecule inhibitor of ASK1 limits mitochondrial-driven cardiac injury.

- This is the likely the mechanism of the sustained myocardial salvage previously observed *in-vivo* in a preclinical model of STEMI treated by reperfusion.

## III. 5. DISCUSSION

ASK1 belongs to the mitogen-activated protein kinase (MAPK) kinase kinase family that activates the MAPK kinase 4 (MKK4)/MKK7-JNK and MKK3/6-p38 pathways through a ROS-dependent mechanism during ischemia-reperfusion [320, 331, 360]. Studies from ASK1 genetic mouse models suggest that ASK1 contributes to the pathogenesis of myocardial ischemia-reperfusion injury [361, 367]. Hence, pharmacological treatment using inhibitor molecules for components of the ASK1-MAPK pathway may potentially decrease cardiac injury during ischemia-reperfusion [388]. In a recent study, pharmacological treatment with ASK1-inhibitor (ASK1-i) at reperfusion led to a significant dose-related reduction in infarct size, inhibition of apoptotic cell death, and preservation of cardiac function at both 24 hours and 7 days [388]. Since cardiac mitochondria are both sources and targets of ischemic damage, we hypothesized that mitochondria could have a possible role in the cardioprotection observed in the *in-vivo* pretreatment with ASK1-i inhibitor. In the current study, we found that the cell-permeable small molecule inhibitor of ASK1 given at the onset of reperfusion protects mitochondrial ETC, decreases susceptibility to MPTP opening and retains cytochrome c in the mitochondria thereby decreasing mitochondrial driven cardiac injury. Thus, this study provides a major translationally relevant pharmacologic strategy to attenuate the cardiac injury which starts at the time of reperfusion.

Mitochondria sustain progressive damage during myocardial ischemia including the electron transport chain, leading to decreased rates of oxidative phosphorylation [203, 204]. Ischemia decreased complex I activity due to increased ROS generation as a

result of electron leakage from the complex [102, 201, 205-207]. Additionally, complex I undergoes ischemia-mediated post-translational modifications including phosphorylation [208] and S-nitrosylation [57]. Ischemia-induced damage to NADH ferricyanide oxidoreductase (NADH dehydrogenase, NFR), a component of the complex I, appears likely due to the loss of the flavin mononucleotide (FMN) component [206, 207]. During ischemia, complex II activity was decreased due to loss of protective glutathionylation of key sulfhydryl groups [62] whereas complex III activity was decreased as a result of the functional inactivation of iron-sulfur protein subunit [214]. Moreover, ischemia damages cytochrome c oxidase by phosphorylation of COXI, COXIVi1, and COXVb subunits causing functional inactivation of the complex [215] and also by selective depletion of cardiolipin [216-218]. While the complex I defect occurs early, as ischemia continues damage increases and involves complex III and cytochrome oxidase.

In our study, 25-min ischemia followed by 30-min reperfusion led to a significant decrease in glutamate+malate-, succinate- and TMPD-dependent respiration. Respiratory control ratios (RCRs) were reduced after ISC-REP independently of the type of substrates used due to slight increase in state 4 and a significant decrease in state 3 rates **(Table 3.1)**. The decrease in integrated respiration was consistent with previous studies of ischemia-reperfusion [102, 201, 206]. The decrease in integrated respiration was not a result of alterations in the phosphorylation apparatus, which consists of ATP synthase, adenine nucleotide and phosphate transporters (DNP rates in **Table 3.1**), thereby localizing the damage to the ETC. Indeed, we observed that complex III activity was decreased **(Table 3.2)**. From the observations including decreased complex III activity (**Table 3.1** and **Figure 3.14**) along with the loss of

cytochrome c **(Figure 3.14)**, it is clear that the distal part of ETC was the key target of ischemic damage.

Ischemic damage to the electron transport chain facilitates ROS generation and sets the stage for myocardial injury during reperfusion. Complex I, in ETC, is one of the major sites for ROS generation during ischemia. The predicted sites of ROS generation from complex I are the FMN, iron sulfur cluster N2, and the two tightly bound ubiquinones [85, 92, 94, 95, 101, 219]. Ischemia increased maximal ROS generation from complex I following blockade with rotenone which localizes the the site for ROS generation proximal to the ubiquinone binding site **(Figure 3.10)** [92]. In this study, the increased production of $H_2O_2$ with succinate as the substrate in the presence of rotenone indicates that complex III remains a key site for ROS generation during ischemia **(Figure 3.11)** [85, 109, 207, 240]. In addition, the blockade of distal ETC with antimycin A increases ROS generation from complex III **(Figure 3.11)** [78, 219]. Most of the ROS generated at complex III are from the $Q_o$ center, whereas the $Q_i$ center can be a site for ROS generation, especially when electron flow into the $Q_o$ center of complex III is limited [85, 105]. Moreover, increase in ROS production from complex I and complex III can also occur due to blocks in distal ETC including cytochrome c peroxidase formation, damage to complex III **(Figure 3.14)** and cytochrome c loss **(Figure 3.13)** with ischemia-reperfusion [219]. Under these conditions, eventhough there was no complex I damage **(Table 3.2)** [78, 85, 219], complex I and complex III generate ROS due to increased relative reduction and electron leak [78, 85, 92] which augments the impact of direct ischemic damage to ETC.

In the present study, ischemia-reperfusion increased the susceptibility to MPTP opening **(Figure 3.12)**. Increased calcium availability during reperfusion enhances mitochondrial calcium loading [244, 245, 391] which in concert with mitochondrial oxidative damage (ROS) predisposes to the onset of MPTP during reperfusion [154, 197]. Opening of MPTP releases cytochrome c and other pro-apoptotic proteins that cause cell death [147, 148]. Moreover, ischemia also depletes cardiolipin that provides binding sites on the inner membrane for cytochrome c [260, 264, 275] as a result of the peroxidase activity of cytochrome c. Depletion of cardiolipin [216, 219] or the oxidative modification of cardiolipin [223, 271, 296, 309, 392] diminishes the affinity of cytochrome c for cardiolipin delocalizing cytochrome c from the inner mitochondrial membrane to the intermembrane space [224, 227]. In normal conditions the outer membrane is impermeable to cytochrome c. However, during ischemia, the loss of BCL-2 triggers oligomerization of the pro-apoptotic BAX and BAK in the outer membrane forming pores [146, 229]. This leads to an increase in the permeability of the outer membrane allowing delocalization of cytochrome c from the inter-membrane space into the cytosol [149]. Furthermore, loss of cytochrome c also inhibits respiration, leading to further increase in ROS production from complex I [94, 102, 393]. This oxidative damage to mitochondrial ETC, further increases susceptibility to MPTP **(Figure 3.12)** that leads to the loss of cytochrome c **(Figure 3.13)** [228, 394] potentially creating a vicious cycle of mitochondrial-driven oxidative injury leading to activation of apoptotic cascades. Thus ischemic damage to the ETC promotes MPTP opening as a mechanism of mitochondrial-dependent cardiac injury during reperfusion, translating ischemic mitochondrial damage into reperfusion injury.

ASK1 is a serine/threonine protein kinase bound directly to thioredoxin and regulates cell death via p38 and c-Jun N-terminal kinase pathways [395]. During oxidative stress, thioredoxin is oxidized which dissociates from ASK1 resulting in activation of ASK1 through phosphorylation of Thr845 [395]. The inhibitor of ASK1 (ASK1-i), GS-459679, competes with the binding pocket of Trx in ASK1 thereby inhibiting ASK1 activation and decreasing cell death. Treatment with ASK1-inhibitor (ASK1-i), at reperfusion led to a significant dose-related reduction in infarct size, inhibition of apoptotic cell death, and preservation of left ventricular dimension and systolic function at both 24 hours and 7 days of reperfusion [388]. The protective effects of ASK1 inhibition during early reperfusion [388] were highly consistent with ASK1 genetic models wherein ASK1-knock out mice decreased infarct size [361] and ASK1 overexpressor mice showed 2-fold increase in infarct size [367] following ischemia-reperfusion. Interestingly, cardiac overexpression of ASK1 in the absence of ischemic injury had no effects in the mice, which proves that ASK1 acts as a cellular sensor, rather than a simple mediator of injury [395].

In this study, we have shown that treatment with ASK1-i before ischemia and during reperfusion significantly improved glutamate respiration whereas the succinate-and TMPD/ascorbate-dependent respiration rates were not **(Table 3.1)**. Interestingly, ASK1-i treatment pre- and post-ischemia decreased susceptibility to MPTP opening **(Figure 3.12)** thereby preventing cytochrome c release from mitochondria **(Figure 3.13)**. We have also shown that, ASK1-i treatment during ischemia and early reperfusion showed a significant increase in the levels of net $H_2O_2$ generated from complex I and III **(Figure 3.10, 3.11)** measured following ISC-REP. This suggests that physiological interaction of

Trx with ASK1 is important for the Trx antioxidant defense system to scavenge ROS release during ischemia [396-398] which probably is a reason why treatment before and after ischemia showed an additional significant increase in ROS release from complex I and complex III compared to ISC-REP.

Prevention of ischemic damage to the ETC by pharmacologic intervention before ischemia salvages myocardium during reperfusion [209, 231, 399, 400]. However, the clinical potential of these approaches are obviously limited because of the unpredictability of clinical ischemic events. Thus, pharmacologic treatment at the onset of reperfusion has great clinical relevance for the reduction of myocardial injury during reperfusion [401, 402]. Remarkably, administration of ASK1-i only during reperfusion protected maximal respiration through complex I, complex II and compex IV **(Figure 3.8)**. Interestingly, pre-treatment with ASK1-i significantly increased the complex III activity **(Figure 3.14)**. In addition, pre-treatment with ASK1-i inhibits MPTP opening **(Figure 3.12)** thereby decreases apoptosis by preventing cytochrome c release **(Figure 3.13)** from mitochondria. To summarize, these results support the observed increased rates of integrated respiration following ASK1-i treatment during reperfusion was indeed due to protection from damage to the distal ETC. Sites of protection include complex III and retention of cytochrome c as a result of decreased susceptibility to MPTP opening. Hence, the ASK1-i treatment during early reperfusion alone protected mitochondria from ETC driven myocardial injury comparable to the regimen that included ASK1-i pre-treatment before ischemia.

Differences in the above mentioned observations in mitochondrial respiration, ETC complex activities and MPTP susceptibility between control, treated and untreated

groups were not due to a preferential selection of “good” mitochondria in the treatment groups during the isolation process. The reason for the above conclusion was because neither the protein content **(Figure 3.7A)** nor the citrate synthase activity (marker for matrix) **(Figure 3.7B)** differed between the four groups which provided a strong evidence of a similar recovery and relative purity of mitochondria from the heart irrespective of ASK1-i treatment. This finding is consistent with published work that the protein yield or the activity of citrate synthase, a mitochondrial matrix marker enzyme, was unaltered [102, 204, 214].

Complex III (ubiquinol: ferricytochrome c oxidoreductase, EC 1.10.2.2) is a dimeric complex with a molecular mass of 485 kDa that is involved in the transfer of electrons from ubiquinol to oxidized cytochrome c coupled to proton translocation [403]. Each monomer consists of 11 subunits, three of which, namely, cytochrome b, cytochrome $c_1$ and the iron-sulfur protein (ISP), have prosthetic groups involved in the electron transfer [66]. Myocardial ischemia decreased complex III activity following *in-vivo* coronary occlusion in the canine model [206] and following global ischemia in the isolated rat heart [201, 214]. Electron paramagnetic resonance (EPR) signal from the ISP subunit containing the [2Fe-2S] cluster decreases after ischemia suggesting that it is the disruption of the cluster that decreases complex III activity. The content of the ISP subunit, cytochromes b and $c_1$ were unchanged by ischemia [214]. Thus, ischemia decreases complex III activity as a result of the functional inactivation of iron-sulfur protein subunit without degradation of the ISP subunit or the remaining eleven subunits of the complex. In addition, ischemia depletes inner membrane enriched phospholipid, cardiolipin [5, 204, 216]. During ischemia excessive generation of ROS converts

cytochrome c to a “peroxidase” leading to oxidation and depletion of cardiolipin. Fusion of mitochondria from ischemic-reperfused hearts with cardiolipin-liposomes resulted in an almost full restoration of complex III activity which highlights the importance of cardiolipin for optimal activity of complex III [404].

ASK1-i treatment during reperfusion improved ETC function by restoring complex III activity. Hence, it can be predicted that the functional inactivation of ISP subunit is a reversible phenomenon. Future studies may include studying the EPR signal of ISP subunit to identify the functional restoration of the ISP catalytic site and the relationship to the improved complex III activity. In addition, it would be interesting to study if ASK1-i treatment restored complex III activity by preserving cardiolipin content. Future studies are required to study the contribution of ASK1-i treatment in preventing cytochrome c peroxidase formation thereby preserving the cardiolipin content which can be probable mechanism through which both complex III activity and cytochrome c content are restored. Also, ASK1 is a MAPK kinase kinase and its possible role in phosphorylation of complex III subunits need to be elucidated. Hence, another possible mechanism through which the inhibitor of ASK1 improves complex III activation is by preventing phosphorylation of complex III subunits thereby decreasing its damage.

Ischemia-damaged mitochondria remain as sources of ROS production and the activators of apoptosis as reperfusion continues [5, 222]. In order for the post-ischemic myocyte to fully recover from ischemia, these damaged mitochondria must eventually undergo repair or removal, through the processes of mitochondrial remodeling or autophagy [138, 192, 193]. Moreover, an approach such as ASK1-i treatment during reperfusion modulates ETC during the course of reperfusion by improving mitochondrial

function, retaining cytochrome c leading to a decrease in the signal for mitophagy. Decreasing mitophagy will prevent the transition to the post-infarction ischemic cardiomyopathy state. We anticipate that the ASK1-i-mediated protection of mitochondria during ischemia favors a pro-survival mitochondrial phenotype and prevents the maladaptive remodeling of the mitochondria by preserving fusion proteins throughout reperfusion. The preservation of fusion proteins will favor the maintenance of mitochondrial membrane potential and bioenergetic function, and will also decrease the stimulus for activation of mitophagy thereby decreasing tissue injury observed after prolonged reperfusion.

In summary, the major finding of the present study was that pharmacological inhibition of ASK1 protects the heart during reperfusion via the modulation of mitochondria that sustained damage during ischemia. This mitochondrial-based mechanism of cardioprotection enhanced the functional integrity of the inner mitochondrial membrane retaining cytochrome c thereby decreasing cell death **(Figure 3.15)**.

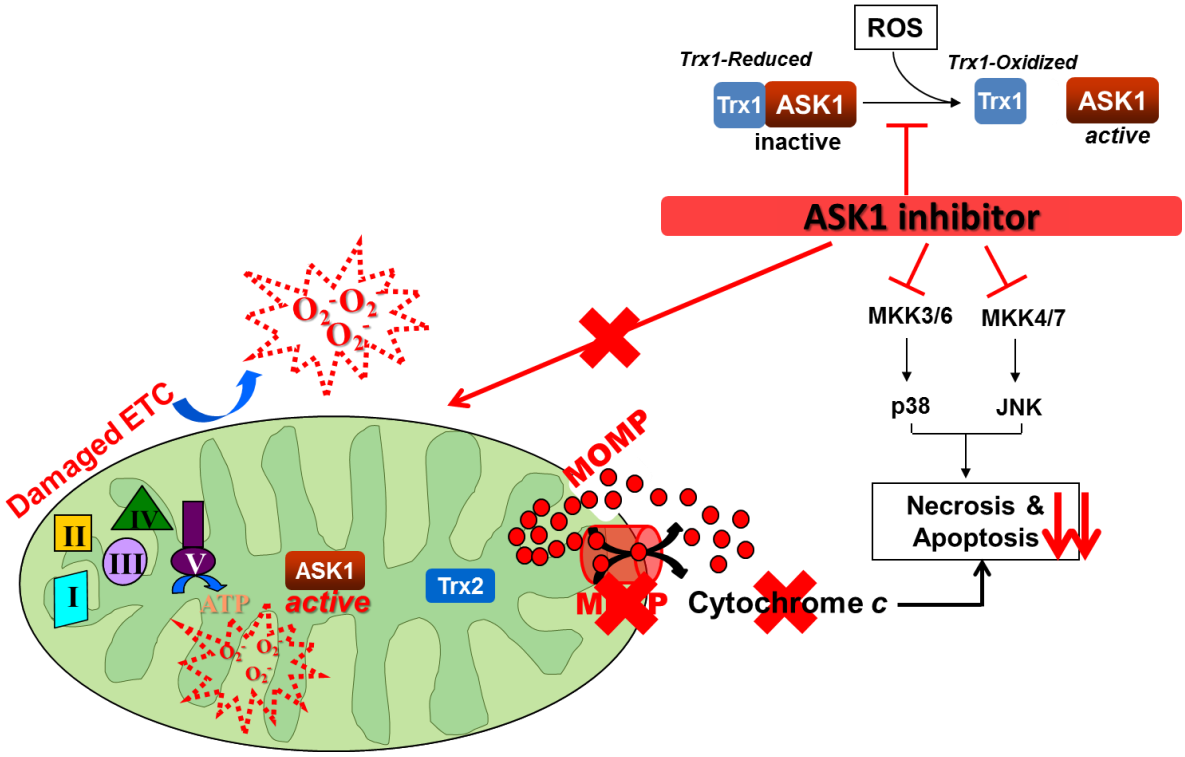


**Figure 3.15. Postulated mechanismof cardioprotection with ASK1-i during ischemia-reperfusion.** The cell-permeable small molecule inhibitor of ASK1 given at the onset of reperfusion protects mitochondrial ETC, decreases susceptibility to MPTP opening and retains cytochrome c in the mitochondria thereby decreasing mitochondrial driven cardiac injury. ASK1, apoptosis signaling kinase 1; MPTP, mitochondrial permeability transition pore opening, Trx, Thioredoxin; ROS, reactive oxygen species.

# CHAPTER IV: CONCLUDING REMARKS

Excessive generation of ROS during oxidative stress conditions oxidize methionine residues in proteins forming methionine sulfoxide and can result in loss of protein's function [405, 406]. Cytochrome c is a small heme protein that transfers electrons between respiratory complexes III and IV located in the inner membrane of mitochondria. Excessive generation of reactive oxygen species (ROS) oxidizes a key methionine residue ($Met_{81}$) of cytochrome c converting it into a pathological peroxidase [264, 271, 406]. Cytochrome c peroxidase oxidizes and depletes cardiolipin releasing pro-apoptotic proteins into the cytosol activating cell death cascades [264, 276]. In order to maintain homeostatis, living organisms have developed a complex and cyclic defense system, the methionine sulfoxide reductase system, comprising enzymatic and non-enzymatic antioxidants to restore the cytochrome c function [407, 408].

Methionine sulfoxide reductases (MSR) are redox repair enzymes which reduce both free and protein bound Met(O) back to methionine (Met) in the presence of thioredoxin

[407, 408]. Oxidized Trx is inactive and unable to bind to ASK1 thereby activating ASK1 and causing cell death via p38/JNK pathways [319, 327, 396]. The oxidized thioredoxin formed is reduced by thioredoxin reductase at the expense of NADPH. Thioredoxin reductases (TrxR) are oxido-reductases that reduce the active site disulfide in Trx maintaining the pool of reduced Trx [409]. Reduced Trx can bind to ASK1 at the N-terminal coiled coil (NCC) domain and inactivates ASK1 by directing it for ubiquitination and degradation [319, 326, 327]. The net result is the catalytic scavenging of ROS by NADPH **(Figure 4.1)**. Hence, it is clear that the cytochrome c and ASK1 cause cell injury through an inter-connected mechanism which is not yet explored during ischemia-reperfusion.

Isoforms of MSRB, MSRB2 and MSRB3B, contain an N-terminal mitochondrial targeting sequence, localizing them to mitochondria [405, 407]. In a recent study, mouse MSRA was shown to be important in cytochrome c repair and protection against cataract [410]. Another study showed that cytosolic MSRA protects the heart from ischemia-reperfusion damage [411]. These studies highlight the pathological role of methionine sulfoxidation in causing cell death and the importance of redox enzymes, methionine sulfoxide reductases, in decreasing cell injury.

Through this study we propose a novel pathway through which mitochondria trigger cell death during ischemia-reperfusion. Excessive generation of ROS and limited NADPH availability, during ischemia-reperfusion burdens and interferes with the methionine redox enzyme system. As a result the cytochrome c oxidized at methionine residue during ischemia is not effectively repaired by MSRB. Oxidized cytochrome c converts to a peroxidase creating an altered electron flow thereby oxidizing and depleting cardiolipin

from the mitochondrial membrane. In addition, high levels of ROS that exceed the capacity of the antioxidant system may lead to an increase in oxidized thioredoxin pool that activates ASK1 and result in cell death.

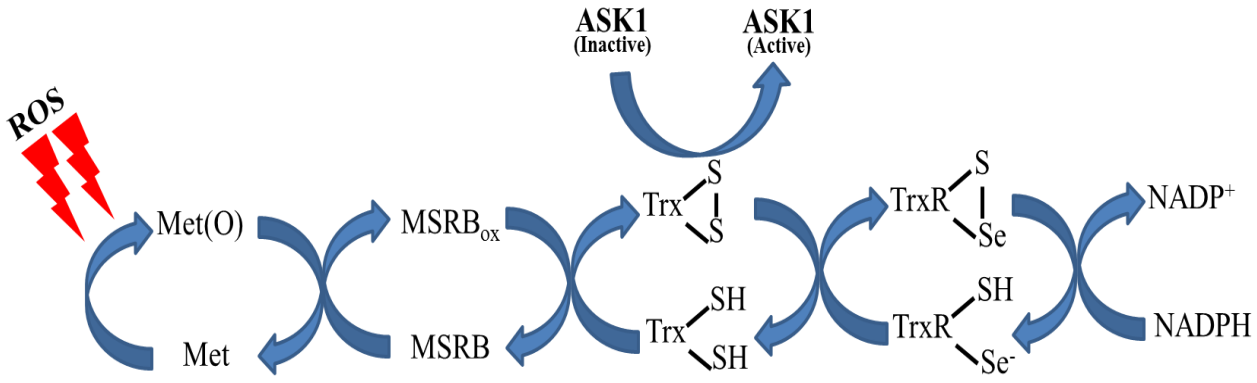


**Figure 4.1. Schematic of the antioxidant defense system created by oxidation and reduction of methionine residues.** ROS is oxidized to Met(O) which is reduced back to Met by MSRB, with the formation of a disulfide bond. The oxidized MSRB is reduced by thioredoxin, forming a disulfide bond. Oxidation of thioredoxin activates ASK1. Oxidized thioredoxin is reduced by thioredoxin reductase containing a selenocysteine residue which is then reduced by NADPH. The net result is that ROS is reduced at the expense of NADPH. Met, methionine; MSRB, methionine sulfoxide reductase B; Trx, thioredoxin; TrxR, thioredoxin reductase; NADPH, nicotinamide adenine dinucleotide phosphate.

## BIBLIOGRAPHY

[1] Henze K, Martin W. Evolutionary biology: essence of mitochondria. Nature. 2003;426:127-8.

[2] McBride HM, Neuspiel M, Wasiak S. Mitochondria: more than just a powerhouse. Current biology : CB. 2006;16:R551-60.

[3] Edmond JC. Mitochondrial disorders. International ophthalmology clinics. 2009;49:27-33.

[4] Hoppel CL, Tandler B, Fujioka H, Riva A. Dynamic organization of mitochondria in human heart and in myocardial disease. The international journal of biochemistry & cell biology. 2009;41:1949-56.

[5] Lesnefsky EJ, Moghaddas S, Tandler B, Kerner J, Hoppel CL. Mitochondrial dysfunction in cardiac disease: ischemia--reperfusion, aging, and heart failure. J Mol Cell Cardiol. 2001;33:1065-89.

[6] Bruce Alberts AJ, Julian Lewis, Martin Raff, Keith Roberts, and Peter Walter. Molecular Biology of the Cell. Fourth Edition ed: Garland Science; 2004.

[7] Margulis L. Symbiosis in Cell Evolution: Life and Its Environment on the Early Earth: W.H. Freeman & Company; 1981.

[8] Voet DJGV, Charlotte W. Pratt. Fundamentals of Biochemistry: Life at the Molecular Level. 4 edition ed: Wiley; 2012.

[9] Neupert W, Herrmann JM. Translocation of proteins into mitochondria. Annual review of biochemistry. 2007;76:723-49.

[10] Rizzuto R, Marchi S, Bonora M, Aguiari P, Bononi A, De Stefani D, et al. Ca(2+) transfer from the ER to mitochondria: when, how and why. Biochim Biophys Acta. 2009;1787:1342-51.

[11] Hayashi T, Rizzuto R, Hajnoczky G, Su TP. MAM: more than just a housekeeper. Trends Cell Biol. 2009;19:81-8.

[12] de Brito OM, Scorrano L. An intimate liaison: spatial organization of the endoplasmic reticulum-mitochondria relationship. The EMBO journal. 2010;29:2715-23.

[13] Chipuk JE, Bouchier-Hayes L, Green DR. Mitochondrial outer membrane permeabilization during apoptosis: the innocent bystander scenario. Cell death and differentiation. 2006;13:1396-402.

[14] Diekert K, de Kroon AI, Ahting U, Niggemeyer B, Neupert W, de Kruijff B, et al. Apocytochrome c requires the TOM complex for translocation across the mitochondrial outer membrane. The EMBO journal. 2001;20:5626-35.

[15] Wiedemann N, Kozjak V, Prinz T, Ryan MT, Meisinger C, Pfanner N, et al. Biogenesis of yeast mitochondrial cytochrome c: a unique relationship to the TOM machinery. Journal of molecular biology. 2003;327:465-74.

[16] Mannella CA. Structure and dynamics of the mitochondrial inner membrane cristae. Biochim Biophys Acta. 2006;1763:542-8.

[17] Anderson S, Bankier AT, Barrell BG, de Bruijn MH, Coulson AR, Drouin J, et al. Sequence and organization of the human mitochondrial genome. Nature. 1981;290:457-65.

[18] Falkenberg M, Larsson NG, Gustafsson CM. DNA replication and transcription in mammalian mitochondria. Annual review of biochemistry. 2007;76:679-99.

[19] DiMauro S. Mitochondrial myopathies. Current opinion in rheumatology. 2006;18:636-41.

[20] Larsson NG, Clayton DA. Molecular genetic aspects of human mitochondrial disorders. Annual review of genetics. 1995;29:151-78.

[21] Taylor RW, Turnbull DM. Mitochondrial DNA mutations in human disease. Nature reviews Genetics. 2005;6:389-402.

[22] Zeviani M, Di Donato S. Mitochondrial disorders. Brain : a journal of neurology. 2004;127:2153-72.

[23] Jacobs HT, Turnbull DM. Nuclear genes and mitochondrial translation: a new class of genetic disease. Trends in genetics : TIG. 2005;21:312-4.

[24] Barnes SJ, Weitzman PD. Organization of citric acid cycle enzymes into a multienzyme cluster. FEBS Lett. 1986;201:267-70.

[25] Jeremy M Berg, John L Tymoczko, Stryer L. Biochemistry: W H Freeman; 2007.

[26] David Keilin JK. The History of Cell Respiration and Cytochrome. 1 edition ed: Cambridge University Press; 1966.

[27] Mitchell P. Coupling of phosphorylation to electron and hydrogen transfer by a chemi-osmotic type of mechanism. Nature. 1961;191:144-8.

[28] Slater EC. Keilin, cytochrome, and the respiratory chain. J Biol Chem. 2003;278:16455-61.

[29] DG N, SJ F. Bioenergetics. 3 edition ed: Academic Press; 2002.

[30] Rich PR. The molecular machinery of Keilin's respiratory chain. Biochemical Society transactions. 2003;31:1095-105.

[31] Schagger H, Pfeiffer K. Supercomplexes in the respiratory chains of yeast and mammalian mitochondria. The EMBO journal. 2000;19:1777-83.

[32] O'Rourke B. Mitochondrial ion channels. Annual review of physiology. 2007;69:19-49.

[33] Kaasik A, Safiulina D, Zharkovsky A, Veksler V. Regulation of mitochondrial matrix volume. Am J Physiol Cell Physiol. 2007;292:C157-63.

[34] Klingenberg M. The ADP and ATP transport in mitochondria and its carrier. Biochim Biophys Acta. 2008;1778:1978-2021.

[35] Solaini G, Sgarbi G, Lenaz G, Baracca A. Evaluating mitochondrial membrane potential in cells. Bioscience reports. 2007;27:11-21.

[36] Distelmaier F, Koopman WJ, Testa ER, de Jong AS, Swarts HG, Mayatepek E, et al. Life cell quantification of mitochondrial membrane potential at the single organelle level. Cytometry Part A : the journal of the International Society for Analytical Cytology. 2008;73:129-38.

[37] Szczepanek K, Chen Q, Larner AC, Lesnefsky EJ. Cytoprotection by the modulation of mitochondrial electron transport chain: the emerging role of mitochondrial STAT3. Mitochondrion. 2012;12:180-9.

[38] Hirst J, Carroll J, Fearnley IM, Shannon RJ, Walker JE. The nuclear encoded subunits of complex I from bovine heart mitochondria. Biochim Biophys Acta. 2003;1604:135-50.

[39] L E. Molecular Mechanisms in Bioenergetics. 1 edition ed: Elsevier Science; 1992.

[40] Hinchliffe P, Sazanov LA. Organization of iron-sulfur clusters in respiratory complex I. Science. 2005;309:771-4.

[41] Sazanov LA, Hinchliffe P. Structure of the hydrophilic domain of respiratory complex I from Thermus thermophilus. Science. 2006;311:1430-6.

[42] Fendel U, Tocilescu MA, Kerscher S, Brandt U. Exploring the inhibitor binding pocket of respiratory complex I. Biochim Biophys Acta. 2008;1777:660-5.

[43] Schagger H. Respiratory chain supercomplexes. IUBMB life. 2001;52:119-28.

[44] Lazarou M, Thorburn DR, Ryan MT, McKenzie M. Assembly of mitochondrial complex I and defects in disease. Biochim Biophys Acta. 2009;1793:78-88.

[45] Hoefs SJ, Dieteren CE, Distelmaier F, Janssen RJ, Epplen A, Swarts HG, et al. NDUFA2 complex I mutation leads to Leigh disease. American journal of human genetics. 2008;82:1306-15.

[46] Martin MA, Blazquez A, Gutierrez-Solana LG, Fernandez-Moreira D, Briones P, Andreu AL, et al. Leigh syndrome associated with mitochondrial complex I deficiency due to a novel mutation in the NDUFS1 gene. Archives of neurology. 2005;62:659-61.

[47] Ugalde C, Hinttala R, Timal S, Smeets R, Rodenburg RJ, Uusimaa J, et al. Mutated ND2 impairs mitochondrial complex I assembly and leads to Leigh syndrome. Molecular genetics and metabolism. 2007;90:10-4.

[48] Mroczek-Tonska K, Kisiel B, Piechota J, Bartnik E. Leber hereditary optic neuropathy--a disease with a known molecular basis but a mysterious mechanism of pathology. Journal of applied genetics. 2003;44:529-38.

[49] Brown MD, Voljavec AS, Lott MT, Torroni A, Yang CC, Wallace DC. Mitochondrial DNA complex I and III mutations associated with Leber's hereditary optic neuropathy. Genetics. 1992;130:163-73.

[50] Keeney PM, Xie J, Capaldi RA, Bennett JP, Jr. Parkinson's disease brain mitochondrial complex I has oxidatively damaged subunits and is functionally impaired and misassembled. The Journal of neuroscience : the official journal of the Society for Neuroscience. 2006;26:5256-64.

[51] Schapira AH, Cooper JM, Dexter D, Jenner P, Clark JB, Marsden CD. Mitochondrial complex I deficiency in Parkinson's disease. Lancet. 1989;1:1269.

[52] Maj MC, Raha S, Myint T, Robinson BH. Regulation of NADH/CoQ oxidoreductase: do phosphorylation events affect activity? The protein journal. 2004;23:25-32.

[53] Taylor ER, Hurrell F, Shannon RJ, Lin TK, Hirst J, Murphy MP. Reversible glutathionylation of complex I increases mitochondrial superoxide formation. J Biol Chem. 2003;278:19603-10.

[54] Beer SM, Taylor ER, Brown SE, Dahm CC, Costa NJ, Runswick MJ, et al. Glutaredoxin 2 catalyzes the reversible oxidation and glutathionylation of mitochondrial

membrane thiol proteins: implications for mitochondrial redox regulation and antioxidant DEFENSE. J Biol Chem. 2004;279:47939-51.

[55] Chen CL, Zhang L, Yeh A, Chen CA, Green-Church KB, Zweier JL, et al. Site-specific S-glutathiolation of mitochondrial NADH ubiquinone reductase. Biochemistry. 2007;46:5754-65.

[56] Ahn BH, Kim HS, Song S, Lee IH, Liu J, Vassilopoulos A, et al. A role for the mitochondrial deacetylase Sirt3 in regulating energy homeostasis. Proceedings of the National Academy of Sciences of the United States of America. 2008;105:14447-52.

[57] Burwell LS, Nadtochiy SM, Tompkins AJ, Young S, Brookes PS. Direct evidence for S-nitrosation of mitochondrial complex I. The Biochemical journal. 2006;394:627-34.

[58] Clementi E, Brown GC, Feelisch M, Moncada S. Persistent inhibition of cell respiration by nitric oxide: crucial role of S-nitrosylation of mitochondrial complex I and protective action of glutathione. Proceedings of the National Academy of Sciences of the United States of America. 1998;95:7631-6.

[59] Sun F, Huo X, Zhai Y, Wang A, Xu J, Su D, et al. Crystal structure of mitochondrial respiratory membrane protein complex II. Cell. 2005;121:1043-57.

[60] Muller FL, Liu Y, Abdul-Ghani MA, Lustgarten MS, Bhattacharya A, Jang YC, et al. High rates of superoxide production in skeletal-muscle mitochondria respiring on both complex I- and complex II-linked substrates. The Biochemical journal. 2008;409:491-9.

[61] Cimen H, Han MJ, Yang Y, Tong Q, Koc H, Koc EC. Regulation of succinate dehydrogenase activity by SIRT3 in mammalian mitochondria. Biochemistry. 2010;49:304-11.

[62] Chen YR, Chen CL, Pfeiffer DR, Zweier JL. Mitochondrial complex II in the post-ischemic heart: oxidative injury and the role of protein S-glutathionylation. J Biol Chem. 2007;282:32640-54.

[63] Salvi M, Morrice NA, Brunati AM, Toninello A. Identification of the flavoprotein of succinate dehydrogenase and aconitase as in vitro mitochondrial substrates of Fgr tyrosine kinase. FEBS Lett. 2007;581:5579-85.

[64] Briere JJ, Favier J, El Ghouzzi V, Djouadi F, Benit P, Gimenez AP, et al. Succinate dehydrogenase deficiency in human. Cellular and molecular life sciences : CMLS. 2005;62:2317-24.

[65] Yanase S, Yasuda K, Ishii N. Adaptive responses to oxidative damage in three mutants of Caenorhabditis elegans (age-1, mev-1 and daf-16) that affect life span. Mechanisms of ageing and development. 2002;123:1579-87.

[66] Xia D, Yu CA, Kim H, Xia JZ, Kachurin AM, Zhang L, et al. Crystal structure of the cytochrome bc1 complex from bovine heart mitochondria. Science. 1997;277:60-6.

[67] Crofts AR. The cytochrome bc1 complex: function in the context of structure. Annual review of physiology. 2004;66:689-733.

[68] Brandt U, Trumpower B. The protonmotive Q cycle in mitochondria and bacteria. Critical reviews in biochemistry and molecular biology. 1994;29:165-97.

[69] Link T, Haase U, Brandt U, von Jagow G. What information do inhibitors provide about the structure of the hydroquinone oxidation site of ubihydroquinone: Cytochromec oxidoreductase? Journal of bioenergetics and biomembranes. 1993;25:221-32.

[70] Schuelke M, Krude H, Finckh B, Mayatepek E, Janssen A, Schmelz M, et al. Septo-optic dysplasia associated with a new mitochondrial cytochrome b mutation. Annals of neurology. 2002;51:388-92.

[71] Wibrand F, Ravn K, Schwartz M, Rosenberg T, Horn N, Vissing J. Multisystem disorder associated with a missense mutation in the mitochondrial cytochrome b gene. Annals of neurology. 2001;50:540-3.

[72] Hinson JT, Fantin VR, Schonberger J, Breivik N, Siem G, McDonough B, et al. Missense mutations in the BCS1L gene as a cause of the Bjornstad syndrome. The New England journal of medicine. 2007;356:809-19.

[73] Visapaa I, Fellman V, Vesa J, Dasvarma A, Hutton JL, Kumar V, et al. GRACILE syndrome, a lethal metabolic disorder with iron overload, is caused by a point mutation in BCS1L. American journal of human genetics. 2002;71:863-76.

[74] Tsukihara T, Aoyama H, Yamashita E, Tomizaki T, Yamaguchi H, Shinzawa-Itoh K, et al. The whole structure of the 13-subunit oxidized cytochrome c oxidase at 2.8 A. Science. 1996;272:1136-44.

[75] Pecina P, Houstkova H, Hansikova H, Zeman J, Houstek J. Genetic defects of cytochrome c oxidase assembly. Physiological research / Academia Scientiarum Bohemoslovaca. 2004;53 Suppl 1:S213-23.

[76] Papadopoulou LC, Sue CM, Davidson MM, Tanji K, Nishino I, Sadlock JE, et al. Fatal infantile cardioencephalomyopathy with COX deficiency and mutations in SCO2, a COX assembly gene. Nature genetics. 1999;23:333-7.

[77] Antonicka H, Mattman A, Carlson CG, Glerum DM, Hoffbuhr KC, Leary SC, et al. Mutations in COX15 produce a defect in the mitochondrial heme biosynthetic pathway,

causing early-onset fatal hypertrophic cardiomyopathy. American journal of human genetics. 2003;72:101-14.

[78] Turrens JF. Mitochondrial formation of reactive oxygen species. The Journal of physiology. 2003;552:335-44.

[79] Balaban RS, Nemoto S, Finkel T. Mitochondria, oxidants, and aging. Cell. 2005;120:483-95.

[80] Raha S, Robinson BH. Mitochondria, oxygen free radicals, disease and ageing. Trends in biochemical sciences. 2000;25:502-8.

[81] Baines CP, Goto M, Downey JM. Oxygen radicals released during ischemic preconditioning contribute to cardioprotection in the rabbit myocardium. J Mol Cell Cardiol. 1997;29:207-16.

[82] Das DK, Maulik N, Sato M, Ray PS. Reactive oxygen species function as second messenger during ischemic preconditioning of heart. Molecular and cellular biochemistry. 1999;196:59-67.

[83] Droge W. Free radicals in the physiological control of cell function. Physiological reviews. 2002;82:47-95.

[84] Liu Y, Fiskum G, Schubert D. Generation of reactive oxygen species by the mitochondrial electron transport chain. Journal of neurochemistry. 2002;80:780-7.

[85] Chen Q, Vazquez EJ, Moghaddas S, Hoppel CL, Lesnefsky EJ. Production of reactive oxygen species by mitochondria: central role of complex III. J Biol Chem. 2003;278:36027-31.

[86] Boveris A. Determination of the production of superoxide radicals and hydrogen peroxide in mitochondria. Methods in enzymology. 1984;105:429-35.

[87] Murphy MP. How mitochondria produce reactive oxygen species. The Biochemical journal. 2009;417:1-13.

[88] Han D, Antunes F, Canali R, Rettori D, Cadenas E. Voltage-dependent anion channels control the release of the superoxide anion from mitochondria to cytosol. J Biol Chem. 2003;278:5557-63.

[89] Kudin AP, Bimpong-Buta NY, Vielhaber S, Elger CE, Kunz WS. Characterization of superoxide-producing sites in isolated brain mitochondria. J Biol Chem. 2004;279:4127-35.

[90] Sazanov LA. Respiratory complex I: mechanistic and structural insights provided by the crystal structure of the hydrophilic domain. Biochemistry. 2007;46:2275-88.

[91] Cadenas E, Boveris A, Ragan CI, Stoppani AO. Production of superoxide radicals and hydrogen peroxide by NADH-ubiquinone reductase and ubiquinol-cytochrome c reductase from beef-heart mitochondria. Arch Biochem Biophys. 1977;180:248-57.

[92] Ohnishi ST, Ohnishi T, Muranaka S, Fujita H, Kimura H, Uemura K, et al. A possible site of superoxide generation in the complex I segment of rat heart mitochondria. Journal of bioenergetics and biomembranes. 2005;37:1-15.

[93] Takeshige K, Minakami S. NADH- and NADPH-dependent formation of superoxide anions by bovine heart submitochondrial particles and NADH-ubiquinone reductase preparation. The Biochemical journal. 1979;180:129-35.

[94] Kushnareva Y, Murphy AN, Andreyev A. Complex I-mediated reactive oxygen species generation: modulation by cytochrome c and NAD(P)+ oxidation-reduction state. The Biochemical journal. 2002;368:545-53.

[95] Kussmaul L, Hirst J. The mechanism of superoxide production by NADH:ubiquinone oxidoreductase (complex I) from bovine heart mitochondria. Proceedings of the National Academy of Sciences of the United States of America. 2006;103:7607-12.

[96] Hansford RG, Hogue BA, Mildaziene V. Dependence of H2O2 formation by rat heart mitochondria on substrate availability and donor age. Journal of bioenergetics and biomembranes. 1997;29:89-95.

[97] Votyakova TV, Reynolds IJ. DeltaPsi(m)-Dependent and -independent production of reactive oxygen species by rat brain mitochondria. Journal of neurochemistry. 2001;79:266-77.

[98] Hinkle PC, Butow RA, Racker E, Chance B. Partial resolution of the enzymes catalyzing oxidative phosphorylation. XV. Reverse electron transfer in the flavin-cytochrome beta region of the respiratory chain of beef heart submitochondrial particles. J Biol Chem. 1967;242:5169-73.

[99] Lambert AJ, Brand MD. Inhibitors of the quinone-binding site allow rapid superoxide production from mitochondrial NADH:ubiquinone oxidoreductase (complex I). J Biol Chem. 2004;279:39414-20.

[100] Hirst J, King MS, Pryde KR. The production of reactive oxygen species by complex I. Biochemical Society transactions. 2008;36:976-80.

[101] Genova ML, Ventura B, Giuliano G, Bovina C, Formiggini G, Parenti Castelli G, et al. The site of production of superoxide radical in mitochondrial Complex I is not a bound ubisemiquinone but presumably iron-sulfur cluster N2. FEBS Lett. 2001;505:364-8.

[102] Chen Q, Moghaddas S, Hoppel CL, Lesnefsky EJ. Ischemic defects in the electron transport chain increase the production of reactive oxygen species from isolated rat heart mitochondria. Am J Physiol Cell Physiol. 2008;294:C460-6.

[103] Turrens JF, Alexandre A, Lehninger AL. Ubisemiquinone is the electron donor for superoxide formation by complex III of heart mitochondria. Arch Biochem Biophys. 1985;237:408-14.

[104] Covian R, Trumpower BL. Regulatory interactions between ubiquinol oxidation and ubiquinone reduction sites in the dimeric cytochrome bc1 complex. J Biol Chem. 2006;281:30925-32.

[105] Raha S, McEachern GE, Myint AT, Robinson BH. Superoxides from mitochondrial complex III: the role of manganese superoxide dismutase. Free Radic Biol Med. 2000;29:170-80.

[106] Sun J, Trumpower BL. Superoxide anion generation by the cytochrome bc1 complex. Arch Biochem Biophys. 2003;419:198-206.

[107] Lesnefsky EJ, Gudz TI, Moghaddas S, Migita CT, Ikeda-Saito M, Turkaly PJ, et al. Aging decreases electron transport complex III activity in heart interfibrillar mitochondria by alteration of the cytochrome c binding site. J Mol Cell Cardiol. 2001;33:37-47.

[108] Muller FL, Liu Y, Van Remmen H. Complex III releases superoxide to both sides of the inner mitochondrial membrane. J Biol Chem. 2004;279:49064-73.

[109] St-Pierre J, Buckingham JA, Roebuck SJ, Brand MD. Topology of superoxide production from different sites in the mitochondrial electron transport chain. J Biol Chem. 2002;277:44784-90.

[110] Andreyev AY, Kushnareva YE, Starkov AA. Mitochondrial metabolism of reactive oxygen species. Biochemistry Biokhimiia. 2005;70:200-14.

[111] Guo J, Lemire BD. The ubiquinone-binding site of the Saccharomyces cerevisiae succinate-ubiquinone oxidoreductase is a source of superoxide. J Biol Chem. 2003;278:47629-35.

[112] Yankovskaya V, Horsefield R, Tornroth S, Luna-Chavez C, Miyoshi H, Leger C, et al. Architecture of succinate dehydrogenase and reactive oxygen species generation. Science. 2003;299:700-4.

[113] Messner KR, Imlay JA. Mechanism of superoxide and hydrogen peroxide formation by fumarate reductase, succinate dehydrogenase, and aspartate oxidase. J Biol Chem. 2002;277:42563-71.

[114] Guzy RD, Sharma B, Bell E, Chandel NS, Schumacker PT. Loss of the SdhB, but Not the SdhA, subunit of complex II triggers reactive oxygen species-dependent hypoxia-inducible factor activation and tumorigenesis. Molecular and cellular biology. 2008;28:718-31.

[115] Zhang L, Yu L, Yu CA. Generation of superoxide anion by succinate-cytochrome c reductase from bovine heart mitochondria. J Biol Chem. 1998;273:33972-6.

[116] Tretter L, Adam-Vizi V. Generation of reactive oxygen species in the reaction catalyzed by alpha-ketoglutarate dehydrogenase. The Journal of neuroscience : the official journal of the Society for Neuroscience. 2004;24:7771-8.

[117] Koza RA, Kozak UC, Brown LJ, Leiter EH, MacDonald MJ, Kozak LP. Sequence and tissue-dependent RNA expression of mouse FAD-linked glycerol-3-phosphate dehydrogenase. Arch Biochem Biophys. 1996;336:97-104.

[118] Hanukoglu I, Rapoport R, Weiner L, Sklan D. Electron leakage from the mitochondrial NADPH-adrenodoxin reductase-adrenodoxin-P450scc (cholesterol side chain cleavage) system. Arch Biochem Biophys. 1993;305:489-98.

[119] Giorgio M, Migliaccio E, Orsini F, Paolucci D, Moroni M, Contursi C, et al. Electron transfer between cytochrome c and p66Shc generates reactive oxygen species that trigger mitochondrial apoptosis. Cell. 2005;122:221-33.

[120] Di Lisa F, Kaludercic N, Carpi A, Menabo R, Giorgio M. Mitochondrial pathways for ROS formation and myocardial injury: the relevance of p66(Shc) and monoamine oxidase. Basic Res Cardiol. 2009;104:131-9.

[121] Zhao H, Joseph J, Fales HM, Sokoloski EA, Levine RL, Vasquez-Vivar J, et al. Detection and characterization of the product of hydroethidine and intracellular superoxide by HPLC and limitations of fluorescence. Proceedings of the National Academy of Sciences of the United States of America. 2005;102:5727-32.

[122] Robinson KM, Janes MS, Pehar M, Monette JS, Ross MF, Hagen TM, et al. Selective fluorescent imaging of superoxide in vivo using ethidium-based probes. Proceedings of the National Academy of Sciences of the United States of America. 2006;103:15038-43.

[123] Zielonka J, Vasquez-Vivar J, Kalyanaraman B. Detection of 2-hydroxyethidium in cellular systems: a unique marker product of superoxide and hydroethidine. Nature protocols. 2008;3:8-21.

[124] Lucas M, Solano F. Coelenterazine is a superoxide anion-sensitive chemiluminescent probe: its usefulness in the assay of respiratory burst in neutrophils. Anal Biochem. 1992;206:273-7.

[125] Cocheme HM, Murphy MP. Complex I is the major site of mitochondrial superoxide production by paraquat. J Biol Chem. 2008;283:1786-98.

[126] Gardner PR. Aconitase: sensitive target and measure of superoxide. Methods in enzymology. 2002;349:9-23.

[127] Loschen G, Flohe L, Chance B. Respiratory chain linked H(2)O(2) production in pigeon heart mitochondria. FEBS Lett. 1971;18:261-4.

[128] Sohal RS. Hydrogen peroxide production by mitochondria may be a biomarker of aging. Mechanisms of ageing and development. 1991;60:189-98.

[129] McCord JM, Fridovich I. Superoxide dismutase: the first twenty years (1968-1988). Free Radic Biol Med. 1988;5:363-9.

[130] Buettner GR, Ng CF, Wang M, Rodgers VG, Schafer FQ. A new paradigm: manganese superoxide dismutase influences the production of H2O2 in cells and thereby their biological state. Free Radic Biol Med. 2006;41:1338-50.

[131] Lesnefsky EJ. Reduction of infarct size by cell-permeable oxygen metabolite scavengers. Free Radic Biol Med. 1992;12:429-46.

[132] Brand MD, Affourtit C, Esteves TC, Green K, Lambert AJ, Miwa S, et al. Mitochondrial superoxide: production, biological effects, and activation of uncoupling proteins. Free Radic Biol Med. 2004;37:755-67.

[133] Wallace DC. A mitochondrial paradigm of metabolic and degenerative diseases, aging, and cancer: a dawn for evolutionary medicine. Annual review of genetics. 2005;39:359-407.

[134] Rhee SG, Kang SW, Chang TS, Jeong W, Kim K. Peroxiredoxin, a novel family of peroxidases. IUBMB life. 2001;52:35-41.

[135] Salvi M, Battaglia V, Brunati AM, La Rocca N, Tibaldi E, Pietrangeli P, et al. Catalase takes part in rat liver mitochondria oxidative stress defense. J Biol Chem. 2007;282:24407-15.

[136] Imai H, Nakagawa Y. Biological significance of phospholipid hydroperoxide glutathione peroxidase (PHGPx, GPx4) in mammalian cells. Free Radic Biol Med. 2003;34:145-69.

[137] Ng CF, Schafer FQ, Buettner GR, Rodgers VG. The rate of cellular hydrogen peroxide removal shows dependency on GSH: mathematical insight into in vivo H2O2 and GPx concentrations. Free radical research. 2007;41:1201-11.

[138] Kubli DA, Gustafsson AB. Mitochondria and mitophagy: the yin and yang of cell death control. Circulation research. 2012;111:1208-21.

[139] Kerr JF, Wyllie AH, Currie AR. Apoptosis: a basic biological phenomenon with wide-ranging implications in tissue kinetics. British journal of cancer. 1972;26:239-57.

[140] Aggarwal BB. Signalling pathways of the TNF superfamily: a double-edged sword. Nature reviews Immunology. 2003;3:745-56.

[141] Wang C, Youle RJ. The role of mitochondria in apoptosis*. Annual review of genetics. 2009;43:95-118.

[142] Parsons MJ, Green DR. Mitochondria in cell death. Essays in biochemistry. 2010;47:99-114.

[143] Gustafsson AB, Gottlieb RA. Bcl-2 family members and apoptosis, taken to heart. Am J Physiol Cell Physiol. 2007;292:C45-51.

[144] Wei MC, Zong WX, Cheng EH, Lindsten T, Panoutsakopoulou V, Ross AJ, et al. Proapoptotic BAX and BAK: a requisite gateway to mitochondrial dysfunction and death. Science. 2001;292:727-30.

[145] Zong WX, Lindsten T, Ross AJ, MacGregor GR, Thompson CB. BH3-only proteins that bind pro-survival Bcl-2 family members fail to induce apoptosis in the absence of Bax and Bak. Genes & development. 2001;15:1481-6.

[146] Kuwana T, Mackey MR, Perkins G, Ellisman MH, Latterich M, Schneiter R, et al. Bid, Bax, and lipids cooperate to form supramolecular openings in the outer mitochondrial membrane. Cell. 2002;111:331-42.

[147] Gustafsson AB, Gottlieb RA. Heart mitochondria: gates of life and death. Cardiovascular research. 2008;77:334-43.

[148] Gustafsson AB, Gottlieb RA. Mechanisms of apoptosis in the heart. Journal of clinical immunology. 2003;23:447-59.

[149] Borutaite V, Budriunaite A, Morkuniene R, Brown GC. Release of mitochondrial cytochrome c and activation of cytosolic caspases induced by myocardial ischaemia. Biochim Biophys Acta. 2001;1537:101-9.

[150] Suzuki Y, Imai Y, Nakayama H, Takahashi K, Takio K, Takahashi R. A serine protease, HtrA2, is released from the mitochondria and interacts with XIAP, inducing cell death. Molecular cell. 2001;8:613-21.

[151] Verhagen AM, Ekert PG, Pakusch M, Silke J, Connolly LM, Reid GE, et al. Identification of DIABLO, a mammalian protein that promotes apoptosis by binding to and antagonizing IAP proteins. Cell. 2000;102:43-53.

[152] Cande C, Cohen I, Daugas E, Ravagnan L, Larochette N, Zamzami N, et al. Apoptosis-inducing factor (AIF): a novel caspase-independent death effector released from mitochondria. Biochimie. 2002;84:215-22.

[153] Li LY, Luo X, Wang X. Endonuclease G is an apoptotic DNase when released from mitochondria. Nature. 2001;412:95-9.

[154] Crompton M. The mitochondrial permeability transition pore and its role in cell death. The Biochemical journal. 1999;341 ( Pt 2):233-49.

[155] Zamzami N, Kroemer G. The mitochondrion in apoptosis: how Pandora's box opens. Nature reviews Molecular cell biology. 2001;2:67-71.

[156] Baines CP. The cardiac mitochondrion: nexus of stress. Annual review of physiology. 2010;72:61-80.

[157] Chiong M, Wang ZV, Pedrozo Z, Cao DJ, Troncoso R, Ibacache M, et al. Cardiomyocyte death: mechanisms and translational implications. Cell death & disease. 2011;2:e244.

[158] Korsmeyer SJ, Wei MC, Saito M, Weiler S, Oh KJ, Schlesinger PH. Pro-apoptotic cascade activates BID, which oligomerizes BAK or BAX into pores that result in the release of cytochrome c. Cell death and differentiation. 2000;7:1166-73.

[159] Shimizu S, Narita M, Tsujimoto Y. Bcl-2 family proteins regulate the release of apoptogenic cytochrome c by the mitochondrial channel VDAC. Nature. 1999;399:483-7.

[160] Whelan RS, Konstantinidis K, Wei AC, Chen Y, Reyna DE, Jha S, et al. Bax regulates primary necrosis through mitochondrial dynamics. Proceedings of the National Academy of Sciences of the United States of America. 2012;109:6566-71.

[161] Steenbergen C, Murphy E, Watts JA, London RE. Correlation between cytosolic free calcium, contracture, ATP, and irreversible ischemic injury in perfused rat heart. Circulation research. 1990;66:135-46.

[162] Inserte J, Garcia-Dorado D, Hernando V, Soler-Soler J. Calpain-mediated impairment of Na+/K+-ATPase activity during early reperfusion contributes to cell death after myocardial ischemia. Circulation research. 2005;97:465-73.

[163] Pattingre S, Tassa A, Qu X, Garuti R, Liang XH, Mizushima N, et al. Bcl-2 antiapoptotic proteins inhibit Beclin 1-dependent autophagy. Cell. 2005;122:927-39.

[164] Strappazzon F, Vietri-Rudan M, Campello S, Nazio F, Florenzano F, Fimia GM, et al. Mitochondrial BCL-2 inhibits AMBRA1-induced autophagy. The EMBO journal. 2011;30:1195-208.

[165] Maiuri MC, Le Toumelin G, Criollo A, Rain JC, Gautier F, Juin P, et al. Functional and physical interaction between Bcl-X(L) and a BH3-like domain in Beclin-1. The EMBO journal. 2007;26:2527-39.

[166] Maiuri MC, Criollo A, Tasdemir E, Vicencio JM, Tajeddine N, Hickman JA, et al. BH3-only proteins and BH3 mimetics induce autophagy by competitively disrupting the interaction between Beclin 1 and Bcl-2/Bcl-X(L). Autophagy. 2007;3:374-6.

[167] Zhang J, Ney PA. Role of BNIP3 and NIX in cell death, autophagy, and mitophagy. Cell death and differentiation. 2009;16:939-46.

[168] Feng Z, Hu W, de Stanchina E, Teresky AK, Jin S, Lowe S, et al. The regulation of AMPK beta1, TSC2, and PTEN expression by p53: stress, cell and tissue specificity, and the role of these gene products in modulating the IGF-1-AKT-mTOR pathways. Cancer research. 2007;67:3043-53.

[169] Budanov AV, Karin M. p53 target genes sestrin1 and sestrin2 connect genotoxic stress and mTOR signaling. Cell. 2008;134:451-60.

[170] Perfettini JL, Kroemer RT, Kroemer G. Fatal liaisons of p53 with Bax and Bak. Nature cell biology. 2004;6:386-8.

[171] Miyashita T, Krajewski S, Krajewska M, Wang HG, Lin HK, Liebermann DA, et al. Tumor suppressor p53 is a regulator of bcl-2 and bax gene expression in vitro and in vivo. Oncogene. 1994;9:1799-805.

[172] Oda E, Ohki R, Murasawa H, Nemoto J, Shibue T, Yamashita T, et al. Noxa, a BH3-only member of the Bcl-2 family and candidate mediator of p53-induced apoptosis. Science. 2000;288:1053-8.

[173] Nakano K, Vousden KH. PUMA, a novel proapoptotic gene, is induced by p53. Molecular cell. 2001;7:683-94.

[174] Sugars KL, Budhram-Mahadeo V, Packham G, Latchman DS. A minimal Bcl-x promoter is activated by Brn-3a and repressed by p53. Nucleic acids research. 2001;29:4530-40.

[175] Pietrzak M, Puzianowska-Kuznicka M. p53-dependent repression of the human MCL-1 gene encoding an anti-apoptotic member of the BCL-2 family: the role of Sp1 and of basic transcription factor binding sites in the MCL-1 promoter. Biological chemistry. 2008;389:383-93.

[176] Chipuk JE, Kuwana T, Bouchier-Hayes L, Droin NM, Newmeyer DD, Schuler M, et al. Direct activation of Bax by p53 mediates mitochondrial membrane permeabilization and apoptosis. Science. 2004;303:1010-4.

[177] Leu JI, Dumont P, Hafey M, Murphy ME, George DL. Mitochondrial p53 activates Bak and causes disruption of a Bak-Mcl1 complex. Nature cell biology. 2004;6:443-50.

[178] Tomita Y, Marchenko N, Erster S, Nemajerova A, Dehner A, Klein C, et al. WT p53, but not tumor-derived mutants, bind to Bcl2 via the DNA binding domain and induce mitochondrial permeabilization. J Biol Chem. 2006;281:8600-6.

[179] Suen DF, Narendra DP, Tanaka A, Manfredi G, Youle RJ. Parkin overexpression selects against a deleterious mtDNA mutation in heteroplasmic cybrid cells. Proceedings of the National Academy of Sciences of the United States of America. 2010;107:11835-40.

[180] Narendra D, Tanaka A, Suen DF, Youle RJ. Parkin is recruited selectively to impaired mitochondria and promotes their autophagy. The Journal of cell biology. 2008;183:795-803.

[181] Geisler S, Holmstrom KM, Skujat D, Fiesel FC, Rothfuss OC, Kahle PJ, et al. PINK1/Parkin-mediated mitophagy is dependent on VDAC1 and p62/SQSTM1. Nature cell biology. 2010;12:119-31.

[182] Gegg ME, Cooper JM, Chau KY, Rojo M, Schapira AH, Taanman JW. Mitofusin 1 and mitofusin 2 are ubiquitinated in a PINK1/parkin-dependent manner upon induction of mitophagy. Human molecular genetics. 2010;19:4861-70.

[183] Wang X, Winter D, Ashrafi G, Schlehe J, Wong YL, Selkoe D, et al. PINK1 and Parkin target Miro for phosphorylation and degradation to arrest mitochondrial motility. Cell. 2011;147:893-906.

[184] Okamoto K, Kondo-Okamoto N, Ohsumi Y. Mitochondria-anchored receptor Atg32 mediates degradation of mitochondria via selective autophagy. Developmental cell. 2009;17:87-97.

[185] Kanki T, Wang K, Cao Y, Baba M, Klionsky DJ. Atg32 is a mitochondrial protein that confers selectivity during mitophagy. Developmental cell. 2009;17:98-109.

[186] Rowe GC, Jiang A, Arany Z. PGC-1 coactivators in cardiac development and disease. Circulation research. 2010;107:825-38.

[187] Lehman JJ, Barger PM, Kovacs A, Saffitz JE, Medeiros DM, Kelly DP. Peroxisome proliferator-activated receptor gamma coactivator-1 promotes cardiac mitochondrial biogenesis. The Journal of clinical investigation. 2000;106:847-56.

[188] Shin JH, Ko HS, Kang H, Lee Y, Lee YI, Pletinkova O, et al. PARIS (ZNF746) repression of PGC-1alpha contributes to neurodegeneration in Parkinson's disease. Cell. 2011;144:689-702.

[189] Kane LA, Youle RJ. Mitochondrial fission and fusion and their roles in the heart. Journal of molecular medicine. 2010;88:971-9.

[190] Chen H, Chan DC. Physiological functions of mitochondrial fusion. Annals of the New York Academy of Sciences. 2010;1201:21-5.

[191] Iglewski M, Hill JA, Lavandero S, Rothermel BA. Mitochondrial fission and autophagy in the normal and diseased heart. Current hypertension reports. 2010;12:418-25.

[192] Kim I, Rodriguez-Enriquez S, Lemasters JJ. Selective degradation of mitochondria by mitophagy. Arch Biochem Biophys. 2007;462:245-53.

[193] Gottlieb RA, Carreira RS. Autophagy in health and disease. 5. Mitophagy as a way of life. Am J Physiol Cell Physiol. 2010;299:C203-10.

[194] Ambrosio G, Zweier JL, Duilio C, Kuppusamy P, Santoro G, Elia PP, et al. Evidence that mitochondrial respiration is a source of potentially toxic oxygen free radicals in intact rabbit hearts subjected to ischemia and reflow. J Biol Chem. 1993;268:18532-41.

[195] Becker LB. New concepts in reactive oxygen species and cardiovascular reperfusion physiology. Cardiovascular research. 2004;61:461-70.

[196] Gottlieb RA, Burleson KO, Kloner RA, Babior BM, Engler RL. Reperfusion injury induces apoptosis in rabbit cardiomyocytes. The Journal of clinical investigation. 1994;94:1621-8.

[197] Weiss JN, Korge P, Honda HM, Ping P. Role of the mitochondrial permeability transition in myocardial disease. Circulation research. 2003;93:292-301.

[198] McCord JM. Free radicals and myocardial ischemia: overview and outlook. Free Radic Biol Med. 1988;4:9-14.

[199] Kloner RA, Jennings RB. Consequences of brief ischemia: stunning, preconditioning, and their clinical implications: part 2. Circulation. 2001;104:3158-67.

[200] Kloner RA, Jennings RB. Consequences of brief ischemia: stunning, preconditioning, and their clinical implications: part 1. Circulation. 2001;104:2981-9.

[201] Veitch K, Hombroeckx A, Caucheteux D, Pouleur H, Hue L. Global ischaemia induces a biphasic response of the mitochondrial respiratory chain. Anoxic pre-perfusion protects against ischaemic damage. The Biochemical journal. 1992;281 ( Pt 3):709-15.

[202] Rouslin W, Ranganathan S. Impaired function of mitochondrial electron transfer complex I in canine myocardial ischemia: loss of flavin mononucleotide. J Mol Cell Cardiol. 1983;15:537-42.

[203] Lesnefsky EJ, Chen Q, Slabe TJ, Stoll MS, Minkler PE, Hassan MO, et al. Ischemia, rather than reperfusion, inhibits respiration through cytochrome oxidase in the isolated, perfused rabbit heart: role of cardiolipin. Am J Physiol Heart Circ Physiol. 2004;287:H258-67.

[204] Lesnefsky EJ, Tandler B, Ye J, Slabe TJ, Turkaly J, Hoppel CL. Myocardial ischemia decreases oxidative phosphorylation through cytochrome oxidase in subsarcolemmal mitochondria. Am J Physiol. 1997;273:H1544-54.

[205] Paradies G, Petrosillo G, Pistolese M, Di Venosa N, Federici A, Ruggiero FM. Decrease in mitochondrial complex I activity in ischemic/reperfused rat heart: involvement of reactive oxygen species and cardiolipin. Circulation research. 2004;94:53-9.

[206] Rouslin W. Mitochondrial complexes I, II, III, IV, and V in myocardial ischemia and autolysis. Am J Physiol. 1983;244:H743-8.

[207] Nohl H. Generation of superoxide radicals as byproduct of cellular respiration. Annales de biologie clinique. 1994;52:199-204.

[208] Chen R, Fearnley IM, Peak-Chew SY, Walker JE. The phosphorylation of subunits of complex I from bovine heart mitochondria. J Biol Chem. 2004;279:26036-45.

[209] Chen Q, Moghaddas S, Hoppel CL, Lesnefsky EJ. Reversible blockade of electron transport during ischemia protects mitochondria and decreases myocardial injury following reperfusion. J Pharmacol Exp Ther. 2006;319:1405-12.

[210] Lesnefsky EJ, Chen Q, Moghaddas S, Hassan MO, Tandler B, Hoppel CL. Blockade of electron transport during ischemia protects cardiac mitochondria. J Biol Chem. 2004;279:47961-7.

[211] Aldakkak M, Stowe DF, Chen Q, Lesnefsky EJ, Camara AK. Inhibited mitochondrial respiration by amobarbital during cardiac ischaemia improves redox state and reduces matrix Ca2+ overload and ROS release. Cardiovascular research. 2008;77:406-15.

[212] Becker LB, vanden Hoek TL, Shao ZH, Li CQ, Schumacker PT. Generation of superoxide in cardiomyocytes during ischemia before reperfusion. Am J Physiol. 1999;277:H2240-6.

[213] Quinlan CL, Orr AL, Perevoshchikova IV, Treberg JR, Ackrell BA, Brand MD. Mitochondrial complex II can generate reactive oxygen species at high rates in both the forward and reverse reactions. J Biol Chem. 2012;287:27255-64.

[214] Lesnefsky EJ, Gudz TI, Migita CT, Ikeda-Saito M, Hassan MO, Turkaly PJ, et al. Ischemic injury to mitochondrial electron transport in the aging heart: damage to the iron-sulfur protein subunit of electron transport complex III. Arch Biochem Biophys. 2001;385:117-28.

[215] Prabu SK, Anandatheerthavarada HK, Raza H, Srinivasan S, Spear JF, Avadhani NG. Protein kinase A-mediated phosphorylation modulates cytochrome c oxidase function and augments hypoxia and myocardial ischemia-related injury. J Biol Chem. 2006;281:2061-70.

[216] Lesnefsky EJ, Slabe TJ, Stoll MS, Minkler PE, Hoppel CL. Myocardial ischemia selectively depletes cardiolipin in rabbit heart subsarcolemmal mitochondria. Am J Physiol Heart Circ Physiol. 2001;280:H2770-8.

[217] Robinson NC, Strey F, Talbert L. Investigation of the essential boundary layer phospholipids of cytochrome c oxidase using Triton X-100 delipidation. Biochemistry. 1980;19:3656-61.

[218] Vik SB, Capaldi RA. Lipid requirements for cytochrome c oxidase activity. Biochemistry. 1977;16:5755-9.

[219] Chen Q, Lesnefsky EJ. Depletion of cardiolipin and cytochrome c during ischemia increases hydrogen peroxide production from the electron transport chain. Free Radic Biol Med. 2006;40:976-82.

[220] Sevanian A, Kim E. Phospholipase A2 dependent release of fatty acids from peroxidized membranes. Journal of free radicals in biology & medicine. 1985;1:263-71.

[221] Parinandi NL, Zwizinski CW, Schmid HH. Free radical-induced alterations of myocardial membrane proteins. Arch Biochem Biophys. 1991;289:118-23.

[222] Chen Q, Lesnefsky E. Mitochondria and cardiac injury: A journey from reperfusion to ischemia and back again. The Research Signpost/Transworld Research Network; 2009.

[223] Paradies G, Petrosillo G, Pistolese M, Di Venosa N, Serena D, Ruggiero FM. Lipid peroxidation and alterations to oxidative metabolism in mitochondria isolated from rat heart subjected to ischemia and reperfusion. Free Radic Biol Med. 1999;27:42-50.

[224] Tyurina YY, Kini V, Tyurin VA, Vlasova, II, Jiang J, Kapralov AA, et al. Mechanisms of cardiolipin oxidation by cytochrome c: relevance to pro- and antiapoptotic functions of etoposide. Molecular pharmacology. 2006;70:706-17.

[225] Jiang J, Huang Z, Zhao Q, Feng W, Belikova NA, Kagan VE. Interplay between bax, reactive oxygen species production, and cardiolipin oxidation during apoptosis. Biochem Biophys Res Commun. 2008;368:145-50.

[226] Kostrzewa A, Pali T, Froncisz W, Marsh D. Membrane location of spin-labeled cytochrome c determined by paramagnetic relaxation agents. Biochemistry. 2000;39:6066-74.

[227] Shidoji Y, Hayashi K, Komura S, Ohishi N, Yagi K. Loss of molecular interaction between cytochrome c and cardiolipin due to lipid peroxidation. Biochem Biophys Res Commun. 1999;264:343-7.

[228] Ott M, Robertson JD, Gogvadze V, Zhivotovsky B, Orrenius S. Cytochrome c release from mitochondria proceeds by a two-step process. Proceedings of the National Academy of Sciences of the United States of America. 2002;99:1259-63.

[229] Esposti MD, Cristea IM, Gaskell SJ, Nakao Y, Dive C. Proapoptotic Bid binds to monolysocardiolipin, a new molecular connection between mitochondrial membranes and cell death. Cell death and differentiation. 2003;10:1300-9.

[230] Chen Q, Hoppel CL, Lesnefsky EJ. Blockade of electron transport before cardiac ischemia with the reversible inhibitor amobarbital protects rat heart mitochondria. J Pharmacol Exp Ther. 2006;316:200-7.

[231] Nadtochiy SM, Burwell LS, Brookes PS. Cardioprotection and mitochondrial S-nitrosation: effects of S-nitroso-2-mercaptopropionyl glycine (SNO-MPG) in cardiac ischemia-reperfusion injury. J Mol Cell Cardiol. 2007;42:812-25.

[232] Stewart S, Lesnefsky EJ, Chen Q. Reversible blockade of electron transport with amobarbital at the onset of reperfusion attenuates cardiac injury. Transl Res. 2009;153:224-31.

[233] Horgan DJ, Singer TP, Casida JE. Studies on the respiratory chain-linked reduced nicotinamide adenine dinucleotide dehydrogenase. 13. Binding sites of rotenone, piericidin A, and amytal in the respiratory chain. J Biol Chem. 1968;243:834-43.

[234] Spiegel HE, Wainio WW. Some features of barbiturate interaction and inhibition of NADH-cytochrome C oxidoreductase in respiring systems. J Pharmacol Exp Ther. 1969;165:23-9.

[235] Flameng W, Andres J, Ferdinande P, Mattheussen M, Van Belle H. Mitochondrial function in myocardial stunning. J Mol Cell Cardiol. 1991;23:1-11.

[236] Kevin LG, Camara AK, Riess ML, Novalija E, Stowe DF. Ischemic preconditioning alters real-time measure of O2 radicals in intact hearts with ischemia and reperfusion. Am J Physiol Heart Circ Physiol. 2003;284:H566-74.

[237] Bolli R, McCay PB. Use of spin traps in intact animals undergoing myocardial ischemia/reperfusion: a new approach to assessing the role of oxygen radicals in myocardial "stunning". Free radical research communications. 1990;9:169-80.

[238] Maupoil V, Rochette L, Tabard A, Clauser P, Harpey C. Evolution of free radical formation during low-flow ischemia and reperfusion in isolated rat heart. Cardiovascular

drugs and therapy / sponsored by the International Society of Cardiovascular Pharmacotherapy. 1990;4 Suppl 4:791-5.

[239] Pietri S, Culcasi M, Cozzone PJ. Real-time continuous-flow spin trapping of hydroxyl free radical in the ischemic and post-ischemic myocardium. European journal of biochemistry / FEBS. 1989;186:163-73.

[240] Gille L, Nohl H. The ubiquinol/bc1 redox couple regulates mitochondrial oxygen radical formation. Arch Biochem Biophys. 2001;388:34-8.

[241] Otani H, Tanaka H, Inoue T, Umemoto M, Omoto K, Tanaka K, et al. In vitro study on contribution of oxidative metabolism of isolated rabbit heart mitochondria to myocardial reperfusion injury. Circulation research. 1984;55:168-75.

[242] Skyschally A, van Caster P, Boengler K, Gres P, Musiolik J, Schilawa D, et al. Ischemic postconditioning in pigs: no causal role for RISK activation. Circulation research. 2009;104:15-8.

[243] Schafer C, Ladilov Y, Inserte J, Schafer M, Haffner S, Garcia-Dorado D, et al. Role of the reverse mode of the Na+/Ca2+ exchanger in reoxygenation-induced cardiomyocyte injury. Cardiovascular research. 2001;51:241-50.

[244] Gunter TE, Pfeiffer DR. Mechanisms by which mitochondria transport calcium. Am J Physiol. 1990;258:C755-86.

[245] Ataka K, Chen D, Levitsky S, Jimenez E, Feinberg H. Effect of aging on intracellular Ca2+, pHi, and contractility during ischemia and reperfusion. Circulation. 1992;86:II371-6.

[246] Halestrap AP, McStay GP, Clarke SJ. The permeability transition pore complex: another view. Biochimie. 2002;84:153-66.

[247] Tsujimoto Y, Shimizu S. Role of the mitochondrial membrane permeability transition in cell death. Apoptosis 2007;12:835-40.

[248] Palmer JW, Tandler B, Hoppel CL. Heterogeneous response of subsarcolemmal heart mitochondria to calcium. Am J Physiol. 1986;250:H741-8.

[249] Chen Q, Paillard M, Gomez L, Li H, Hu Y, Lesnefsky EJ. Postconditioning modulates ischemia-damaged mitochondria during reperfusion. J Cardiovasc Pharmacol. 2012;59:101-8.

[250] Paillard M, Gomez L, Augeul L, Loufouat J, Lesnefsky EJ, Ovize M. Postconditioning inhibits mPTP opening independent of oxidative phosphorylation and membrane potential. J Mol Cell Cardiol. 2009;46:902-9.

[251] Lesnefsky EJ, Lundergan CF, Hodgson JM, Nair R, Reiner JS, Greenhouse SW, et al. Increased left ventricular dysfunction in elderly patients despite successful thrombolysis: the GUSTO-I angiographic experience. J Am Coll Cardiol. 1996;28:331-7.

[252] Balakumar P, Singh H, Singh M, Anand-Srivastava MB. The impairment of preconditioning-mediated cardioprotection in pathological conditions. Pharmacological research : the official journal of the Italian Pharmacological Society. 2009;60:18-23.

[253] Tani M, Honma Y, Hasegawa H, Tamaki K. Direct activation of mitochondrial K(ATP) channels mimics preconditioning but protein kinase C activation is less effective in middle-aged rat hearts. Cardiovascular research. 2001;49:56-68.

[254] Chen Q, Yin G, Stewart S, Hu Y, Lesnefsky EJ. Isolating the segment of the mitochondrial electron transport chain responsible for mitochondrial damage during cardiac ischemia. Biochem Biophys Res Commun. 2010;397:656-60.

[255] Chen Q, Camara AK, Stowe DF, Hoppel CL, Lesnefsky EJ. Modulation of electron transport protects cardiac mitochondria and decreases myocardial injury during ischemia and reperfusion. Am J Physiol Cell Physiol. 2007;292:C137-47.

[256] Rytomaa M, Kinnunen PK. Evidence for two distinct acidic phospholipid-binding sites in cytochrome c. J Biol Chem. 1994;269:1770-4.

[257] Rytomaa M, Kinnunen PK. Reversibility of the binding of cytochrome c to liposomes. Implications for lipid-protein interactions. J Biol Chem. 1995;270:3197-202.

[258] Kawai C, Prado FM, Nunes GL, Di Mascio P, Carmona-Ribeiro AM, Nantes IL. pH-Dependent interaction of cytochrome c with mitochondrial mimetic membranes: the role of an array of positively charged amino acids. J Biol Chem. 2005;280:34709-17.

[259] Tuominen EK, Wallace CJ, Kinnunen PK. Phospholipid-cytochrome c interaction: evidence for the extended lipid anchorage. J Biol Chem. 2002;277:8822-6.

[260] Gorbenko GP, Molotkovsky JG, Kinnunen PK. Cytochrome C interaction with cardiolipin/phosphatidylcholine model membranes: effect of cardiolipin protonation. Biophysical journal. 2006;90:4093-103.

[261] Belikova NA, Vladimirov YA, Osipov AN, Kapralov AA, Tyurin VA, Potapovich MV, et al. Peroxidase activity and structural transitions of cytochrome c bound to cardiolipin-containing membranes. Biochemistry. 2006;45:4998-5009.

[262] Chattopadhyay K, Mazumdar S. Stabilization of partially folded states of cytochrome c in aqueous surfactant: effects of ionic and hydrophobic interactions. Biochemistry. 2003;42:14606-13.

[263] Kalanxhi E, Wallace CJ. Cytochrome c impaled: investigation of the extended lipid anchorage of a soluble protein to mitochondrial membrane models. The Biochemical journal. 2007;407:179-87.

[264] Kagan VE, Bayir HA, Belikova NA, Kapralov O, Tyurina YY, Tyurin VA, et al. Cytochrome c/cardiolipin relations in mitochondria: a kiss of death. Free Radic Biol Med. 2009;46:1439-53.

[265] Pinheiro TJ, Watts A. Lipid specificity in the interaction of cytochrome c with anionic phospholipid bilayers revealed by solid-state 31P NMR. Biochemistry. 1994;33:2451-8.

[266] Pinheiro TJ, Elove GA, Watts A, Roder H. Structural and kinetic description of cytochrome c unfolding induced by the interaction with lipid vesicles. Biochemistry. 1997;36:13122-32.

[267] Muga A, Mantsch HH, Surewicz WK. Membrane binding induces destabilization of cytochrome c structure. Biochemistry. 1991;30:7219-24.

[268] Spooner PJ, Watts A. Cytochrome c interactions with cardiolipin in bilayers: a multinuclear magic-angle spinning NMR study. Biochemistry. 1992;31:10129-38.

[269] Radi R, Turrens JF, Freeman BA. Cytochrome c-catalyzed membrane lipid peroxidation by hydrogen peroxide. Arch Biochem Biophys. 1991;288:118-25.

[270] Stellwagen E. Carboxymethylation of horse heart ferricytochrome c and cyanferricytochrome c. Biochemistry. 1968;7:2496-501.

[271] Kagan VE, Borisenko GG, Tyurina YY, Tyurin VA, Jiang J, Potapovich AI, et al. Oxidative lipidomics of apoptosis: redox catalytic interactions of cytochrome c with cardiolipin and phosphatidylserine. Free Radic Biol Med. 2004;37:1963-85.

[272] Chen YR, Deterding LJ, Sturgeon BE, Tomer KB, Mason RP. Protein oxidation of cytochrome C by reactive halogen species enhances its peroxidase activity. J Biol Chem. 2002;277:29781-91.

[273] Cassina AM, Hodara R, Souza JM, Thomson L, Castro L, Ischiropoulos H, et al. Cytochrome c nitration by peroxynitrite. J Biol Chem. 2000;275:21409-15.

[274] Prasad S, Maiti NC, Mazumdar S, Mitra S. Reaction of hydrogen peroxide and peroxidase activity in carboxymethylated cytochrome c: spectroscopic and kinetic studies. Biochim Biophys Acta. 2002;1596:63-75.

[275] Sinibaldi F, Fiorucci L, Patriarca A, Lauceri R, Ferri T, Coletta M, et al. Insights into cytochrome c-cardiolipin interaction. Role played by ionic strength. Biochemistry. 2008;47:6928-35.

[276] Kagan VE, Tyurin VA, Jiang J, Tyurina YY, Ritov VB, Amoscato AA, et al. Cytochrome c acts as a cardiolipin oxygenase required for release of proapoptotic factors. Nature chemical biology. 2005;1:223-32.

[277] Nilsson OS, Dallner G. Transverse asymmetry of phospholipids in subcellular membranes of rat liver. Biochim Biophys Acta. 1977;464:453-8.

[278] Sperka-Gottlieb CD, Hermetter A, Paltauf F, Daum G. Lipid topology and physical properties of the outer mitochondrial membrane of the yeast, Saccharomyces cerevisiae. Biochim Biophys Acta. 1988;946:227-34.

[279] Daum G. Lipids of mitochondria. Biochim Biophys Acta. 1985;822:1-42.

[280] Ardail D, Privat JP, Egret-Charlier M, Levrat C, Lerme F, Louisot P. Mitochondrial contact sites. Lipid composition and dynamics. J Biol Chem. 1990;265:18797-802.

[281] Pfeiffer K, Gohil V, Stuart RA, Hunte C, Brandt U, Greenberg ML, et al. Cardiolipin stabilizes respiratory chain supercomplexes. J Biol Chem. 2003;278:52873-80.

[282] Sharpley MS, Shannon RJ, Draghi F, Hirst J. Interactions between phospholipids and NADH:ubiquinone oxidoreductase (complex I) from bovine mitochondria. Biochemistry. 2006;45:241-8.

[283] Hovius R, Thijssen J, van der Linden P, Nicolay K, de Kruijff B. Phospholipid asymmetry of the outer membrane of rat liver mitochondria. Evidence for the presence of cardiolipin on the outside of the outer membrane. FEBS Lett. 1993;330:71-6.

[284] Tyurin VA, Tyurina YY, Osipov AN, Belikova NA, Basova LV, Kapralov AA, et al. Interactions of cardiolipin and lyso-cardiolipins with cytochrome c and tBid: conflict or assistance in apoptosis. Cell death and differentiation. 2007;14:872-5.

[285] Liu J, Dai Q, Chen J, Durrant D, Freeman A, Liu T, et al. Phospholipid scramblase 3 controls mitochondrial structure, function, and apoptotic response. Molecular cancer research : MCR. 2003;1:892-902.

[286] Lutter M, Fang M, Luo X, Nishijima M, Xie X, Wang X. Cardiolipin provides specificity for targeting of tBid to mitochondria. Nature cell biology. 2000;2:754-61.

[287] Gonzalvez F, Pariselli F, Dupaigne P, Budihardjo I, Lutter M, Antonsson B, et al. tBid interaction with cardiolipin primarily orchestrates mitochondrial dysfunctions and subsequently activates Bax and Bak. Cell death and differentiation. 2005;12:614-26.

[288] Van Q, Liu J, Lu B, Feingold KR, Shi Y, Lee RM, et al. Phospholipid scramblase-3 regulates cardiolipin de novo biosynthesis and its resynthesis in growing HeLa cells. The Biochemical journal. 2007;401:103-9.

[289] Liu J, Chen J, Dai Q, Lee RM. Phospholipid scramblase 3 is the mitochondrial target of protein kinase C delta-induced apoptosis. Cancer research. 2003;63:1153-6.

[290] Tyurina YY, Kawai K, Tyurin VA, Liu SX, Kagan VE, Fabisiak JP. The plasma membrane is the site of selective phosphatidylserine oxidation during apoptosis: role of cytochrome C. Antioxidants & redox signaling. 2004;6:209-25.

[291] Tyurina YY, Serinkan FB, Tyurin VA, Kini V, Yalowich JC, Schroit AJ, et al. Lipid antioxidant, etoposide, inhibits phosphatidylserine externalization and macrophage clearance of apoptotic cells by preventing phosphatidylserine oxidation. J Biol Chem. 2004;279:6056-64.

[292] Tyurina YY, Tyurin VA, Epperly MW, Greenberger JS, Kagan VE. Oxidative lipidomics of gamma-irradiation-induced intestinal injury. Free Radic Biol Med. 2008;44:299-314.

[293] Tyurin VA, Tyurina YY, Kochanek PM, Hamilton R, DeKosky ST, Greenberger JS, et al. Oxidative lipidomics of programmed cell death. Methods in enzymology. 2008;442:375-93.

[294] Belikova NA, Jiang J, Tyurina YY, Zhao Q, Epperly MW, Greenberger J, et al. Cardiolipin-specific peroxidase reactions of cytochrome C in mitochondria during irradiation-induced apoptosis. International journal of radiation oncology, biology, physics. 2007;69:176-86.

[295] Bayir H, Tyurin VA, Tyurina YY, Viner R, Ritov V, Amoscato AA, et al. Selective early cardiolipin peroxidation after traumatic brain injury: an oxidative lipidomics analysis. Annals of neurology. 2007;62:154-69.

[296] Huang Z, Jiang J, Tyurin VA, Zhao Q, Mnuskin A, Ren J, et al. Cardiolipin deficiency leads to decreased cardiolipin peroxidation and increased resistance of cells to apoptosis. Free Radic Biol Med. 2008;44:1935-44.

[297] Sevanian A, Hochstein P. Mechanisms and consequences of lipid peroxidation in biological systems. Annual review of nutrition. 1985;5:365-90.

[298] Borutaite V, Brown GC. Mitochondria in apoptosis of ischemic heart. FEBS Lett. 2003;541:1-5.

[299] Vlasova, II, Tyurin VA, Kapralov AA, Kurnikov IV, Osipov AN, Potapovich MV, et al. Nitric oxide inhibits peroxidase activity of cytochrome c.cardiolipin complex and blocks cardiolipin oxidation. J Biol Chem. 2006;281:14554-62.

[300] Wang H, Blair DF, Ellis WR, Jr., Gray HB, Chan SI. Temperature dependence of the reduction potential of CuA in carbon monoxide inhibited cytochrome c oxidase. Biochemistry. 1986;25:167-71.

[301] Basova LV, Kurnikov IV, Wang L, Ritov VB, Belikova NA, Vlasova, II, et al. Cardiolipin switch in mitochondria: shutting off the reduction of cytochrome c and turning on the peroxidase activity. Biochemistry. 2007;46:3423-34.

[302] Lesnefsky EJ, Minkler P, Hoppel CL. Enhanced modification of cardiolipin during ischemia in the aged heart. J Mol Cell Cardiol. 2009;46:1008-15.

[303] Chance B, Williams GR. Respiratory enzymes in oxidative phosphorylation. IV. The respiratory chain. J Biol Chem. 1955;217:429-38.

[304] Chance B, Williams GR. Respiratory enzymes in oxidative phosphorylation. III. The steady state. J Biol Chem. 1955;217:409-27.

[305] RW E. Mitochondrial respiratory control and the polarographic measurement of ADP: O ratios1967.

[306] Chen Q, Paillard M, Gomez L, Ross T, Hu Y, Xu A, et al. Activation of mitochondrial mu-calpain increases AIF cleavage in cardiac mitochondria during ischemia-reperfusion. Biochem Biophys Res Commun. 2011;415:533-8.

[307] Nold MJ, Cerda BA, Wesdemiotis C. Proton affinities of the N- and C-terminal segments arising upon the dissociation of the amide bond in protonated peptides. Journal of the American Society for Mass Spectrometry. 1999;10:1-8.

[308] Lesnefsky EJ, Stoll MS, Minkler PE, Hoppel CL. Separation and quantitation of phospholipids and lysophospholipids by high-performance liquid chromatography. Anal Biochem. 2000;285:246-54.

[309] Lesnefsky EJ, Hoppel CL. Cardiolipin as an oxidative target in cardiac mitochondria in the aged rat. Biochim Biophys Acta. 2008;1777:1020-7.

[310] Lesnefsky EJ, Hoppel CL. Ischemia-reperfusion injury in the aged heart: role of mitochondria. Arch Biochem Biophys. 2003;420:287-97.

[311] Thariat J, Collin F, Marchetti C, Ahmed-Adrar NS, Vitrac H, Jore D, et al. Marked difference in cytochrome c oxidation mediated by HO(*) and/or O(2)(*-) free radicals in vitro. Biochimie. 2008;90:1442-51.

[312] Godoy LC, Munoz-Pinedo C, Castro L, Cardaci S, Schonhoff CM, King M, et al. Disruption of the M80-Fe ligation stimulates the translocation of cytochrome c to the cytoplasm and nucleus in nonapoptotic cells. Proceedings of the National Academy of Sciences of the United States of America. 2009;106:2653-8.

[313] Liu W, Porter NA, Schneider C, Brash AR, Yin H. Formation of 4-hydroxynonenal from cardiolipin oxidation: Intramolecular peroxyl radical addition and decomposition. Free Radic Biol Med. 2011;50:166-78.

[314] Rauniyar N, Prokai L. Detection and identification of 4-hydroxy-2-nonenal Schiff-base adducts along with products of Michael addition using data-dependent neutral loss-driven MS3 acquisition: method evaluation through an in vitro study on cytochrome c oxidase modifications. Proteomics. 2009;9:5188-93.

[315] Genestra M. Oxyl radicals, redox-sensitive signalling cascades and antioxidants. Cellular signalling. 2007;19:1807-19.

[316] Janssen-Heininger YM, Mossman BT, Heintz NH, Forman HJ, Kalyanaraman B, Finkel T, et al. Redox-based regulation of signal transduction: principles, pitfalls, and promises. Free Radic Biol Med. 2008;45:1-17.

[317] Orrenius S, Gogvadze V, Zhivotovsky B. Mitochondrial oxidative stress: implications for cell death. Annual review of pharmacology and toxicology. 2007;47:143-83.

[318] Powis G, Montfort WR. Properties and biological activities of thioredoxins. Annual review of pharmacology and toxicology. 2001;41:261-95.

[319] Katagiri K, Matsuzawa A, Ichijo H. Regulation of apoptosis signal-regulating kinase 1 in redox signaling. Methods in enzymology. 2010;474:277-88.

[320] Hattori K, Naguro I, Runchel C, Ichijo H. The roles of ASK family proteins in stress responses and diseases. Cell communication and signaling : CCS. 2009;7:9.

[321] Matsui M, Oshima M, Oshima H, Takaku K, Maruyama T, Yodoi J, et al. Early embryonic lethality caused by targeted disruption of the mouse thioredoxin gene. Developmental biology. 1996;178:179-85.

[322] Mitsui A, Hamuro J, Nakamura H, Kondo N, Hirabayashi Y, Ishizaki-Koizumi S, et al. Overexpression of human thioredoxin in transgenic mice controls oxidative stress and life span. Antioxidants & redox signaling. 2002;4:693-6.

[323] Nishiyama A, Matsui M, Iwata S, Hirota K, Masutani H, Nakamura H, et al. Identification of thioredoxin-binding protein-2/vitamin D(3) up-regulated protein 1 as a negative regulator of thioredoxin function and expression. J Biol Chem. 1999;274:21645-50.

[324] Junn E, Han SH, Im JY, Yang Y, Cho EW, Um HD, et al. Vitamin D3 up-regulated protein 1 mediates oxidative stress via suppressing the thioredoxin function. Journal of immunology. 2000;164:6287-95.

[325] Patwari P, Higgins LJ, Chutkow WA, Yoshioka J, Lee RT. The interaction of thioredoxin with Txnip. Evidence for formation of a mixed disulfide by disulfide exchange. J Biol Chem. 2006;281:21884-91.

[326] Yoshihara E, Chen Z, Matsuo Y, Masutani H, Yodoi J. Thiol redox transitions by thioredoxin and thioredoxin-binding protein-2 in cell signaling. Methods in enzymology. 2010;474:67-82.

[327] Lu J, Holmgren A. Thioredoxin system in cell death progression. Antioxidants & redox signaling. 2012;17:1738-47.

[328] Saxena G, Chen J, Shalev A. Intracellular shuttling and mitochondrial function of thioredoxin-interacting protein. J Biol Chem. 2010;285:3997-4005.

[329] Bodnar JS, Chatterjee A, Castellani LW, Ross DA, Ohmen J, Cavalcoli J, et al. Positional cloning of the combined hyperlipidemia gene Hyplip1. Nature genetics. 2002;30:110-6.

[330] Saitoh M, Nishitoh H, Fujii M, Takeda K, Tobiume K, Sawada Y, et al. Mammalian thioredoxin is a direct inhibitor of apoptosis signal-regulating kinase (ASK) 1. The EMBO journal. 1998;17:2596-606.

[331] Ichijo H, Nishida E, Irie K, ten Dijke P, Saitoh M, Moriguchi T, et al. Induction of apoptosis by ASK1, a mammalian MAPKKK that activates SAPK/JNK and p38 signaling pathways. Science. 1997;275:90-4.

[332] Matsuzawa A, Saegusa K, Noguchi T, Sadamitsu C, Nishitoh H, Nagai S, et al. ROS-dependent activation of the TRAF6-ASK1-p38 pathway is selectively required for TLR4-mediated innate immunity. Nature immunology. 2005;6:587-92.

[333] Nishitoh H, Matsuzawa A, Tobiume K, Saegusa K, Takeda K, Inoue K, et al. ASK1 is essential for endoplasmic reticulum stress-induced neuronal cell death triggered by expanded polyglutamine repeats. Genes & development. 2002;16:1345-55.

[334] Nishitoh H, Saitoh M, Mochida Y, Takeda K, Nakano H, Rothe M, et al. ASK1 is essential for JNK/SAPK activation by TRAF2. Molecular cell. 1998;2:389-95.

[335] Noguchi T, Ishii K, Fukutomi H, Naguro I, Matsuzawa A, Takeda K, et al. Requirement of reactive oxygen species-dependent activation of ASK1-p38 MAPK pathway for extracellular ATP-induced apoptosis in macrophage. J Biol Chem. 2008;283:7657-65.

[336] Takeda K, Matsuzawa A, Nishitoh H, Tobiume K, Kishida S, Ninomiya-Tsuji J, et al. Involvement of ASK1 in Ca2+-induced p38 MAP kinase activation. EMBO reports. 2004;5:161-6.

[337] Tobiume K, Matsuzawa A, Takahashi T, Nishitoh H, Morita K, Takeda K, et al. ASK1 is required for sustained activations of JNK/p38 MAP kinases and apoptosis. EMBO reports. 2001;2:222-8.

[338] Sayama K, Hanakawa Y, Shirakata Y, Yamasaki K, Sawada Y, Sun L, et al. Apoptosis signal-regulating kinase 1 (ASK1) is an intracellular inducer of keratinocyte differentiation. J Biol Chem. 2001;276:999-1004.

[339] Hatai T, Matsuzawa A, Inoshita S, Mochida Y, Kuroda T, Sakamaki K, et al. Execution of apoptosis signal-regulating kinase 1 (ASK1)-induced apoptosis by the mitochondria-dependent caspase activation. J Biol Chem. 2000;275:26576-81.

[340] Kanamoto T, Mota M, Takeda K, Rubin LL, Miyazono K, Ichijo H, et al. Role of apoptosis signal-regulating kinase in regulation of the c-Jun N-terminal kinase pathway and apoptosis in sympathetic neurons. Molecular and cellular biology. 2000;20:196-204.

[341] Gotoh Y, Cooper JA. Reactive oxygen species- and dimerization-induced activation of apoptosis signal-regulating kinase 1 in tumor necrosis factor-alpha signal transduction. J Biol Chem. 1998;273:17477-82.

[342] Tobiume K, Saitoh M, Ichijo H. Activation of apoptosis signal-regulating kinase 1 by the stress-induced activating phosphorylation of pre-formed oligomer. Journal of cellular physiology. 2002;191:95-104.

[343] Fujino G, Noguchi T, Matsuzawa A, Yamauchi S, Saitoh M, Takeda K, et al. Thioredoxin and TRAF family proteins regulate reactive oxygen species-dependent

activation of ASK1 through reciprocal modulation of the N-terminal homophilic interaction of ASK1. Molecular and cellular biology. 2007;27:8152-63.

[344] Kim AH, Khursigara G, Sun X, Franke TF, Chao MV. Akt phosphorylates and negatively regulates apoptosis signal-regulating kinase 1. Molecular and cellular biology. 2001;21:893-901.

[345] Yuan ZQ, Feldman RI, Sussman GE, Coppola D, Nicosia SV, Cheng JQ. AKT2 inhibition of cisplatin-induced JNK/p38 and Bax activation by phosphorylation of ASK1: implication of AKT2 in chemoresistance. J Biol Chem. 2003;278:23432-40.

[346] Nagai H, Noguchi T, Homma K, Katagiri K, Takeda K, Matsuzawa A, et al. Ubiquitin-like sequence in ASK1 plays critical roles in the recognition and stabilization by USP9X and oxidative stress-induced cell death. Molecular cell. 2009;36:805-18.

[347] Morita K, Saitoh M, Tobiume K, Matsuura H, Enomoto S, Nishitoh H, et al. Negative feedback regulation of ASK1 by protein phosphatase 5 (PP5) in response to oxidative stress. The EMBO journal. 2001;20:6028-36.

[348] Saito J, Toriumi S, Awano K, Ichijo H, Sasaki K, Kobayashi T, et al. Regulation of apoptosis signal-regulating kinase 1 by protein phosphatase 2Cepsilon. The Biochemical journal. 2007;405:591-6.

[349] Wang Y. Mitogen-activated protein kinases in heart development and diseases. Circulation. 2007;116:1413-23.

[350] Hausenloy DJ, Yellon DM. Survival kinases in ischemic preconditioning and postconditioning. Cardiovascular research. 2006;70:240-53.

[351] Bogoyevitch MA, Gillespie-Brown J, Ketterman AJ, Fuller SJ, Ben-Levy R, Ashworth A, et al. Stimulation of the stress-activated mitogen-activated protein kinase

subfamilies in perfused heart. p38/RK mitogen-activated protein kinases and c-Jun N-terminal kinases are activated by ischemia/reperfusion. Circulation research. 1996;79:162-73.

[352] Yin T, Sandhu G, Wolfgang CD, Burrier A, Webb RL, Rigel DF, et al. Tissue-specific pattern of stress kinase activation in ischemic/reperfused heart and kidney. J Biol Chem. 1997;272:19943-50.

[353] Knight RJ, Buxton DB. Stimulation of c-Jun kinase and mitogen-activated protein kinase by ischemia and reperfusion in the perfused rat heart. Biochem Biophys Res Commun. 1996;218:83-8.

[354] Cuevas BD, Abell AN, Johnson GL. Role of mitogen-activated protein kinase kinase kinases in signal integration. Oncogene. 2007;26:3159-71.

[355] Winter-Vann AM, Johnson GL. Integrated activation of MAP3Ks balances cell fate in response to stress. Journal of cellular biochemistry. 2007;102:848-58.

[356] Derijard B, Raingeaud J, Barrett T, Wu IH, Han J, Ulevitch RJ, et al. Independent human MAP-kinase signal transduction pathways defined by MEK and MKK isoforms. Science. 1995;267:682-5.

[357] Sanchez I, Hughes RT, Mayer BJ, Yee K, Woodgett JR, Avruch J, et al. Role of SAPK/ERK kinase-1 in the stress-activated pathway regulating transcription factor c-Jun. Nature. 1994;372:794-8.

[358] Tournier C, Whitmarsh AJ, Cavanagh J, Barrett T, Davis RJ. Mitogen-activated protein kinase kinase 7 is an activator of the c-Jun NH2-terminal kinase. Proceedings of the National Academy of Sciences of the United States of America. 1997;94:7337-42.

[359] Brancho D, Tanaka N, Jaeschke A, Ventura JJ, Kelkar N, Tanaka Y, et al. Mechanism of p38 MAP kinase activation in vivo. Genes & development. 2003;17:1969-78.

[360] Harding SJ, Browne GJ, Miller BW, Prigent SA, Dickens M. Activation of ASK1, downstream MAPKK and MAPK isoforms during cardiac ischaemia. Biochim Biophys Acta. 2010;1802:733-40.

[361] Watanabe T, Otsu K, Takeda T, Yamaguchi O, Hikoso S, Kashiwase K, et al. Apoptosis signal-regulating kinase 1 is involved not only in apoptosis but also in non-apoptotic cardiomyocyte death. Biochem Biophys Res Commun. 2005;333:562-7.

[362] Giordano FJ. Oxygen, oxidative stress, hypoxia, and heart failure. The Journal of clinical investigation. 2005;115:500-8.

[363] Zou Y, Zhu W, Sakamoto M, Qin Y, Akazawa H, Toko H, et al. Heat shock transcription factor 1 protects cardiomyocytes from ischemia/reperfusion injury. Circulation. 2003;108:3024-30.

[364] Brundel BJ, Shiroshita-Takeshita A, Qi X, Yeh YH, Chartier D, van Gelder IC, et al. Induction of heat shock response protects the heart against atrial fibrillation. Circulation research. 2006;99:1394-402.

[365] Zhang L, Jiang H, Gao X, Zou Y, Liu M, Liang Y, et al. Heat shock transcription factor-1 inhibits H2O2-induced apoptosis via down-regulation of reactive oxygen species in cardiac myocytes. Molecular and cellular biochemistry. 2011;347:21-8.

[366] Zhang H, Tao L, Jiao X, Gao E, Lopez BL, Christopher TA, et al. Nitrative thioredoxin inactivation as a cause of enhanced myocardial ischemia/reperfusion injury in the aging heart. Free Radic Biol Med. 2007;43:39-47.

[367] Liu Q, Sargent MA, York AJ, Molkentin JD. ASK1 regulates cardiomyocyte death but not hypertrophy in transgenic mice. Circulation research. 2009;105:1110-7.

[368] Nakamura T, Kataoka K, Fukuda M, Nako H, Tokutomi Y, Dong YF, et al. Critical role of apoptosis signal-regulating kinase 1 in aldosterone/salt-induced cardiac inflammation and fibrosis. Hypertension. 2009;54:544-51.

[369] Hikoso S, Ikeda Y, Yamaguchi O, Takeda T, Higuchi Y, Hirotani S, et al. Progression of heart failure was suppressed by inhibition of apoptosis signal-regulating kinase 1 via transcoronary gene transfer. J Am Coll Cardiol. 2007;50:453-62.

[370] Milano G, Morel S, Bonny C, Samaja M, von Segesser LK, Nicod P, et al. A peptide inhibitor of c-Jun NH2-terminal kinase reduces myocardial ischemia-reperfusion injury and infarct size in vivo. Am J Physiol Heart Circ Physiol. 2007;292:H1828-35.

[371] Bogoyevitch MA, Ngoei KR, Zhao TT, Yeap YY, Ng DC. c-Jun N-terminal kinase (JNK) signaling: recent advances and challenges. Biochim Biophys Acta. 2010;1804:463-75.

[372] Martin JL, Avkiran M, Quinlan RA, Cohen P, Marber MS. Antiischemic effects of SB203580 are mediated through the inhibition of p38alpha mitogen-activated protein kinase: Evidence from ectopic expression of an inhibition-resistant kinase. Circulation research. 2001;89:750-2.

[373] Nagarkatti DS, Sha'afi RI. Role of p38 MAP kinase in myocardial stress. J Mol Cell Cardiol. 1998;30:1651-64.

[374] Sucher R, Gehwolf P, Kaier T, Hermann M, Maglione M, Oberhuber R, et al. Intracellular signaling pathways control mitochondrial events associated with the

development of ischemia/ reperfusion-associated damage. Transplant international : official journal of the European Society for Organ Transplantation. 2009;22:922-30.

[375] Aleshin A, Sawa Y, Ono M, Funatsu T, Miyagawa S, Matsuda H. Myocardial protective effect of FR167653; a novel cytokine inhibitor in ischemic-reperfused rat heart. European journal of cardio-thoracic surgery : official journal of the European Association for Cardio-thoracic Surgery. 2004;26:974-80.

[376] Clanachan AS, Jaswal JS, Gandhi M, Bottorff DA, Coughlin J, Finegan BA, et al. Effects of inhibition of myocardial extracellular-responsive kinase and P38 mitogen-activated protein kinase on mechanical function of rat hearts after prolonged hypothermic ischemia. Transplantation. 2003;75:173-80.

[377] Ma XL, Kumar S, Gao F, Louden CS, Lopez BL, Christopher TA, et al. Inhibition of p38 mitogen-activated protein kinase decreases cardiomyocyte apoptosis and improves cardiac function after myocardial ischemia and reperfusion. Circulation. 1999;99:1685-91.

[378] Gao F, Yue TL, Shi DW, Christopher TA, Lopez BL, Ohlstein EH, et al. p38 MAPK inhibition reduces myocardial reperfusion injury via inhibition of endothelial adhesion molecule expression and blockade of PMN accumulation. Cardiovascular research. 2002;53:414-22.

[379] Kompa AR, See F, Lewis DA, Adrahtas A, Cantwell DM, Wang BH, et al. Long-term but not short-term p38 mitogen-activated protein kinase inhibition improves cardiac function and reduces cardiac remodeling post-myocardial infarction. J Pharmacol Exp Ther. 2008;325:741-50.

[380] Liu YH, Wang D, Rhaleb NE, Yang XP, Xu J, Sankey SS, et al. Inhibition of p38 mitogen-activated protein kinase protects the heart against cardiac remodeling in mice with heart failure resulting from myocardial infarction. Journal of cardiac failure. 2005;11:74-81.

[381] Kaiser RA, Lyons JM, Duffy JY, Wagner CJ, McLean KM, O'Neill TP, et al. Inhibition of p38 reduces myocardial infarction injury in the mouse but not pig after ischemia-reperfusion. Am J Physiol Heart Circ Physiol. 2005;289:H2747-51.

[382] Schulz R, Belosjorow S, Gres P, Jansen J, Michel MC, Heusch G. p38 MAP kinase is a mediator of ischemic preconditioning in pigs. Cardiovascular research. 2002;55:690-700.

[383] Schreiber S, Feagan B, D'Haens G, Colombel JF, Geboes K, Yurcov M, et al. Oral p38 mitogen-activated protein kinase inhibition with BIRB 796 for active Crohn's disease: a randomized, double-blind, placebo-controlled trial. Clinical gastroenterology and hepatology : the official clinical practice journal of the American Gastroenterological Association. 2006;4:325-34.

[384] Cohen SB, Cheng TT, Chindalore V, Damjanov N, Burgos-Vargas R, Delora P, et al. Evaluation of the efficacy and safety of pamapimod, a p38 MAP kinase inhibitor, in a double-blind, methotrexate-controlled study of patients with active rheumatoid arthritis. Arthritis and rheumatism. 2009;60:335-44.

[385] Damjanov N, Kauffman RS, Spencer-Green GT. Efficacy, pharmacodynamics, and safety of VX-702, a novel p38 MAPK inhibitor, in rheumatoid arthritis: results of two randomized, double-blind, placebo-controlled clinical studies. Arthritis and rheumatism. 2009;60:1232-41.

[386] Sweeney SE. The as-yet unfulfilled promise of p38 MAPK inhibitors. Nature reviews Rheumatology. 2009;5:475-7.

[387] Hammaker D, Firestein GS. "Go upstream, young man": lessons learned from the p38 saga. Annals of the rheumatic diseases. 2010;69 Suppl 1:i77-82.

[388] Toldo S, Breckenridge DG, Mezzaroma E, Tassell BW, Shryock J, Kannan H, et al. Inhibition of apoptosis signal-regulating kinase 1 reduces myocardial ischemia-reperfusion injury in the mouse. J Am Heart Assoc. 2012;1:e002360.

[389] Zhang R, Al-Lamki R, Bai L, Streb JW, Miano JM, Bradley J, et al. Thioredoxin-2 inhibits mitochondria-located ASK1-mediated apoptosis in a JNK-independent manner. Circulation research. 2004;94:1483-91.

[390] Ichas F, Jouaville LS, Sidash SS, Mazat JP, Holmuhamedov EL. Mitochondrial calcium spiking: a transduction mechanism based on calcium-induced permeability transition involved in cell calcium signalling. FEBS Lett. 1994;348:211-5.

[391] Grover GJ, Dzwonczyk S, Sleph PG. Ruthenium red improves postischemic contractile function in isolated rat hearts. J Cardiovasc Pharmacol. 1990;16:783-9.

[392] Paradies G, Petrosillo G, Paradies V, Ruggiero FM. Role of cardiolipin peroxidation and Ca2+ in mitochondrial dysfunction and disease. Cell calcium. 2009;45:643-50.

[393] Ricci JE, Gottlieb RA, Green DR. Caspase-mediated loss of mitochondrial function and generation of reactive oxygen species during apoptosis. The Journal of cell biology. 2003;160:65-75.

[394] Petrosillo G, Ruggiero FM, Paradies G. Role of reactive oxygen species and cardiolipin in the release of cytochrome c from mitochondria. FASEB J. 2003;17:2202-8.

[395] Hori M, Nishida K. Oxidative stress and left ventricular remodelling after myocardial infarction. Cardiovascular research. 2009;81:457-64.

[396] Hsieh CC, Papaconstantinou J. Thioredoxin-ASK1 complex levels regulate ROS-mediated p38 MAPK pathway activity in livers of aged and long-lived Snell dwarf mice. FASEB J. 2006;20:259-68.

[397] Li X, Rong Y, Zhang M, Wang XL, LeMaire SA, Coselli JS, et al. Up-regulation of thioredoxin interacting protein (Txnip) by p38 MAPK and FOXO1 contributes to the impaired thioredoxin activity and increased ROS in glucose-treated endothelial cells. Biochem Biophys Res Commun. 2009;381:660-5.

[398] Oh J, Hur MW, Lee CE. SOCS1 protects protein tyrosine phosphatases by thioredoxin upregulation and attenuates Jaks to suppress ROS-mediated apoptosis. Oncogene. 2009;28:3145-56.

[399] Halestrap AP, Connern CP, Griffiths EJ, Kerr PM. Cyclosporin A binding to mitochondrial cyclophilin inhibits the permeability transition pore and protects hearts from ischaemia/reperfusion injury. Molecular and cellular biochemistry. 1997;174:167-72.

[400] Shiva S, Sack MN, Greer JJ, Duranski M, Ringwood LA, Burwell L, et al. Nitrite augments tolerance to ischemia/reperfusion injury via the modulation of mitochondrial electron transfer. The Journal of experimental medicine. 2007;204:2089-102.

[401] Ovize M, Baxter GF, Di Lisa F, Ferdinandy P, Garcia-Dorado D, Hausenloy DJ, et al. Postconditioning and protection from reperfusion injury: where do we stand? Position paper from the Working Group of Cellular Biology of the Heart of the European Society of Cardiology. Cardiovascular research. 2010;87:406-23.

[402] Piot C, Croisille P, Staat P, Thibault H, Rioufol G, Mewton N, et al. Effect of cyclosporine on reperfusion injury in acute myocardial infarction. The New England journal of medicine. 2008;359:473-81.

[403] Hatefi Y. The mitochondrial electron transport and oxidative phosphorylation system. Annual review of biochemistry. 1985;54:1015-69.

[404] Petrosillo G, Ruggiero FM, Di Venosa N, Paradies G. Decreased complex III activity in mitochondria isolated from rat heart subjected to ischemia and reperfusion: role of reactive oxygen species and cardiolipin. FASEB J. 2003;17:714-6.

[405] Vogt W. Oxidation of methionyl residues in proteins: tools, targets, and reversal. Free Radic Biol Med. 1995;18:93-105.

[406] Stadtman ER, Van Remmen H, Richardson A, Wehr NB, Levine RL. Methionine oxidation and aging. Biochim Biophys Acta. 2005;1703:135-40.

[407] Moskovitz J. Roles of methionine suldfoxide reductases in antioxidant defense, protein regulation and survival. Current pharmaceutical design. 2005;11:1451-7.

[408] Ruan H, Tang XD, Chen ML, Joiner ML, Sun G, Brot N, et al. High-quality life extension by the enzyme peptide methionine sulfoxide reductase. Proceedings of the National Academy of Sciences of the United States of America. 2002;99:2748-53.

[409] Arner ES. Focus on mammalian thioredoxin reductases--important selenoproteins with versatile functions. Biochim Biophys Acta. 2009;1790:495-526.

[410] Brennan LA, Lee W, Cowell T, Giblin F, Kantorow M. Deletion of mouse MsrA results in HBO-induced cataract: MsrA repairs mitochondrial cytochrome c. Molecular vision. 2009;15:985-99.

[411] Kim JI, Choi SH, Jung KJ, Lee E, Kim HY, Park KM. Protective Role of Methionine Sulfoxide Reductase A Against Ischemia/Reperfusion Injury in Mouse Kidney and Its Involvement in the Regulation of Trans-Sulfuration Pathway. Antioxidants & redox signaling. 2012.

# VITA

Hema Santhi Aluri was born on May 21, 1984 in Nuzividu, Visakhapatnam. She graduated from St. Francis De Sales high school in Visakhapatnam, Andhra Pradesh in 1999. She received her Bachelor of Pharmacy in 2005 from the Andhra University, in Visakhapatnam, Andhra Pradesh (INDIA). She completed Master of chemistry in 2009 from Virginia Commonwealth University, Richmond, Virginia. She joined the Physiology and Biophysics program for post-doctoral degree in 2010.